Investigating the Role of BMP Antagonists in Vertebrate Eye Development

by

Jennifer Michelle Weekes

A thesis submitted in partial fulfillment of the requirements for the degree of

Master of Science

in

Molecular Biology and Genetics

Department of Biological Sciences
University of Alberta

Abstract

Vertebrate eye development is a dynamic process that couples morphogenesis, migration of extraocular periocular mesenchyme (POM) cells to the eye, and retinal patterning along the nasotemporal and dorsoventral (DV) axes. Aberrant patterning during ocular development often results in defects including microphthalmia (small eyes), anophthalmia (no eyes), and coloboma (MAC). Coloboma occurs when the choroid fissure, a transient opening needed for vascularization and optic nerve formation, fails to close later in development. The eye is patterned in much the same way that the body axes are patterned via morphogen gradients established by the spatially restricted expression of diffusible extracellular molecules. Antagonists can further modify and shape morphogen gradients by establishing an opposing gradient. How these morphogen gradients work during eye patterning has been thoroughly studied in NT patterning, but much less is known about DV retinal patterning.

The dorsal retina is specified by BMP signaling restricted to the dorsal eye. Loss of BMP signaling results in a ventralized retina and ventral eye defects including coloboma. The ventral eye defects that occur with aberrant dorsoventral patterning suggest that dorsalizing and ventralizing signals must be balanced for proper patterning and structure; however, our knowledge of ventral retinal patterning remains incomplete. Evidence in chick indicates that BMP antagonists restricted to the ventral retina specify ventral retinal fate, but the BMP antagonists characterized appear to be chick specific, and to date no BMP

antagonist restricted to the ventral eye in other vertebrates has been characterized.

This work has identified three putative BMP inhibitors restricted to the ventral retina or surrounding cells during eye development: SPARC-related modular calcium binding 1 (Smoc1), Smoc2, and Gremlin2b (Grem2b). Expression of *smoc1* and *smoc2* was found to be restricted to the ventral retina while *grem2b* is expressed in what appears to be a novel subpopulation of POM cells that migrate exclusively to the ventral retina and choroid fissure. Reducing levels of these three proteins using antisense morpholino oligonucleotides resulted in microphthalmia, suggesting that inhibition of BMP signaling is necessary to regulate ocular size. Further loss of function studies revealed that Grem2b regulates BMP signaling in the dorsal eye while Smoc1 regulates BMP signaling in the dorsal eye and choroid fissure, indicating that Smoc1 could be involved in choroid fissure closure or vascularization. Reducing Smoc1 protein levels showed that Smoc1 is involved in DV retinal patterning, but likely during maintenance of DV patterning rather than initial specification. Together, these results provide an initial characterization of three BMP inhibitors during early vertebrate eye development and have surprisingly revealed that inhibition of BMP signaling occurs in the ventral retina although the source of these BMP signals remains unknown.

Preface

This thesis is an original work by Jennifer Weekes. The research project, of which this thesis is a part, received research ethics approval from the University of Alberta Animal Policy and Welfare Committee. The author has met the Canadian Council on Animal Care (CCAC) mandatory training requirements for animal users on the Care and Use of Animals in Research, Teaching and Testing.

Acknowledgements

I would like to thank my supervisor Dr. Andrew Waskiewicz for giving me the opportunity to work in the lab during my undergraduate and graduate degree. I would like to thank Drs. Heather McDermid and Dave Pilgrim for agreeing to be on my examination committee.

I would like to thank my family and friends for their constant support and encouragement throughout my degree. To all of the past and present lab members: thank you for making the lab a great environment to work in. Thank-you for everything you have taught me and thank-you for always providing an amazing source of entertainment. I would also like to thank my fellow graduate students for almost never turning down an opportunity for beer or travel.

Table of Contents

Chapter 1 ..... **1**

Vertebrate eye development is highly conserved 2

Specification of the eye field 2

Early eye morphogenesis 3

Eye patterning and retinotectal mapping 5

Dorsoventral retinal patterning is established by BMP signaling 7

The choroid fissure and coloboma 9

Microphthalmia and anophthalmia 11

Human genetics of congenital ocular defects 12

Periocular mesenchyme is essential for ventral eye development 14

BMP signaling, regulation, and its role in early embryogenesis 15

BMP signaling in eye development 18

Regulation of BMP signaling in eye development 19

Purpose of study 20

Chapter 2 ..... **27**

Zebrafish lines and maintenance 28

Embryo manipulation and care 28

General 28

Morpholino oligonucleotide preparation and injection 28

mRNA preparation and injection 29

Isolation of genomic DNA 29

PCR and Cloning 29

PCR 29

RNA extraction 30

cDNA synthesis 30

One-Step RT-PCR 31
TOPO Cloning and transformation 31
Sequencing 32
Overexpression constructs 33
Primer and construct design 33
Restriction digests 33
In vitro mRNA synthesis 34
In situ hybridization 35
Digoxigenin labeled riboprobe synthesis 35
Whole Mount mRNA *In Situ* Hybridization (ISH) 36
Microscopy 38
Eye measurements 38
Aldh1a3 genotyping 38
Chapter 3 49
Introduction 50
Results & Discussion 52
Smoc1 sequence 52
Smoc2 sequence 53
smoc1 & *smoc2* expression patterns 53
Expression of *smoc1* & *smoc2* is expanded in *gdf6a* mutants 56
Knockdown of *smoc1* and *smoc2* results in microphthalmia 57
Smoc1 morphants have abnormal optic stalks 59
Smoc1 regulates BMP signaling in the choroid fissure 59
Knockdown of *smoc1* alters dorsoventral retinal patterning 60
Knockdown of *smoc2* does not affect dorsoventral retinal patterning 61
smoc1 and *smoc2* do not act synergistically 62

Overexpression of *smoc1* and *smoc2* does not alter dorsoventral retinal patterning 62
Summary & Future directions 64
Chapter 4 85
Introduction 86
Results & Discussion 87
Gremlin proteins are highly conserved 87
grem2b expression 88
grem2b expression is altered in *gdf6a* mutants 89
grem2b morphants have microphthalmia 91
grem2b morphants have expanded BMP signaling 93
Summary and Future directions 94
Chapter 5 104
Introduction 105
Results and Discussion 107
aldh1a3 mutants are strong hypomorphs 107
aldh1a3 mutant phenotype 108
Retinal patterning is normal in *aldh1a3* mutants 109
POM migration is normal in *aldh1a3* mutants 109
Retinoic acid signaling in *aldh1a3* mutants 110
Development of photoreceptors in *aldh1a3* mutants 111
Discussion and conclusions 112
Chapter 6 122
Literature Cited 128

List of Tables

Table 2.1: translation blocking morpholino oligonucleotides used. **.....40**

Table 2.2: Primers used to amplify the Grem2b and Smoc2 coding sequences to generate overexpression constructs. **..... 41**

Table 2.3: Primers used to generate templates for riboprobe synthesis. **..... 45**

Table 2.4: Information for plasmid-based riboprobes used in this study. **.....46**

Table 2.5: Primers used for *aldh1a3* genotyping. **.....48**

List of Figures

Figure 1.1: Vertebrate eye morphogenesis. **23**

Figure 1.2: Establishment of the dorsoventral (DV) retinal axis during eye development. **25**

Figure 1.3: Bone morphogenetic protein (BMP) signaling pathway. **26**

Figure 2.1: Sequence alignment of the zebrafish smoc1 coding sequence (input) with the codon optimized sequence synthesized by Genscript (optimized). **43**

Figure 2.2: Amino acid alignment of the *smoc1* input sequence with the codon optimized output sequenced used to generate a *smoc1* overexpression construct. **44**

Figure 2.3: The *aldh1a3*^{sa118} mutant allele results in a severely truncated protein. **47**

Figure 3.1: Smoc1 is a highly conserved protein with two isoforms in zebrafish and mice. **69**

Figure 3.2: Conserved domains and alignment of zebrafish Smoc2. **71**

Figure 3.3: Expression of smoc1 and smoc2 in zebrafish from 14 hpf to 48 hpf. **72**

Figure 3.4: Expression of smoc1 and smoc2 is expanded in *gdf6a*$^{-/-}$ mutants. **73**

Figure 3.5: Reduction of Smoc1 protein levels results in microphthalmia in a p53 dependent manner. **74**

Figure 3.6: *smoc2* morphants have microphthalmia. **75**

Figure 3.7: *smoc1* morphants have abnormal optic stalks. **76**

Figure 3.8: BMP signaling is expanded throughout the eye and into the choroid fissure when Smoc1 protein levels are reduced. **77**

Figure 3.9: Smoc1 plays a minor role in patterning the DV retinal axis in zebrafish. **78**

Figure 3.10: *smoc2* morphants have normal DV retinal patterning. **79**

Figure 3.11: Smoc1 and Smoc2 do not act synergistically to pattern the DV retinal axis. **80**

Figure 3.12: Overexpression of *smoc1* does not alter DV retinal patterning but does cause axis defects. **82**

Figure 3.13: Overexpression of smoc2 does not alter DV retinal patterning, but it does cause axial defects similar to loss of a BMP. **83**

Figure 4.1: Grem2 proteins are highly conserved. **97**

Figure 4.2: The zebrafish Grem2 paralogs, Grem2a and Grem2b, are highly conserved. **98**

Figure 4.3: Expression of *grem2b* between 16 and 48 hpf of zebrafish development. **99**

Figure 4.4: Expression of *grem2b* is altered in *gdf6a*$^{-/-}$ mutants. **100**

Figure 4.5: Reduction of Grem2b protein levels results in microphthalmia and ventral eye defects. **101**

Figure 4.6: *grem2b* morphants exhibit microphthalmia. **102**

Figure 4.7: BMP signaling is expanded in *grem2b* morphants. **103**

Figure 5.1: Retinoic acid (RA) synthesis and signaling pathway. **114**

Figure 5.2: Expression of *aldh1a3* is reduced in *aldh1a3* mutants. **115**

Figure 5.3: Eye defects observed in embryos from *aldh1a3*$^{+/-}$ incrosses. **116**

Figure 5.4: *aldh1a3* mutants have normal dorsoventral retinal patterning. **117**

Figure 5.5: POM migration is unaffected in *aldh1a3* mutants. **118**

Figure 5.6: RA signaling is attenuated in *aldh1a3* mutants. **119**

Figure 5.7: *aldh1a3* mutants have normal *opn1sw2* expression and cone distribution. **121**

Figure 6.1: The BMP inhibitors Smoc1, Smoc2, and Grem2b are involved in **127**

early zebrafish eye morphogenesis. **127**

List of Abbreviations

ALDH: aldehyde dehydrogenase

Aldh1a2: aldehyde dehydrogenase 1a2

Aldh1a3: aldehyde dehydrogenase 1a3

ANB: anterior neural border

Bambi: BMP and activin membrane-bound protein

BCIP: 5-bromo-4-chloro-3- indolyl-phosphate

BLAST: basic local alignment search tool

BLAT: BLAST like alignment tool

BMP: bone morphogenetic protein

Bmpr-I: BMP receptor, type I

Bmpr-II: BMP receptor, type II

Bra: brachyury

BRE: BMP response element

BSA: bovine serum albumin

CAPs: cleaved amplified polymorphism

CDS: coding sequence

CMZ: ciliary marginal zone

CNCC: cranial neural crest cell

CRABP: cellular retinoic acid binding protein

CTCK: C-terminal cysteine knot

CV2: crossveinless 2

Cyp1b1: cytochrome P450, family 1, subfamily B, polypeptide 1

CYP26: cytochrome p450, family 26

DAN: differential screening-selected gene aberrative in neuroblastoma

DEPC: diethylpyrocarbonate

DNA: deoxyribonucleic acid

Dpf: days post fertilization

Dpp: Decapentaplegic

DRM: down regulated by v-*mos*

DV: dorsoventral

ECM: extracellular matrix

Efnb2a: ephrin-B2a

Ephb4a: eph receptor B4a

FACs: fluorescence activated cell sorting

FGF: fibroblast growth factor

FS: follistatin

Fsta: follistatin a

GCL: ganglion cell layer

Gdf6a: growth and differentiation factor 6a

Grem: gremlin

Grem2: gremlin2

hpf: hours post fertilization

INL: inner nuclear layer

IPL: inner plexiform layer

iSmad: inhibitory Smad

LCA: Leber congenital amaurosis

MAC: microphthalmia, anophthalmia, coloboma

mRNA: messenger RNA

NBT: 4-nitro blue tetrazolium

Nrp2b: neuropilin 2b

NT: nasotemporal

ONL: outer nuclear layer

OPL: outer plexiform layer

Opn1sw2: opsin 1, short-wave sensitive 2

Otx2: Orthodenticle homeobox 2

Pax6: Paired box 6

PFA: paraformaldehyde

POM: periocular mesenchyme

PRDC: protein related to DAN and Cerberus

PTU: N-phenylthiourea

RA: retinoic acid

RALDH: retinaldehyde dehydrogenase

RAR: retinoic acid receptor

RARB: retinoic acid receptor beta

RARE: retinoic acid response element

RBP: retinol binding protein

RDH: retinol dehydrogenase

Rdh10a: retinol dehydrogenase 10a

RGC: retinal ganglion cell

RNA: ribonucleic acid

RPC: retinal progenitor cell

RPE: retinal pigmented epithelium

rSmad: receptor-activated Smad

Rx: retinal homeobox

Rx1: retinal homeobox 1

Rx2: retinal homeobox 2

Rx3: retinal homeobox 3

RXR: retinoid X receptor

SDS: sodium dodecyl sulfate

Sema3fa: semaphorin 3fa

Sema3fb: semaphorin 3fb

Sfrp: secreted frizzled related protein

Shh: sonic hedgehog

Slit2: slit homolog 2

Smoc1: Sparc related modular calcium binding 1

Smoc2: Sparc related modular calcium binding 2

Sox2: SRY-box 2

SPARC: secreted protein acidic and rich in cysteine

Stra6: stimulated by retinoic acid 6

Tbx5a: T-box 5a

TGF- β: transforming growth factor-β

Tsg: twisted gastrulation

Ty: thyroglobulin

VAD: vitamin A deficiency

Vasna: vasorin a

Vax2: ventral anterior homeobox 2

X-vent1: VENT homeobox 1 gene 2

Chapter 1

Introduction

Vertebrate eye development is highly conserved

Development of the eye is a tightly coordinated process that requires the precise orchestration of spatial and temporal gene expression with morphogenetic movements that shape the eye. When either of these processes goes awry, congenital eye defects and blindness can result. How exactly these processes are regulated and coordinated are not fully understood; further study of these processes is essential to fully comprehend the complex etiology of congenital eye disorders.

Vertebrate eye development is a highly conserved process that has been studied in model systems including, but not limited to, mice, chick, *Xenopus*, medaka and zebrafish. Zebrafish (*Danio rerio*) have been increasingly used as a model to study human disease as zebrafish provide a genetically tractable system that has many advantages over other potential model systems (Ablain & Zon 2013). In particular, zebrafish are an excellent model for studying eye development and eye disorders. The zebrafish genome has been sequenced, and unlike other teleost species used in developmental biology, the zebrafish genome is well annotated. This facilitates the use of many genetic tools including antisense morpholino oligonucleotides to inhibit splicing or translation of mRNA and targeted mutagenesis to disrupt gene function. Many mutant and transgenic lines have been generated that are invaluable for studying the eye. Eye development can be easily observed in zebrafish due to the transparency of the embryos and external fertilization, which allows for development to be observed continuously.

Specification of the eye field

Eye development begins with specification of the eye field, which occurs shortly after gastrulation at 10 hours post fertilization (hpf) in zebrafish (Loosli et al. 2003). Eye field specification is preceded by neural induction and anterior-posterior (AP) patterning of the forebrain (Sinn & Wittbrodt 2013). Both neural induction and patterning require the combined action of different morphogens. Induction of the neurectoderm is achieved through fibroblast growth factor

(FGF) signaling in combination with the inhibition of Wnt and bone morphogenetic protein (BMP) signaling (Wilson & Houart 2004; Sinn & Wittbrodt 2013). Following neural induction, neural tissue of the forebrain is patterned along the AP axis and partitioned into the telencephalon and diencephalon. High Wnt activity specifies posterior, or diencephalic, neural fate while low Wnt activity in the anterior neurectoderm, in part achieved through the secretion of the Wnt antagonist Tlc from the anterior neural border (ANB), is necessary for the telencephalon and eye field to form (Houart et al. 2002).

Low Wnt activity is further reinforced in the anterior neural plate through the expression and autologous positive regulation of the transcriptional repressor *six3* in the telencephalon and presumptive eye field (Kobayashi et al. 2001; Wilson & Houart 2004). Expression of *six3* and other eye field transcription factors is mediated by SRY-box 2 (Sox2) and Orthodenticle homeobox 2 (Otx2) which allows for the initiation of eye field formation in part by making the anterior neural tissue competent to form the eye field (Beccari et al. 2012; Beby & Lamonerie 2013). A network of transcription factors, including Six3, establish the eye field in part by the reciprocal regulation of the transcription factors Six3 and Paired box 6 (Pax6) (Carl et al. 2002; Sinn & Wittbrodt 2013). The eye field transcriptional network is further established by the regulation of expression of the *retinal homeobox* (*rx1, rx2,* and *rx3*) genes via Six3 (Loosli et al. 1999; Carl et al. 2002; Sinn & Wittbrodt 2013). The *rx* genes, in particular *rx3,* maintains eye field fate, regulates proliferation within the eye field, and facilitates separation of eye field cells from the forebrain through the upregulation of *ephrin b2a* (*efnb2a*) (Stigloher et al. 2006; Loosli et al. 2001; Chuang & Raymond 2001; Cavodeassi et al. 2013). Following specification of the single eye field by the host of transcription factors described above, the eye field is split into bilateral optic primordia by the posterior to anterior movement of diencephalic cells (Varga et al. 1999; Wilson & Houart 2004).

Early eye morphogenesis

In zebrafish, the optic primordia form by 11 hpf and begin to evaginate (Figure 1.1) (Schmitt & Dowling 1994). The optic vesicles begin to grow as

evagination occurs as retinal progenitor cells (RPCs) intercalate into the optic vesicle. The lateral morphogenetic movement of the optic vesicle is facilitated in part through Rx3; Rx3 in the eye field is necessary for the eye field cells to not retain the epithelial characteristics of other forebrain cells (Rembold et al. 2006; Sinn & Wittbrodt 2013). The optic vesicle continues to evaginate until it makes contact with the overlying ectoderm. Contact with the surface ectoderm induces formation of the lens vesicle from ectodermal tissue concurrent with the invagination of the optic vesicle to form the bilayered optic cup which occurs around 16 hpf (Figure 1.1) (Adler & Canto-Soler 2007). FGF signaling originating from the surface ectoderm induces the differentiation of the innder layer of the optic cup to become neural retina while the outer layer becomes the retinal pigmented epithelium (RPE) (Hyer et al. 1998; Adler & Canto-Soler 2007; Martínez-Morales & Wittbrodt 2009).

Optic cup formation occurs simultaneously with other morphological changes. The tissue connecting the brain to the anterior optic cup begins to lengthen and constrict to form the optic stalk, which will go on to form the optic nerve (Schmitt & Dowling 1994). As invagination of the optic cup continues, two grooves form in the posterior and anterior regions of the eye. The posterior groove is shallow and transient; the function of this transient structure is still unknown. In the anterior eye, the groove that forms around 18 hpf continues to invaginate and forms a gap in the anterior eye known as the choroid fissure (Figure 1.1 B) (Schmitt & Dowling 1994). Like the posterior groove, the choroid fissure is also transient, but remains open until 48 hpf. This transient opening is necessary for vasculature to enter and exit the eye and for retinal ganglion cell (RGC) axons to exit the eye and reach the brain through the optic nerve (Schmitt & Dowling 1994; Adler & Canto-Soler 2007). As optic cup invagination completes around 24 hpf, the lens is formed and the eye begins to rotate so that the choroid fissure and optic stalk have a ventral rather than anterior orientation (Schmitt & Dowling 1994).

Following the morphogenetic movements that occur to give the eye its structure, retinal precursor cells begin to differentiate and form the neural retina. The vertebrate retina is a highly conserved and highly organized laminar tissue

divided into three nuclear layers: the outer nuclear layer (ONL), the inner nuclear layer (INL) and ganglion cell layer (GCL) (Stenkamp 2007). Plexiform layers where cells from one nuclear layer synapse with cells from the adjacent layer are found between the ONL and INL (outer plexiform layer; OPL) and between the INL and GCL (inner plexiform layer; IPL) (Hoon et al. 2014). Between 24 and 36 hpf, RGCs are the first cell type of the retina that begin to differentiate. By 36 hpf, these cells begin to project to the brain through the optic nerve and reach and innervate the optic tectum by 48 hpf and 72 hpf, respectively (Schmitt & Dowling 1994; Kita et al. 2014; Stuermer 1988; Stenkamp 2007). Following the differentiation of RGCs at 36 hpf, cells of the INL (horizontal, amacrine, and bipolar cells) begin to differentiate. The last cells to differentiate and divide starting at 48 hpf are the photoreceptors of the ONL, the layer closest to the RPE (Stenkamp 2007).

After formation of the visual system is complete, light enters the eye through the lens and passes through the GCL and INL to reach the photoreceptors in the ONL. Photoreceptors transmit signals to bipolar cells in the INL. These signals can be further refined through contact with horizontal cells in the INL. Bipolar cells then synapse with RGCs in the GCL. Visual processing is further fine-tuned by amacrine cells that synapse with bipolar cells and RGCs. RGCs transmit this action potential through the optic nerve to the optic tectum in the midbrain where visual signals are processed (Hoon et al. 2014).

Eye patterning and retinotectal mapping

In order for visual cues to be properly processed into a single coherent image, the spatial organization of RGCs in the retina must be preserved when the axons of these cells innervate the tectum. This maintenance of the topographical organization of RGCs from the eye to the tectum, known as retinotectal mapping, requires positional information to be imparted on the RGCs within the retina so that the axons migrate to the correct target within the tectum. This positional identity and directed axon migration occurs through patterning of the dorsoventral (DV) and nasotemporal (NT) axes of the eye and through the spatially restricted expression of Eph and Ephrin guidance molecules in the

retina and tectum (Lemke & Reber 2005). By patterning the retina along the DV and NT axes, the retina can be divided into quadrants: nasal, temporal, dorsal, and ventral. The posterior and anterior regions of the optic tectum are innervated by RGCs from the nasal and temporal regions of the retina, respectively. RGCs in the dorsal retina project to the lateral tectum while RGCs in the ventral retina project medially (Lemke & Reber 2005).

RGC axons are guided from their respective quadrant to the correct region of the tectum by interactions between Eph receptors and Ephrin ligands (Lemke & Reber 2005). Repulsive interactions between EphA receptors and Ephrin A ligands guide RGC axons from the nasal and temporal retina to the posterior and anterior tectum, while attractive interactions between EphB receptors and EphrinB ligands guide axons from the dorsal and ventral regions of the eye to the lateral and medial regions of the tectum. Eph receptors are expressed in a gradient across the retina with EphA receptor expression highest in the temporal retina and EphB receptor expression highest in the ventral retina. RGC axons from the temporal retina are repelled from the posterior tectum where EphrinA ligands are expressed and innervate the anterior tectum where there are low levels of EphrinA ligands. As RGCs from the nasal retina have low EphA receptor expression, the axons are guided to the posterior tectum where there are high levels of the repellent EphrinA ligands. Conversely, RGC axons from the ventral retina express high levels of EphB receptors and are guided to the medial tectum where EphrinB ligands are expressed and serve as an attractive cue while RGC axons with low levels of EphB receptor innervate the lateral tectum where there is low EphrinB expression (Lemke & Reber 2005).

An essential step in establishing the Eph receptor gradients in the retina for retinotectal mapping is the patterning of the DV and NT axes of the eye. Vertebrate eye patterning is coupled with early eye morphogenesis. Like eye morphogenesis, patterning largely relies on spatially restricted expression of diffusible morphogens. NT patterning occurs shortly after the optic primordia form at 11 hpf when the optic vesicle is beginning to evaginate and the dorsal forebrain is in close proximity to what will become the nasal retina after the optic cup rotates. The nasal retina is specified by FGF signaling; Fgf3 and Fgf8 diffuse

from the dorsal forebrain while Fgf24 diffuses from the olfactory placode to the presumptive nasal retina (Picker & Brand n.d.; Picker et al. 2009). Fgf3/8/24 promotes nasal retinal fate by activating expression of the forkhead box transcription factor *foxg1* and represses temporal retinal fate by inhibiting expression of *foxd1* (Picker et al. 2009). The nasal and temporal halves of the retina become demarcated by the expression of *foxg1* and *foxd1*, respectively. These transcription factors act antagonistically to maintain NT identity and to spatially restrict the expression of *epha3* to the temporal retina, thereby providing RGCs with positional identity and facilitating proper retinotectal mapping (Takahashi et al. 2009; Picker et al. 2009).

Like NT patterning, DV retinal patterning is required for the topographical projection of dorsal and ventral RGC axons to the lateral and medial tectum, respectively (Lemke & Reber 2005). Although the end result of DV and NT patterning is largely the same, how these two axes are patterned differs. As described above, the nasal retina is specified by the presence of Fgf ligands and the temporal retina is specified by the lack of these signals. NT patterning and subsequent morphogenetic movements and retinotectal mapping have been thoroughly characterized in multiple vertebrate model systems, but much less is known about DV patterning, and in particular, how ventral retinal identity if established.

Dorsoventral retinal patterning is established by BMP signaling

DV retinal patterning has two phases: initiation and maintenance. Patterning of the DV axis occurs early in zebrafish eye development shortly after the NT axis is patterned and the optic vesicles have evaginated at 12 hpf (Veien et al. 2008; Picker et al. 2009). Dorsal eye patterning is initiated by the diffusion of the transforming growth factor β (TGF-β) ligand growth and differentiation factor 6a (Gdf6a) from lateral extraocular ectoderm to the presumptive dorsal retina (Kruse-Bend et al. 2012). Gdf6a, along with bone and morphogenetic protein 2b (Bmp2b) activate expression of the transcription factor *T-box 5a* (*tbx5a*) in the dorsal retina (Kruse-Bend et al. 2012; French et al. 2009). The ventral retina is

specified by sonic hedgehog (Shh) diffusing from the midline to the presumptive ventral retina which then activates expression of the ventral retinal transcription factor *ventral anterior homeobox 2* (*vax2*) (Figure 1.2) (Ekker et al. 1995; Zhang & Yang 2001; Sasagawa et al. 2002; Zhao et al. 2010; Take-uchi et al. 2003).

Maintenance of DV retinal patterning occurs between 14 and 16 hpf (Veien et al. 2008). While initiation of retinal patterning involves extraocular diffusible morphogens, the maintenance phase is characterized by these morphogens being expressed within the eye (Veien et al. 2008; Kruse-Bend et al. 2012). Wnt ligands originating from the dorsal RPE diffuse to the dorsal retina and initiate expression of *gdf6a, bmp2b*, and *bmp4* within the dorsal retina which maintains expression of *tbx5a* (Veien et al. 2008). The initiation and maintenance phases have only been described for specification of dorsal retinal identity. Although Shh is required for ventral retinal fate, it is not clear if ventral retinal specification, like dorsal retinal specification, occurs in two phases where ventral identity and *vax2* expression is established by Hh signaling and then maintained by another morphogen (Ekker et al. 1995; Zhang & Yang 2001; Sasagawa et al. 2002; Zhao et al. 2010).

Similar to the restricted expression of the transcription factors *foxg1* and *foxd1* to the nasal and temporal retina, the restriction of *tbx5a* and *vax2* expression to the dorsal and ventral regions of the retina is necessary for retinotectal mapping where misexpression results in misprojected RGC axons (Koshiba-Takeuchi et al. 2000; Barbieri et al. 2002). Based on mechanisms of NT patterning where transcription factors restricted to the nasal and temporal lobes of the eye reciprocally repress each other to promote nasal and temporal cell fate, the demarcation of the dorsal and ventral halves of the eye by *tbx5a* and *vax2,* respectively, suggest that a similar mechanism could occur to establish and maintain dorsoventral patterning; however, loss of *tbx5a* or *vax2* does not affect the expression domain of the other gene, indicating that these transcription factors do not reciprocally repress each other (French et al. 2009; Mui et al. 2002).

The absence of reciprocal repression between Tbx5a and Vax2 suggests that instead there are upstream antagonistic regulators that act to restrict dorsal

and ventral retinal identity. Indeed, the retina becomes ventralized and *vax2* expression is expanded at the expense of dorsal eye identity and *tbx5a* expression when the BMP ligands Gdf6a or Bmp2b are absent (French et al. 2009) (Gosse & Baier 2009; Kruse-Bend et al. 2012). Similarly, overexpression of *gdf6a* results in a dorsalized eye where *tbx5a* expression is expanded at the expense of *vax2* (French et al. 2009). Together, these results indicate that BMP ligands in the dorsal eye promote dorsal retinal identity while restricting ventral identity and that there are unidentified factors in the ventral retina that do the opposite. Since BMP ligands specify the dorsal eye, the most likely explanation is that BMP inhibitors restricted to the ventral eye restrict dorsal retinal fate while promoting ventral fate. In chickens, *ventroptin*, a chordin-like BMP antagonist, is expressed in the ventral retina and opposes BMP signals originating from the dorsal retina. Expression of *ventroptin* in the ventral retina has only been observed in chickens and is not expressed in the zebrafish or mouse ventral retina, leaving open the possibility that there remain unidentified BMP inhibitors within the ventral retina that are necessary for DV retinal patterning (Sakuta et al. 2001).

In addition to misprojected RGC axons and abnormal retinotectal mapping, aberrant DV retinal patterning also results in a spectrum of eye defects. The same genes that are involved in early eye development and eye patterning also appear to have a role in eye morphogenesis although it is not entirely understood how alterations in eye patterning can lead to such defects which include microphthalmia, anophthalmia, and coloboma.

The choroid fissure and coloboma

As mentioned previously, the choroid fissure is a transient opening in the optic cup that is required for RGC axons to exit the eye through the optic nerve and for vasculature to enter and exit the eye. Although this opening in the eye is required during early eye development, it is essential that the choroid fissure closes to produce a structurally sound eye. When the choroid fissure fails to close, coloboma occurs. Coloboma accounts for 3.2-11% of pediatric blindness (Onwochei et al. 2000). The severity of coloboma varies depending on how the where the fissure fails to close along the proximal distal axis of the eye. Distal

failure of fissure closure typically only involves the iris and RPE whereas proximal failure of fissure closure, or posterior segment coloboma, affects distal regions of the eye including the retina and optic nerve resulting in a poorer visual prognosis when compared to more anterior colobomata (Onwochei et al. 2000).

The etiology of coloboma is not fully understood, but appears to be caused by environmental and genetic factors with the majority of genetic cases being syndromic (Gregory-Evans, Vieira, et al. 2004a). In addition to genetic causes of coloboma mentioned above, coloboma and eye development can be influenced by environmental factors including diet. Countries where Vitamin A deficiency (VAD) and resulting night blindness are prevalent have an increased incidence of coloboma (Gregory-Evans, Williams, et al. 2004b). Maternal VAD in rats has been shown to result in coloboma in their offspring (See & Clagett-Dame 2009). Vitamin A is a precursor to the diffusible morphogen retinoic acid (RA), which is an essential morphogen for hindbrain patterning and is thought to be necessary for ventral eye development and choroid fissure closure since RA synthesis enzymes are spatially restricted to the dorsal and ventral regions of the eye (Rhinn & Dollé 2012; Duester 2009). The study of RA in zebrafish eye development has largely relied on the use of pharmacological treatments; RA signaling antagonist and exogenous RA treatments have both been shown to result in coloboma, although the mechanism through which this happens has not yet been fully elucidated (Hyatt, Schmitt, Marsh-Armstrong, McCaffery, Dräger & Dowling 1996a; Lupo et al. 2011). One possibility is that rather than RA signaling within the ventral eye to direct fissure closure, RA signals to nearby periocular mesenchyme, a migratory cell population that is thought to be required for fissure closure (Matt et al. 2008; Lupo et al. 2011).

Alterations in DV retinal patterning are known to cause coloboma, although the underlying mechanisms through which this occurs is not clear. In zebrafish, coloboma has been associated with a ventralized retina as is seen in *gdf6a* mutants, *patched1* mutants and *secreted frizzled related protein* (*sfrp1a/sfrp5*) morphants (French et al. 2009; French et al. 2013; Lee et al. 2008; Holly et al. 2014). In *patched1* mutants, which lack the negative regulator of the Hedgehog receptor, increased Hedgehog signaling ventralizes the eye and also

expands the optic stalk which impedes fissure closure (Lee et al. 2008). Zebrafish *gdf6a* mutants and *sfrp1a/sfrp5* morphants also have coloboma, although the underlying mechanism is not clear in these cases (French et al. 2013; Holly et al. 2014). Failure of fissure closure is also observed when the eye is dorsalized by the overexpression of *BMP4* due to reduced epithelial flow from the presumptive RPE to the presumptive retina during optic cup formation (Heermann et al. 2015). Together, these studies show that DV retinal patterning, and in particular BMP signaling, must be finely regulated for choroid fissure closure to occur. Often when fissure closure fails due to aberrant DV patterning or through another mechanism, other eye defects such as microphthalmia occur.

Microphthalmia and anophthalmia

Microphthalmia, anophthalmia, and coloboma (MAC) encompass a spectrum of eye disorders. Microphthalmia is characterized by a small eye whereas anophthalmia is characterized by the absence of eyes. Anophthalmia is classified by the amount of remaining ocular tissue with true anophthalmia being the complete absence of the globe and all associated structures including the optic nerve (Gerth-Kahlert et al. 2013). As can be imagined from the complexity of eye morphogenesis, aberrant processes at multiple steps in development can cause microphthalmia and anophthalmia. Aberrant steps of early eye development including eye field specification and optic vesicle evagination have the most profound effect and typically result in anophthalmia, whereas abnormal eye development at later stages can result in less severe eye defects such as microphthalmia or anophthalmia with remaining eye tissue.

The loss of the eye field markers *rx3* and *six3* both result in anophthalmia in medaka although the eye field still initially forms (Loosli et al. 2001; Carl et al. 2002). Since *six3* maintains *rx3* expression, the phenotypes caused by the loss of *six3* and *rx3* are similar. The loss of *rx3*, an early eye field marker, results in anophthalmia by disrupting many processes. In *rx3* mutants, retinal progenitor cell field specification and retinal progenitor cell proliferation are reduced and during optic vesicle evagination, retinal progenitor cells converge on the midline and not all cells enter the evaginating optic vesicle (Loosli et al. 2001; Rembold et

al. 2006). Anophthalmia can also occur after the optic vesicle has evaginated and the optic cup begins to form if induction between the lens and optic vesicle does not occur and the optic vesicle degenerates, as has been observed in *Bmp7* null mutant mice (Verma & FitzPatrick 2007; Morcillo et al. 2006).

The severity of microphthalmia, like anophthalmia, is variable and can be attributed to mutations in many of the same genes that have been associated with anophthalmia and coloboma. Microphthalmia can be caused by increased apoptosis or decreased proliferation during eye development. Like coloboma, loss of DV retinal patterning genes can also cause microphthalmia. Zebrafish *gdf6a* mutants, as mentioned previously, have altered DV patterning and coloboma, but also exhibit microphthalmia due to a combination of a reduced number of progenitor cells in the eye, increased apoptosis, and decreased proliferation (Asai-Coakwell et al. 2013; French et al. 2013). As aberrant DV retinal patterning has been associated with MAC phenotypes in several studies, fully understanding how the eye DV axis is specified can also further elucidate the underlying causative mechanisms for microphthalmia, anophthalmia, and coloboma.

Human genetics of congenital ocular defects

MAC encompasses a spectrum of rare eye disorders that occurs in 1/10 000 to 1/5000 live births (Gerth-Kahlert et al. 2013; Morrison et al. 2002; Slavotinek 2011). MAC can manifest unilaterally or bilaterally with variable severity. The majority of MAC cases present with other developmental anomalies with 20-40% of all MAC cases being syndromic with an identified genetic lesion (Slavotinek 2011). Of the MAC cases that occur from chromosomal aberrations, most present as bilateral ocular defects. Inherited MAC disorders have variable penetrance and modes of inheritance with phenotypes typically showing a strong genotype phenotype correlation (Slavotinek 2011). The most common cause of microphthalmia and anophthalmia is lesions in the early eye field development genes *SOX2* and *OTX2*, which account for up to 20% and 8% of microphthalmia and anophthalmia cases, respectively (Gerth-Kahlert et al. 2013; Slavotinek 2011). Other eye field specification and early patterning genes have been reported to cause microphthalmia and anophthalmia including *SIX3, PAX6,* and *SHH*, but

the incidence of these mutations is very low, possibly due to the reduced viability that would be expected from mutations in genes that also are involved in brain development (Slavotinek 2011). Mutations in *RAX*, the human ortholog of teleost *rx3*, has been associated with microphthalmia, anophthalmia, and coloboma and is one of the few genes that when mutated does not cause extraocular phenotypes (Slavotinek 2011).

Another common cause of MAC is recessive mutations in *Aldhehyde dehydrogenase 1a3* (*ALDH1A3*), which encodes an RA synthesis enzyme. Mutations in *ALDH1A3* have been estimated to be present in up to 10% of MAC cases where phenotypes range from microphthalmia, to microphthalmia with coloboma or anophthalmia (Abouzeid et al. 2014; Aldahmesh et al. 2013; Fares-Taie et al. 2013; Mory et al. 2013; Williamson & Fitzpatrick 2014). Unlike most genetically attributable MAC cases, mutations in *ALDH1A3* often do not exhibit any extraocular phenotypes (Williamson & Fitzpatrick 2014). Mutations in a transporter involved in the RA pathway, *Stimulated by retinoic acid 6* (*STRA6*), as well as the nuclear RA receptor, *Retinoic acid receptor beta* (*RARB*), have been identified in MAC patients, although unlike mutations in *ALDH1A3*, mutations in *STRA6* and *RARB* present with extraocular findings and are syndromic in nature (Slavotinek 2011; Williamson & Fitzpatrick 2014). Occurrence of *STRA6* and *RARB* mutations in MAC is rare when compared to the frequency of *ALDH1A3* mutations likely due to the reduction in viability associated with mutations in these genes (Williamson & Fitzpatrick 2014). The number of MAC cases that have been attributed to mutations in RA pathway genes and the increased incidence of MAC in countries where VAD is prevalent strongly suggests that RA, and in particular *ALDH1A3,* is essential for eye morphogenesis (Gregory-Evans, Williams, et al. 2004b). Surprisingly, studies in model systems have not yet elucidated the complete role of RA in vertebrate eye development.

Similar to model systems, humans with mutations in genes known to be involved in dorsoventral retinal patterning exhibit MAC phenotypes and degenerative retinal disorders. Mutations in *GDF6* have been associated with microphthalmia, anophthalmia and coloboma in addition to the degenerative

retinal dystrophy Leber congenital amaurosis (LCA) (Asai-Coakwell et al. 2007; Asai-Coakwell et al. 2013; Slavotinek 2011). Humans with mutations in *BMP4* exhibit a variety of phenotypes quite similar to those seen with *GDF6* mutations and include MAC, glaucoma, and retinal dystrophies (Slavotinek 2011). Mutations in the BMP inhibitor *SMOC1* are associated with Waardenburg anophthalmia, a syndrome characterized by microphthalmia and anophthalmia with the most severe cases having true anophthalmia where no ocular remnants remain (Okada et al. 2011; Abouzeid et al. 2011; Rainger et al. 2011). While loss of function of *GDF6* and *BMP4* has been studied in model systems, little work has been done on *SMOC1* and it is not known how exactly mutations in *SMOC1* can lead to MAC phenotypes.

Periocular mesenchyme is essential for ventral eye development

Periocular mesenchyme (POM) is a neural crest derived migratory cell population that migrates to the eye and contributes to ocular structures primarily within the anterior segment of the eye including the cornea, sclera, trabecular meshwork, Schlemm's canal, extraocular and ciliary muscles, and vasculature (Gage et al. 2005). How exactly POM cells are directed to migrate to the eye is currently unknown, but it is thought that a signal emanating from the eye directs migration (Langenberg et al. 2008). POM cells migrate to the choroid fissure, where these cells appear to be necessary to direct fissure closure (Matt et al. 2008; Lupo et al. 2011). It is thought that POM cells could be directed to the eye and choroid fissure by RA since inhibition of RA signaling in zebrafish results in decreased POM migration to the eye and choroid fissure, increased apoptosis, and coloboma (Lupo et al. 2011). In mice, the reduction of RA synthesis in the eye results in POM overgrowth and decreased apoptosis (Molotkov et al. 2006). Pan-neural crest markers such as *sox10* and POM specific markers including *pitx2, foxc1a,* and *eya2* have been utilized to track POM migration to the eye, but it is still not known what genes distinguish POM cells from other migratory neural crest cells.

BMP signaling, regulation, and its role in early embryogenesis

Bone morphogenetic protein (BMP) signaling is a highly conserved signaling pathway essential for many aspects of development. BMP ligands are members of the transforming growth factor β (TGF-β) superfamily. BMPs are characterized by seven conserved cysteine residues, six of which form disulfide bonds and form a cysteine knot, while the seventh cysteine is involved in dimerization. Signals from extracellular BMP ligands are transduced through receptor serine-threonine kinases, which then regulate downstream gene expression. BMP ligands are secreted in their active form following proteolysis of the pro-domain and dimerization in the Golgi network (Bragdon et al. 2011). BMP ligands bind to type-I BMP receptors that exist in a receptor complex with type-II BMP receptors (Figure 1.3). Both type-I and type-II are receptor serine-threonine kinases, but only type-II receptors are constitutively active. BMP ligand binding to the receptor complex and subsequent recruitment of type-II receptors triggers the cross phosphorylation of type-I receptors by type-II receptors. Following cross phosphorylation and activation of type-I receptors, type-I receptors then phosphorylate and activate the receptor-activated SMADs (rSmads), Smad1/5/8. Phosphorylation of these rSmads triggers a conformational change that exposes the DNA binding domain and allows Smad1/5/8 to complex with the co-Smad, Smad4. Once this complex is formed, it translocates to the nucleus and regulates downstream gene expression either by directly binding DNA or through interactions with coactivators and corepressors. Once this signaling cascade occurs, inhibitory Smads (iSmads) smad6/7 are exported from the nucleus and exert negative feedback by competing for binding of type-I receptors, Smad4, and cofactors in the nucleus (Figure 1.3) (Nohe et al. 2004; Sieber et al. 2009).

In addition to negative regulation by the iSmads, BMP signaling can be regulated at many different steps in the signaling cascade. A BMP pseudoreceptor, BMP and activin membrane-bound protein (BAMBI) lacks the intracellular serine-threonine kinase domain. Without the intracellular kinase domain typical

of type-I receptors, BAMBI inhibits BMP signaling by sequestering BMP ligand away from functional receptors and by competing with type-I receptors to form a complex with type-II receptors (Nohe et al. 2004; Sieber et al. 2009). BMP signaling is also regulated extracellularly by secreted BMP inhibitors. Modulation of BMP signaling by these secreted diffusible inhibitors is arguably one of the most important forms of BMP regulation as these small molecules play a key role in shaping BMP gradients during early embryogenesis.

Secreted BMP antagonists are highly variable and are classified based on the number of conserved cysteine residues. Members of the differential screening-selected gene aberrative in neuroblastoma (DAN) family, which includes DAN, Cerberus, and Gremlin, most closely resemble TGF-β ligands with eight conserved cysteine residues. Twisted gastrulation (Tsg) is the only BMP antagonist with nine conserved cysteine residues. The Chordin family, which comprises multiple inhibitors known to play a crucial role in early embryogenesis including Chordin, Crossveinless2 (CV2), Ventroptin, and Noggin, is characterized by the presence of ten conserved cysteine residues. Follistatin, and other antagonists with Follistatin-like domains including Sparc related modular calcium binding 1 (Smoc1) and Smoc2 also contain ten conserved cysteine residues within the Follistatin domain, but the number of Follistatin domains in the proteins vary (Bragdon et al. 2011). Similar to TGF-β ligands, these conserved cysteine residues form disulfide bonds with the majority of disulfide bonds forming a cysteine knot. The remaining cysteine residues are thought to be involved in dimerization and other protein interactions (Bragdon et al. 2011; Rider & Mulloy 2010; Nolan et al. 2013). Most secreted BMP antagonists function in a similar manner with the exception of follistatin. While BMP antagonists including Chordin, Noggin, and Gremlin are secreted and sequester BMP ligands from their receptors, Follistatin binds the ligand and forms an inhibitory complex with the receptor (Balemans & Van Hul 2002; Iemura et al. 1998). Although Follistatin differs mechanistically from other antagonists, Follistatin together with Chordin and Noggin function during early development to establish the dorsoventral axis during gastrulation.

Spemann and Mangold first described the properties of an organizer in 1924 based on the ability of the organizer, when transplanted, to dorsalize and neuralize tissue, and induce the formation of a secondary axis (J. C. Smith & Slack 1983; De Robertis 2006). Although it was unknown at the time, the organizer establishes dorsal identity and allows for differentiation of neural tissue from ectoderm through the secretion of the BMP inhibitors Chordin, Noggin, and Follistatin. Chordin and Noggin were first identified using similar methods; these two BMP inhibitors were first identified in a differential screen using dorsalized embryos to identify dorsal specific transcripts capable of inducing a secondary axis when overexpressed (W. C. Smith & Harland 1992; Sasai et al. 1994). Follistatin was initially described based on it's inhibitory activity on follicle stimulating hormone secretion and was described as an inhibitor of the TGF- β ligand activin. Later work demonstrated that *follistatin* is expressed in the organizer, and like Noggin, has the ability to neuralize an embryo when overexpressed (Hemmati-Brivanlou et al. 1994).

During gastrulation, Chordin, Noggin, and Follistatin promote dorsal and neural fate by inhibiting BMP4. BMP4 levels are highest in the ventral portion of the embryo while Chordin, Noggin, and Follistatin levels are highest in the posterior of the embryo at the organizer. This apposition of a BMP4 gradient that is highest ventrally and a BMP inhibitor gradient highest dorsally further refines the BMP4 gradient so that regions with high BMP4 are specified as ventral and ectodermal and where BMP4 signaling is inhibited, dorsal and neural fates are induced. Loss of Chordin, Noggin, and Follistatin and BMP4 overexpression produces similar results where dorsal tissue and neurectoderm is lost while ventral tissues are expanded (Hammerschmidt et al. 1996; Khokha et al. 2005; Schmidt et al. 1995). Secreted BMP inhibitors are typically thought to refine BMP gradients through their inhibitory activity; however, secreted BMP antagonists have also been shown to enable gradient formation by preventing immediate high affinity ligand receptor binding and facilitating diffusion of BMP ligands away from their source (Umulis et al. 2009).

BMP signaling in eye development

BMP signaling is essential for many steps of eye development, and in particular, Gdf6 has been well established in humans, mice, and zebrafish to play a critical role. As mentioned previously, as the optic vesicle begins to evaginate, Bmp2 and Gdf6 from the lateral extraocular ectoderm diffuses to the lateral optic vesicle to specify the dorsal retina (Kruse-Bend et al. 2012). As eye development progresses, Bmp2, Bmp4, and Gdf6 begin to be expressed in the dorsal retina where Gdf6 has an antiapoptotic effect. As the eye enters the maintenance phase of DV patterning and these BMP ligands are found within the dorsal retina, Bmp4 is involved in regulating maintenance of dorsal gene expression (Veien et al. 2008; Behesti et al. 2006). Choroid fissure closure requires a precise balance of BMP signaling, with the loss of BMP ligands or the overexpression of ligands both resulting in coloboma (French et al. 2009; Heermann et al. 2015).

In addition to BMPs being required for fissure closure, Bmp7 is required for fissure formation. *Bmp7* null mice have either an anophthalmic or microphthalmic phenotype, where the microphthalmic eyes never form a choroid fissure and as a result do not develop hyaloid vasculature and RGC axons do not exit the eye. *Bmp7* null mutants also have a reduced number of apoptotic cells where the fissure would form, indicating that apoptosis regulated by Bmp7 is a necessary component of choroid fissure formation (Morcillo et al. 2006; Ozeki et al. 2000).

As the optic cup is forming, the spatially restricted expression of Bmp ligands that specify the dorsal retina appear to be necessary to distinguish between the dorsal and ventral ciliary marginal zone (CMZ) (Heermann et al. 2015). The CMZ is a region of the retina next to the lens that contains multipotent retinal progenitors (Centanin & Wittbrodt 2014). BMPs in the dorsal eye prevent streaming of cells into the dorsal CMZ, although the exact function of a polarized CMZ is still not known (Heermann et al. 2015). Later in development, after the eye has formed and as progenitors are being added to the eye from the CMZ, Gdf6 positively regulates cell proliferation by regulating expression of cell cycle regulators (French et al. 2013). Gdf6a is also involved in the differentiation of

blue cones and is required for photoreceptor maintenance (Duval et al. 2014; Asai-Coakwell et al. 2013).

Regulation of BMP signaling in eye development

The role of BMP signaling in vertebrate eye development has been thoroughly characterized, but far less is known about how BMP signaling is regulated during development. In zebrafish, Sfrps have a concentration dependent effect on BMP signaling. When Sfrps are present at low levels, as is seen in the developing eye, Sfrps facilitate BMP signaling, but when Sfrps are overexpressed, BMP signaling is inhibited (Holly et al. 2014). Another extracellular BMP inhibitor, *follistatin a* (*fsta*) is expressed within the developing zebrafish eye. BMP inhibition by Follistatin a is thought to be necessary to allow for epithelial flow from the presumptive RPE to the presumptive retina early in development and is believed to facilitate streaming of multipotent retinal progenitor cells to the ventral CMZ (Heermann et al. 2015). Although Fsta is likely involved in early eye morphogenesis, it is a poor candidate for patterning the DV retinal axis by inhibiting BMP signaling as *fsta* is expressed throughout the eye (Heermann et al. 2015).

In chick, Ventroptin has been identified as a BMP4 antagonist that restricted to the ventral retina. Ventroptin and BMP4 corepress expression of each other. As would be expected of a BMP inhibitor localized to the ventral retina, Ventroptin maintains ventral retinal identity by inhibiting *tbx5* expression and maintaining *vax2* expression. As has been observed with other cases of abnormal DV patterning, overexpression of *ventroptin* results in misprojected RGC axons and altered retinotectal mapping (Sakuta et al. 2001). Despite Ventroptin appearing as the perfect candidate to regulate DV retinal patterning, in zebrafish and mice, *ventroptin* is not expressed in the ventral retina. Furthermore, Ventroptin has been characterized as only being able to inhibit BMP4, when in zebrafish and mice, other BMPs including Gdf6 and Bmp2 are also essential for DV retinal patterning (Sakuta et al. 2001).

Purpose of study

BMP morphogen gradients are crucial for embryonic development, but what is perhaps as important is how BMP signaling is regulated. Extracellular BMP antagonists are an essential part of this regulatory network. Not only do BMP antagonists block BMP signaling and create a more defined BMP gradient, these antagonists have also been shown to be necessary for the formation of BMP gradients by sequestering BMP ligands from receptors and allowing for diffusion of these ligands to occur (Vuilleumier et al. 2010; Umulis et al. 2009). The necessity of these extracellular BMP inhibitors has been demonstrated in multiple model systems and for many developmental processes, yet the function of BMP inhibitors in vertebrate eye development and dorsoventral retinal patterning has not been thoroughly characterized.

Dorsal retinal identity is specified by the diffusion of Bmp2b and Gdf6a to the presumptive dorsal retina (Kruse-Bend et al. 2012; Gosse & Baier 2009; French et al. 2009). Shortly thereafter, DV patterning enters a maintenance phase where dorsal retinal identity is maintained by Wnt mediated regulation of localized expression of Bmp ligands within the dorsal retina (Veien et al. 2008). In mice and zebrafish, BMP signaling has been shown to be positively regulated by diffusible Sfrp proteins that appear to facilitate ligand diffusion in much the same way that BMP antagonists do at low concentrations (Holly et al. 2014; Esteve et al. 2011; Vuilleumier et al. 2010). Although in mice and zebrafish only facilitation of Bmp signaling during eye development has been described, previous work showing that the loss of Gdf6a results in complete ventralization of the retina suggests that dorsal and ventral retinal fate is finely balanced meaning that there should be some mechanism to negatively regulate Bmp signaling during eye development (French et al. 2009). Ventroptin, a BMP4 antagonist, has been described in chick as having this exact function; Ventroptin is localized to the ventral eye and is necessary to specify ventral retinal fate (Sakuta et al. 2001). Suprisingly, this function of Ventroptin appears to be limited to chick as Ventroptin is not found within the ventral retina of mice or zebrafish. Logically it follows that other Bmp antagonists in species other than chick have the same

function as Ventroptin, but to date, no other ventral retina specific BMP antagonist has been described.

The goal of this work is to determine if three putative BMP antagonists are involved in regulating ventral retinal identity and mediating other aspects of BMP directed eye morphogenesis. Two of these candidates, *sparc related modular calcium binding 1* (*smoc1*) and *smoc2* appear to have expression restricted to the ventral retina (Abouzeid et al. 2011; Mommaerts et al. 2014). Expression of the other candidate gene, *gremlin 2b* (*grem2b*), looks to be restricted to the periphery of the ventral retina and in the neural crest (Müller et al. 2006). These three candidate BMP inhibitors have mainly been studied through bioinformatic analyses and cell culture experiments, but little is known about their function in a developmental context. Based on the localized expression pattern of these three genes and knowing that inhibition of BMP signaling by Ventroptin is essential for eye development, it is hypothesized that either alone or in combination, these three BMP inhibitors modulate BMP signaling within the eye during early eye development, morphogenesis, and DV retinal patterning. To test this hypothesis, zebrafish were utilized as a model for vertebrate eye development. The role of Smoc1, Smoc2, and Grem2b in regulating ocular size, DV retinal patterning, and ocular BMP signaling was further elucidated using a loss of function approach with translation blocking morpholino oligonucleotides and a gain of function approach using mRNA overexpression. Together, these results show that inhibition of BMP signaling within the eye is regulated by ocular and extraocular sources of BMP antagonists, which appears to be necessary within the eye to regulate ocular size, optic stalk morphogenesis, and is involved in an unknown process in the choroid fissure.

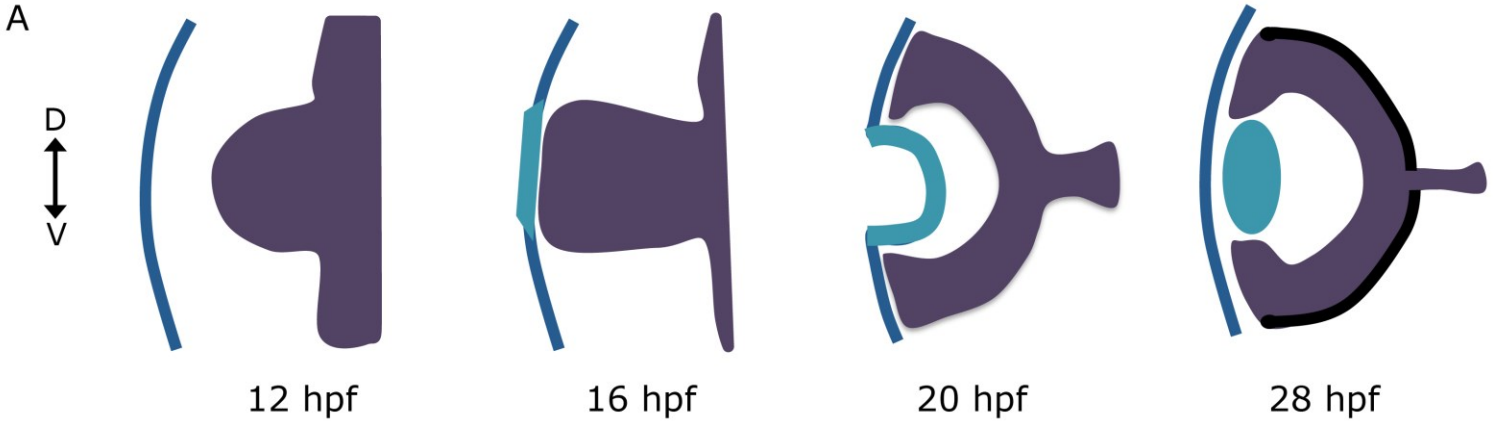
A
D
V
12 hpf
16 hpf
20 hpf
28 hpf

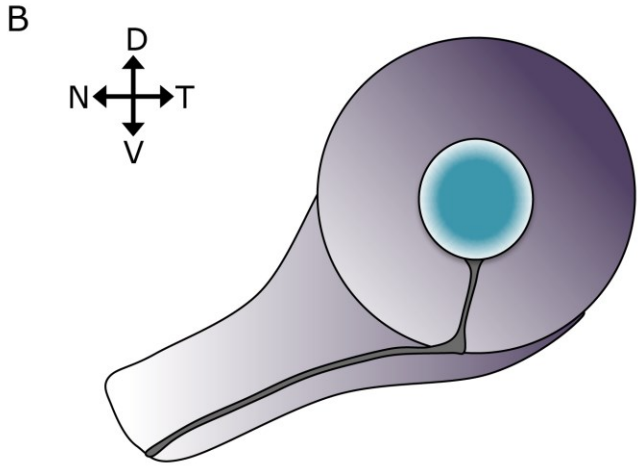
B
D
N
T
V

Figure 1.1: Vertebrate eye morphogenesis. (A) Diagrams showing cross sections of zebrafish eye morphogenesis at the indicated timepoints. By 12 hpf, the optic primordia (purple) have started evaginating from the diencephalon towards the overlying surface ectoderm (blue). Contact of the optic vesicle with the overlying ectoderm induces formation of the lens (turquoise) around 16 hpf and initiates transition of the optic vesicle to the bilayered optic cup. By 20 hpf, the lens has started to form and the bilayered optic cup continues to develop. At 28 hpf, the lens is fully formed and inner layer of the bilayered optic cup will become the retina, while the outer layer will become the RPE (black). (B) Diagram showing the location of the choroid fissure. The choroid fissure is a transient opening in the ventral region of the eye that is needed for RGC axon exit from the eye and for vascularization of the eye.

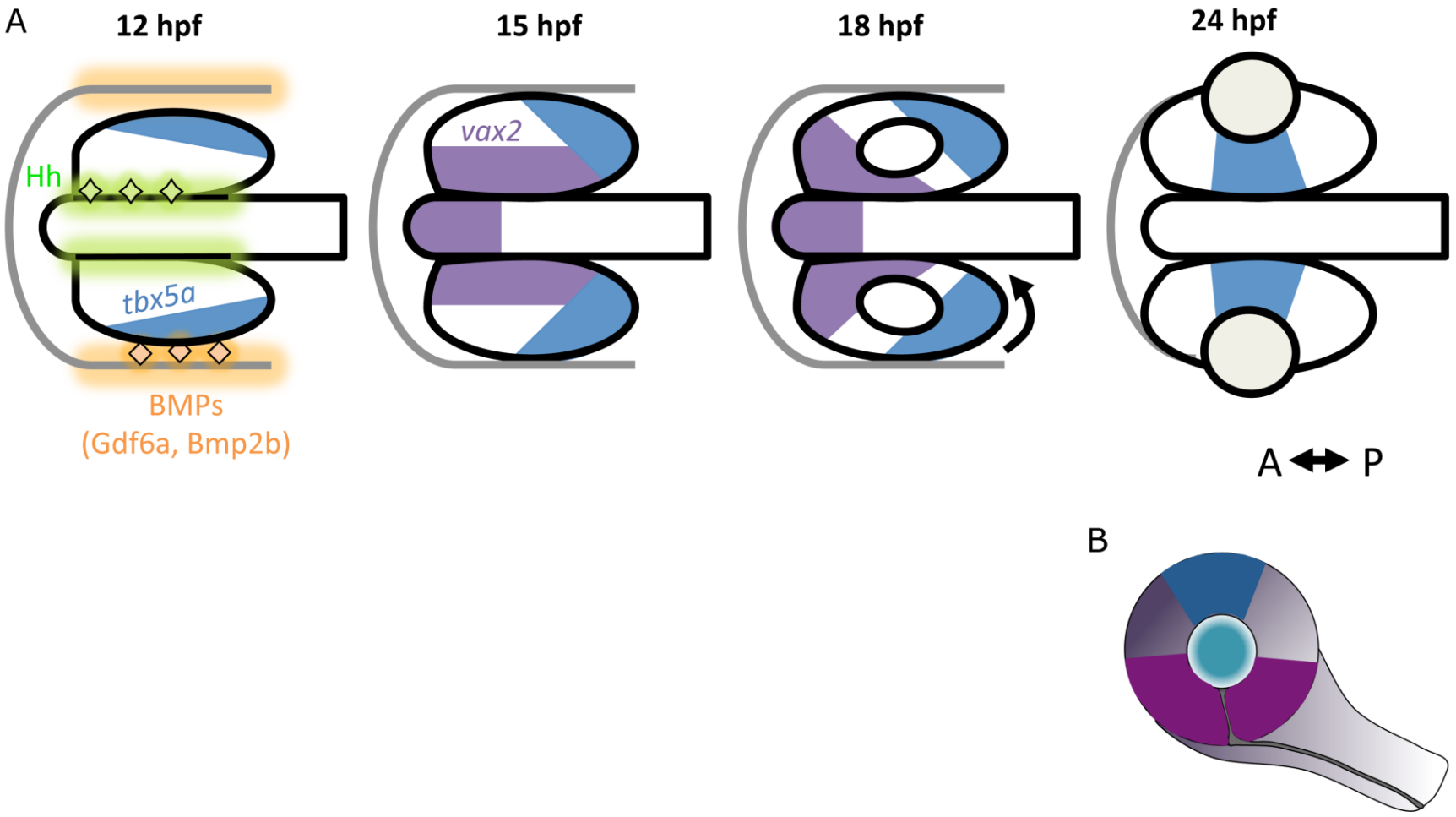
A
12 hpf
15 hpf
18 hpf
24 hpf
Hh
tbx5a
vax2
BMPs
(Gdf6a, Bmp2b)
A
P
B

Figure 1.2: Establishment of the dorsoventral (DV) retinal axis during eye development. (A) The DV axis is established early in development when the optic vesicles have completed evagination at 12 hpf. BMP ligands (orange) diffuse from overlying ectoderm to the lateral region of the developing eye to induce expression of *tbx5a* (blue) and specify the presumptive dorsal retina. Shortly after the dorsal retina has been specified, Hedgehog (Hh; green) diffuses from the midline to the medial optic vesicle to induce expression of *vax2* and specify the ventral retina. By 15 hpf, expression of *tbx5a* and *vax2* in the presumptive dorsal and ventral regions of the retina is apparent. The eye begins to rotate at 18 hpf and completes rotation at 24 hpf so that the lateral optic vesicle is repositioned to be dorsal and the medial optic vesicle is now ventral. (B) Frontal view of the eye at 24 hpf. By 24 hpf, *tbx5a* expression (blue) is restricted to the dorsal eye and *vax2* expression (purple) is restricted to the ventral eye.

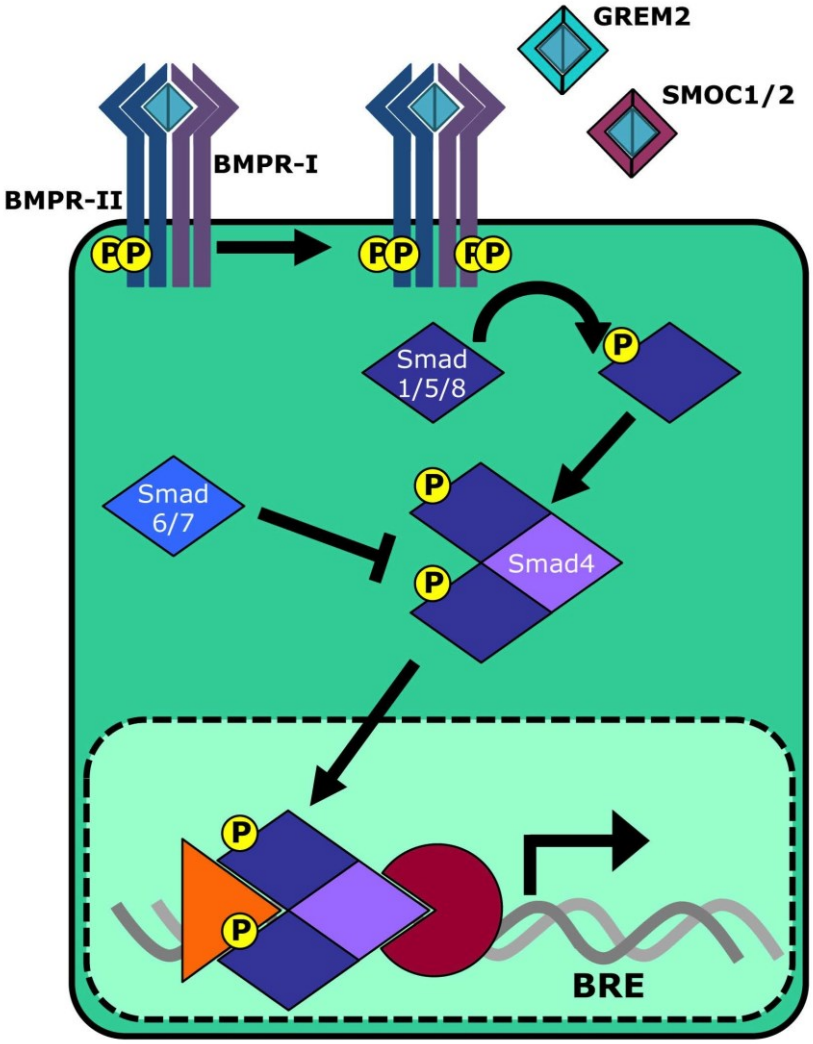

Figure 1.3: Bone morphogenetic protein (BMP) signaling pathway. Secreted and dimerized BMP ligands bind to type-1 BMP serine-threonine kinase receptors which recruits constitutively active type-II receptors to the complex and initiates cross phorphorylation by type-I receptors (BMPR-I) by type-II receptors (BMPR-II). Receptor Smads (rSmads), Smad1/5/8, interact with phosphorylated type-I receptors and are subsequently phosphorylated which enables Smad1/5/8 interaction with the co-Smad, Smad4, and translocation into the nucleus where Smads regulate gene expression by binding to BMP response elements (BRE) with coactivators or corepressors. The inhibitory Smads (iSmads), smad6/7, negatively regulate BMP signaling by competing with R-Smads for receptor and Smad4 binding.

Chapter 2

Materials & Methods

Zebrafish lines and maintenance

Work done with zebrafish embryos and adults was done as specified in (Westerfield 2007) and in accordance with the Canadian Council for Animal Care guidelines and approved by the University of Alberta Animal Care and Use Committee for Biosciences. All experiments were done on the AB strain of zebrafish, except for experiments using the *gdf6a*^{s327} (Gosse & Baier 2009) and *aldh1a3*^{sa118} (Kettleborough et al. 2013) mutant lines and experiments using the *Tg(BMPRE-AAV.Mlp:eGFP)* (Collery & Link 2011) and *Tg(12xRARE-ef1μ:eGFP)* (Waxman & Yelon 2011) transgenic lines.

Embryo manipulation and care

General

Embryos were grown in embryo medium (EM: 15 mM NaCl, 500 nM KCl, 1 mM CaCl2, 150 nM KH2PO4, 1 mM MgSO4, 715 nM NaHCO3) with 10 ml of Penicillin-Streptomycin (10 000 units penicillin, 10 mg/ml streptomycin; Sigma-Aldrich, St. Louis MO, USA) added per liter of embryo media. Embryos were incubated at 25-33°C and staged according to developmental landmarks described in (Kimmel et al. 1995). To block pigment formation, embryos that were used for *in situ* hybridization were raised in embryo media with 0.006% phenylthiourea (PTU) (Sigma-Aldrich, St. Louis MO, USA) starting at 22 hours post fertilization (hpf). Embryo media was changed every 24 hours. Embryos were manually dechorionated using Dumont #5 forceps.

Morpholino oligonucleotide preparation and injection

Translation blocking morpholino oligonucleotides (MOs) were designed by and ordered from Gene Tools, LLC (Philomath OR, USA) (Table 1). Lyophilized morpholinos were dissolved in sterile distilled water to a stock concentration of 10 mg/ml. Stock morpholinos were diluted to 1-4 mg/ml using Danieau buffer (58 mM NaCl, 0.7 mM KCl, 0.4 mM MgSO4, 0.6 mM Ca(NO3)2, 5 mM HEPES [4-(2-hydroxethyl)piperazine- 1-ethanesulfonic acid], pH 7.6). Prior to injection, MOs were heated to 65°C for 10 minutes and cooled to room temperature. Embryos were injected at the 1-4 cell stage with 1-4 nl (1-8 ng) of morpholino.

Dose was estimated based on known concentration and bolus size delivered by an ASI MPPI-2 Pressure Injector (Applied Scientific Instrumentation, Eugene OR, USA).

mRNA preparation and injection

Following synthesis and clean up, mRNA was stored at -80°C. Before injection, mRNA was thawed on ice and diluted to the appropriate working concentrations using nuclease free water. mRNA was injected directly into the cell of one-cell stage embryos using a ASI MPPI-2 Pressure Injector (Applied Scientific Instrumentation, Eugene OR, USA).

Isolation of genomic DNA

Genomic DNA was extracted using established protocols (Meeker et al. 2007). Embryos or fin clips were transferred to 0.2 ml PCR tubes and 50mM sodium hydroxide was added to each tube. For fin clips and single embryos, 50 µl of 50 mM sodium hydroxide was used, while 200 µl of 50 mM sodium hydroxide was used when extracting DNA from 20 or more embryos. PCR tubes were heated to 95 °C for 10 minutes for non-fixed embryos and 20 minutes for fin clips and fixed tissue. Tubes were then cooled to 4 °C and vortexed until the material was homogenized. The solution was neutralized by adding 1/10 volume of Tris-HCl pH 8 (5 µl for single embryos and fin clips, 20 µl for multiple embryos). Genomic DNA was stored at 4 °C.

PCR and Cloning

PCR

PCR reactions were done using either isolated genomic DNA or cDNA that had been synthesized from total RNA as a template. PCR reactions consisted of 2 µl of template DNA or cDNA, 2 µl each of 5 µM forward and reverse primers, 2 µl 10 mM dNTPs, 0.2 µl ExTaq, and sterile water to a final volume of 25 µl. The thermocycler program used consisted of an initial denaturation at 94°C for 3 minutes followed by 30-40 cycles of 94°C for 15 seconds, annealing 2-5°C below

the melting temperature of the primers for 25 seconds, and extension at 72°C for 1 minute/kilobase followed by a single 3 minute incubation at 72°C.

RNA extraction

RNA was extracted from 24 hours post fertilization (hpf) to 48 hpf embryos using the RNAqueous®-4PCR Total RNA Isolation Kit (Life Technologies Inc., Burlington ON, Canada). Before starting RNA extraction, 70 µl of elution buffer for each sample was preheated to 70°C. 20-60 embryos were dechorionated and homogenized by vortexing in 350 µl of lysis/binding solution. 350 µl of 64% ethanol was added to the homogenized embryos, the solution was mixed, and the entire contents were added to a filter cartridge. The filter cartridge was placed in a collection tube and centrifuged for 1 minute at 14 800 rpm and the flow through was discarded. Filter cartridges were rinsed with 700 µl of Wash Solution1 and twice with 500 µl of Wash Solution 2/3. After each rinse step, filter cartridges were centrifuged for 1 minute at 14 800 rpm and the flow through was discarded. After rinsing, the filter cartridges were transferred to clean RNase free tubes. RNA was eluted from filter cartridges using Elution Solution heated to 70 °C. Elution was done in two steps: 40 µl of Elution Solution was added to filter cartridges and filter cartridges were centrifuged for 30 seconds at 14 800 rpm followed by adding 30 µl of Elution Solution to the filter cartridges and centrifuging for another 30 seconds. DNA was removed from isolated RNA by adding 1 µl of DNase I, 10 µl of 10x DNase I Buffer, and 19 µl of diethylpyrocarbonate (DEPC) treated water to each tube of RNA followed by incubation at 37 °C for 30 minutes. Following isolation and DNA removal, RNA was stored at -80 °C.

cDNA synthesis

cDNA was synthesized using Superscript III® Reverse Transcriptase (Life Technologies Inc., Burlington ON, Canada). Reactions were set up on ice in PCR tubes by adding 4 µl RNA, 1 µl oligo dT, 1 µl dNTPs, and 4 µl DEPC treated water. Reactions were heated to 65°C for 5 minutes and cooled for 1 minute on ice.

Following cooling, 2 µl of 10x RT buffer, 4 µl 25mM $MgCl_2$, 2 µl 0.1M DTT, 1 µl RNase OUT, and 1 µl of Superscript III RT was added to each tube and incubated for 1 hour at 50°C. Reactions were heat killed by incubating at 85°C for 5 minutes followed by a 5 minute ice incubation. Remaining RNA was removed by adding 1 µl of RNase H and incubating at 37°C for 20 minutes. cDNA was stored at -20°C.

One-Step RT-PCR

The Superscript III® One-Step RT-PCR System with Platinum® Taq Polymerase (Life Technologies Inc., Burlington ON, Canada) was used to amplify PCR products directly from total RNA. Each reaction consisted of 12.5 µl 2x Reaction mix, 1 µl of Superscript III® RT/Platinum ® Taq Mix, 1 µl of 5 µM forward and reverse primers, 1 µl of total RNA, and 9.5 µl of DEPC treated water. Reactions were incubated for 30 minutes at 54 °C then denatured at 94°C for 2 minutes followed by 40 cycles of 94°C for 15 seconds, annealing 2-5°C below the melting temperature of the primers for 30 seconds, and extension at 68°C for 1 minute/kilobase. A final extension was done at 68°C for 5 minutes. RT-PCR products were run on an agarose gel and the appropriate sized band was gel extracted.

TOPO Cloning and transformation

TOPO®-TA cloning was used for the ligation of blunt ended PCR products. For inserts used as a template for riboprobe synthesis, pCR®4-TOPO® TA vector (Life Technologies Inc., Burlington ON, Canada) was used. The pCR®2.1-TOPO® vector was used for all other purposes. PCR products were run on a 1% agarose gel and gel extracted using a QIAquick Gel Extraction Kit (Qiagen, Hilden Germany) as per the manufacturer's instructions. For PCR products amplified with a non-proofreading Taq that adds 3' adenine overhangs, undiluted gel extracted PCR product was used for the TOPO®TA ligation. For PCR products amplified using a proofreading polymerase, 3' adenine overhangs were added after gel purification using ExTaq (TaKaRa, Japan). In a PCR tube, 16 µl of gel extracted PCR product was added with 2 µl 10x ExTaq buffer, 1 µl 10 mM dNTPs, and 1 µl of ExTaq. The reaction was incubated for 10 minutes at 72°C and purified

using the GeneJET PCR Purification Kit (ThermoFisher, Waltham MA, USA). Each ligation consisted of 2 μl of purified PCR product, 0.5 μl salt solution, and 0.25 μl of either pCR®4-TOPO® or pCR®2.1-TOPO® vector. Reactions were incubated for 5 minutes at room temperature and the entire ligation was added to 20-50 μl of One-Shot® Top10 chemically competent *E. coli* (Life Technologies Inc., Burlington ON, Canada). The transformation mixture was left on ice for 20 minutes followed by a 45 second heat shock at 42°C and a 5 minute incubation on ice. Next, 250 μl of super optimal broth with catabolite repression (SOC: 2% bacto tryptone, 0.5% bacto yeast extract, 10 mM NaCl, 2.5 mM KCl, 10 mM MgCl2, 10 mM MgSO4, 20 mM glucose) was added to the cells and the cells were incubated for one hour at 37°C. Following incubation, cells were plated on Luria broth agar plates (LB: 1% bacto tryptone, 0.5% bacto yeast extract, 0.17 M NaCl, 1.5% bacto agar, pH 7) containing the appropriate antibiotic. Plates were incubated overnight at 37°C. Single colonies were picked and used to inoculate liquid LB containing the appropriate antibiotic and incubated for 16-18 hours at 37°C. Plasmid DNA was isolated from the liquid culture using the Qiaprep Spin Miniprep Kit (Qiagen, Hilden, Germany). Plasmids were then sequenced to verify that the correct insert was cloned.

Sequencing

Sequencing reactions were done using the BigDye Terminator v3.1 Cycle Sequencing Kit (Life Technologies Inc., Burlington ON, Canada). Reactions consisted of 2 μl 10x BigDye premix, 3 μl 5x buffer, 300 ng template plasmid DNA, 1 μl 5 μM sequencing primer, with sterile water to a final volume of 20 μl. Template was denatured by incubating the reaction at 96°C for 2 minutes followed by 25 cycles of 96°C for 30 seconds, 50°C for 15 seconds, 60°C for 1.5 minutes. The reaction was then incubated for 5 minutes at 60°C.
Sequencing reactions were purified by adding 2 μl 1.5M NaOAc/250 mM EDTA to the reaction followed by 80 μl of 95% ethanol. The reaction was mixed, cooled to -20°C for 30 minutes, then centrifuged at >14 000 xg for 10 minutes at 4°C. The supernatant was removed and the pellet was washed with 500 μl 70% ethanol and centrifuged again. The supernatant was removed and the pellet was dried.

Sequencing reactions were submitted to the Molecular Biology Service Unit at the University of Alberta.

Overexpression constructs

Primer and construct design

The *smoc1* coding sequence (CDS) was synthesized and inserted into pUC57-Kan by Genscript (Piscataway, NJ, USA). The 5' end of the *smoc1* CDS is preceded by a BamHI site (5'-GGATCC-3') followed by a Kozak sequence (5'-GCCGCCACC-3') while the 3' end of the *smoc1* CDS is followed by an XbaI site (5'-TCTAGA-3'). The *smoc1* CDS was codon optimized by Genscript to prevent any frameshift elements, remove stem-loop structures that would prevent translation, optimize GC content, and maximize the stability of the transcript (Figure 2.1).

Primers for *smoc2* and *gremlin2* overexpression constructs were designed to amplify the entire coding sequence. The forward primer consisted of a 6 bp stuffer sequence, a BamHI site (5'-GGATCC-3'), and a Kozak sequence (5'-GCCGCCACC-3') followed by the first 22 bp of coding sequence. The reverse primers consisted of a 6 bp stuffer sequence and an XbaI site (5'-TCTAGA-3') followed by the last 22 bp of coding sequence (Table 2.2). Primers were used to amplify the coding sequence from 24 hpf total RNA using the Superscript III® One-Step RT-PCR System With Platinum® *Taq* DNA Polymerase kit (Life Technologies Inc., Burlington ON, Canada). PCR products were run on a 1% agarose gel and the bands corresponding to the size of the CDS were gel purified using the QIAquick Gel Extraction Kit (Qiagen, Hilden, Germany) as per the manufacturer's instructions. PCR products were eluted using 30μl of sterile water.

Restriction digests

The *smoc1* CDS and Kozak sequence were subcloned into pCS2+ by digesting smoc1-pUC57-Kan with BamHI and XbaI and gel extracting the appropriate sized fragment. The insert was ligated into pCS2+ that had also been digested with BamHI and XbaI. For *smoc2* and *grem2*, 25 μl of gel extracted PCR product was digested with BamHI and XbaI and ligated into pCS2+ that had been

digested with BamHI and XbaI. Ligation reactions were done with 25 ng of linearized pCS2+ and the corresponding volumes of insert for 3:1 and 5:1 molar ratios with 1 µl 10x T4 DNA ligase buffer, 1 µl ATP, 1 µl T4 DNA ligase (New England Biolabs, Ipwich, MA, USA), and sterile water to a final volume of 10 µl. Reactions were incubated overnight at 16°C and 5 µl of the reaction was transformed into 25-50 µl of One-Shot® Top10 chemically competent *E. coli* (Life Technologies Inc., Burlington ON, Canada). Colonies containing inserts of the correct size were identified using colony PCR with the universal SP6 primer and pCS2+ specific T7 primer. Following identification of insert containing colonies, plasmid DNA was isolated from these colonies and sequenced using the SP6 and T7 (pCS2+) primers.

In vitro mRNA synthesis

NotI was used to linearize overexpression constructs that had been ligated into pCS2+. Following linearization, RNase removal was done by adding DEPC treated water to the completed linearization reaction to a total volume of 50 µl. Next, 2.5 µl of 10% sodium dodecyl sulphate (SDS) and 2 µl of 10 mg/ml Proteinase K was added and incubated for one hour at 50°C. Following incubation, 50 µl of DEPC treated water and 10 µl of 3M sodium acetate pH 5.3 was added to the tube and mixed. After mixing, 85.5 µl of DEPC treated water was added to bring the final volume to 200 µl.

Linearized, RNase free construct was purified using a phenol-chloroform extraction. 200 µl of phenol:chloroform:isoamyl alcohol (25:24:1) was added to the reaction. The tube was vortexed for 20 seconds and centrifuged for 5 minutes at 14 800 rpm. The upper layer of liquid was transferred to an RNase free tube and 200 µl of chloroform was added to the mixture. The tube was vortexed for 20 seconds, centrifuged for 5 minutes at 14 800 rpm, and the upper layer of liquid was transferred to 1.5 ml RNase free tube. DNA was precipitated by adding 600 µl of 100% RNase free ethanol and incubating at -20°C for at least 20 minutes. The sample was centrifuged for 15 minutes at 14 800 rpm at 4°C. The liquid was removed from the tube, the pellet was washed with 100 µl of 70% RNase free

ethanol, and the sample was centrifuged for 10 minutes at 14 800 rpm at 4°C. Following centrifugation, liquid was removed and the DNA pellet was dried. The pellet was resuspended in 15 μl of DEPC treated water.

Capped mRNA was transcribed from linearized overexpression constructs using the SP6 mMessage mMachine® kit (Life Technologies Inc., Burlington ON, Canada). Each reaction consisted of 2 μg of linearized DNA, 10 μl 2x NTP/CAP, 2 μl 10x SP6 reaction buffer, 2 μl SP6 enzyme mix, and DEPC treated water to a final volume of 20 μl. Reactions were incubated for 2 hours at 37 °C and DNA template was removed by adding 1 μl of TURBO™ DNase for 10 minutes at 37 °C. Synthesized mRNA was purified using Amicon Ultra-0.5 ml Centrifugal Filters (Millipore, Billerica MA, USA). Reactions were topped up to a total volume of 500 μl by adding 480 μl of DEPC treated water. The liquid was transferred to a column placed in a collection tube and centrifuged for 4 minutes at 14 000 xg. The column was then inverted, transferred to a clean collection tube, and centrifuged for 3 minutes at 1000 xg. The liquid in the collection tube was topped up to a total volume of 500 μl with 480 μl of DEPC treated water. The columns were centrifuged again as described above and the purified mRNA remaining after inverting the column and centrifuging was diluted to the appropriate concentration and stored at -80°C.

In situ hybridization

Digoxigenin labeled riboprobe synthesis

Antisense digoxigenin (DIG) riboprobes were synthesized from total RNA using the Superscript III Reverse Transcriptase One-Step RT-PCR kit (Life Technologies Inc., Burlington ON, Canada) as described above. For all probes, the reverse primer had a T7 RNA polymerase binding site (5'-TAATACGACTCACTATAGGG -3') at the 5' end of the primer (Table 2.3). Primers were designed to amplify the 3' UTR and generate a 800-1200 bp product, if possible. For plasmid based riboprobe synthesis, the PCR product was TOPO cloned and linearized at the 5' end of the insert before riboprobe synthesis (Table 2.4). The riboprobe synthesis reaction was set up by adding 10 μl (~400 ng) of gel

extracted PCR product or linearized plasmid to 2 µl 10x Transcription buffer (Roche Applied Sciences, Penzberg, Germany), 2 µl 10x DIG RNA labeling mix (Roche Applied Sciences, Penzberg, Germany), 1 µl T7 RNA polymerase (Roche Applied Sciences, Penzberg, Germany), RNase-OUT™ Recombinant Ribonuclease Inhibitor (Life Technologies Inc., Burlington ON, Canada). DEPC treated water was added to a final volume of 20 µl. Reactions were incubated at 37°C. After the first hour of incubation 1 µl of T7 RNA polymerase was added and the reactions were incubated for another hour. Riboprobe synthesis was stopped by adding 2 µl 0.2 M EDTA.

Synthesized riboprobes were purified using SigmaSpin™ Post-Reaction Clean-Up Columns (Sigma-Aldrich, St. Louis MO, USA). Columns were placed in 2 ml collection tubes and centrifuged for 2 minutes at 2500 rpm. The end of the column was broken off and the columns were centrifuged for another 2 minutes at 2500 rpm. The column was transferred to a clean tube and the riboprobe synthesis contents were added to the column. The column was then centrifuged for 4 minutes at 2500 rpm. Following purification, 0.5 µl RNase-OUT was added to the riboprobe.

Whole Mount mRNA *In Situ* Hybridization (ISH)

The described protocol is based on previously described methods (C. Thisse & B. Thisse 2008). All washes were done on a shaker and at room temperature unless otherwise specified. Embryos were fixed in 4% paraformaldehyde (PFA) in phosphate buffered saline (PBS: 137 mM NaCl, 2.7 mM KCl, 10 mM Na2HPO4, 1.8 mM KH2PO4, pH 7.4) overnight at 4°C. Embryos older than 2 dpf were anesthetized in 0.0168% ethyl 3-aminobenzoate methanesulfonate (MS-222) (Sigma-Aldrich, St. Louis MO, USA) before fixation. Embryos were rinsed out of fixative by rinsing in PBST (PBS + 0.1% Tween 20) 5 x 5 minutes. For long-term storage (>5 days) or to further permeabilize embryos, embryos were transferred to 100% methanol/0.1% Tween 20 and stored at -20°C. Embryos were rehydrated in successive 5 minute rinses of 75% methanol/25% PBST, 50% methanol/50% PBST, 25% methanol/75% PBST followed by 5 x 5

minute PBST washes. Permeabilization was done with 10 μg/ml proteinase K. Permeabilization times varied with embryonic stage as follows: 10-14 somites (1 minute), 19-22 hpf (3 minutes), 24-32 hpf (5 minutes), 48 hpf (40 minutes), 4 dpf (1.5 hours). Following permeabilization, embryos were re-fixed in 4% PFA for 20 minutes. Embryos were rinsed 4 x 5 minutes in PBST. Pre-hybridization was done for at least one hour at 65°C in 500 μl in hybridization solution (hyb: 50% formamide, 5X SSC [saline sodium citrate buffer], 50 μg/ml heparin, 0.1% Tween-20, 0.092 M citric acid in sterile water) with 500 μg/ml yeast tRNA (hyb + tRNA). Hybridization was done for 16-40 hours at 65°C using riboprobes diluted in hyb + tRNA 1:50-1:200.

All rinses used 1 ml of liquid unless otherwise specified. Following hybridization, embryos were rinsed in successive five minute washes at 65°C of 66% hyb/33% 2x SSC, 33% hyb/66% 2xSSC, 2x SSC. Embryos were then rinsed at 65°C for 20 minutes in 0.2x SSC/0.1% Tween-20 follwed by two 20 minute washes in 0.1x SSC/0.1% Tween-20. Embryos were washed for 5 minutes each in 66% 2x SSC/33% PBST, 33% 2x SSC/66% PBST, and PBST. Blocking solution (2% sheep serum and 2 mg/ml bovine serum albumin [BSA] in PBST) was added and left to block for at least one hour. Embryos were then incubated for 2 hours at room temperature or at 4°C overnight in Anti-Digoxigenin-AP Fab fragments (Roche Applied Science, Penzberg, Germany) diluted 1:5000 in blocking solution. Embryos were then rinsed 5 x 15 minutes with PBST.

For the coloration reaction, embryos were rinsed 4 x 5 minutes in coloration buffer (100 mM Tris-HCl pH 9.5, 50 mM MgCl2, 100 mM NaCl and 0.1% Tween-20 in sterile water). The coloration reaction was done by incubating embryos in the dark at room temperature in coloration buffer with 0.45 mg/ml nitro blue tetrazolium chloride (NBT) and 0.175 mg/ml 5-bromo-4-chloro-3-indolyl-phosphate (BCIP). The coloration reaction was stopped by two rinses in 100% methanol/0.1% Tween-20 followed by a minimum 10 minute rinse in 100% methanol/0.1% Tween-20. Prior to photographing or further manipulation, embryos were rehydrated as described above.

Microscopy

An Olympus SZX12 stereomicroscope (Olympus, Richmond Hill ON, Canada) with a Micropublisher 5.0 RTV camera was used to photograph whole embryos using QCapture Suite PLUS Software v3.3.1.10 (QImaging, Surrey BC, Canada). For dorsal views or dissected eyes, embryos were run through 30% glycerol/70% PBST, 50%glycerol/50% PBST, and 70% glycerol/30% PBST. Embryos were dissected off of the yolk and the eyes were removed and mounted in 70% glycerol/30% PBST. Photographs were taken using a Zeiss AxioImager.Z1 compound microscope using an AxioCam HRm camera and Axiovision SE64 Rel.4.8 software (Zeiss, Oberkochen, Germany). For frontal views of embryos, embryos were mounted in a drop of 1% UltraPure™ low melting point agarose (Life Technologies, Burlington ON, Canada) on a 30 mm Petri Dish and covered with 1x PBS. Embryos were imaged using a 20x dipping lens with the same microscope configuration as for dissected embryos as described above.

Eye measurements

Live embryos were imaged at 48 or 72 hpf using an Olympus SZX12 stereomicroscope (Olympus, Richmond Hill ON, Canada) with a Micropublisher 5.0 RTV camera was used to photograph whole embryos using QCapture Suite PLUS Software v3.3.1.10 (QImaging, Surrey BC, Canada). All images were taken at the same magnification. Eye area was measured using ImageJ software (National Institutes of Health, Bethesda MD, USA). Statistical analysis was done using student's t-tests for two categories and ANOVA for three categories.

Aldh1a3 genotyping

The *aldh1a3*^{sa118} mutant allele was generated through an ENU mutagenesis screen carried out by the Sanger Centre as part of the Zebrafish Mutation Project (Kettleborough et al. 2013). The mutant allele has a G to A transition at the 264th nucleotide within the third exon that results in a stop codon at codon 88, resulting in a severely truncated protein (Figure 2.3). Cleaved amplified polymorphism (CAPs) PCR using ExTaq (TaKaRa, Japan) was used with DNA extracted from finclips or individual embryos (Table 2.5) (Neff et al. 2002). The

PCR program consisted of an initial denaturation at 94°C for 2 minutes followed by 40 cycles of 94°C for 15 seconds, 62°C for 25 seconds, 72°C for 3 minutes followed by a final extension at 72°C for 3 minutes. Following PCR, 10 μl of PCR product was digested with Tsp45I (New England Biolabs, Ipwich, MA, USA) at 65°C for 2-4 hours for heterozygotes and for 8 hours to identify homozygotes or with NmuCI (ThermoFisher, Waltham MA, USA) at 37°C for 2 hours. Digested PCR products were ran on a 2% agarose gel. The wild-type allele produces a 253 bp band while the mutant allele produces 96 and 154 bp bands.

Table 2.1: translation blocking morpholino oligonucleotides used.

Gene	Sequence (5'-3')
grem2	CACAGCGCCACCTTACTGCTCATCC
p53	GCGCCATTGCTTTGCAAGAATTG
smoc1	CACATAAATGAAGCGATGAGGGCAT
smoc2	GCAGCAGCAGCACCGATACGCGCAT

Table 2.2: Primers used to amplify the Grem2b and Smoc2 coding sequences to generate overexpression constructs.

Gene	Name	Sequence (5'-3')	Tm (°C)	size (bp)
grem2	grem2 OE F	ACGTTAGGATCCGCCGCCACCATGAGCAGTAAGGTGGCGCTGT	65.5	534
	grem2 OE R	ACGTTATCTAGATCACTGTTTCCCCGACTCGGAC	67.9	
smoc2	smoc2 OE F	ACGTTAGGATCCGCCGCCACCATGCGCGTATCGGTGCTGCTGC	76.2	1347
	smoc2 OE R	ACGTTATCTAGATTAGCCTTGTTTCTTTGACAGG	58.6	


input
optimized

Figure 2.1: Sequence alignment of the zebrafish smoc1 coding sequence (input) with the codon optimized sequence synthesized by Genscript (optimized). Unshaded regions indicate changes in sequence between the input and optimized sequence.

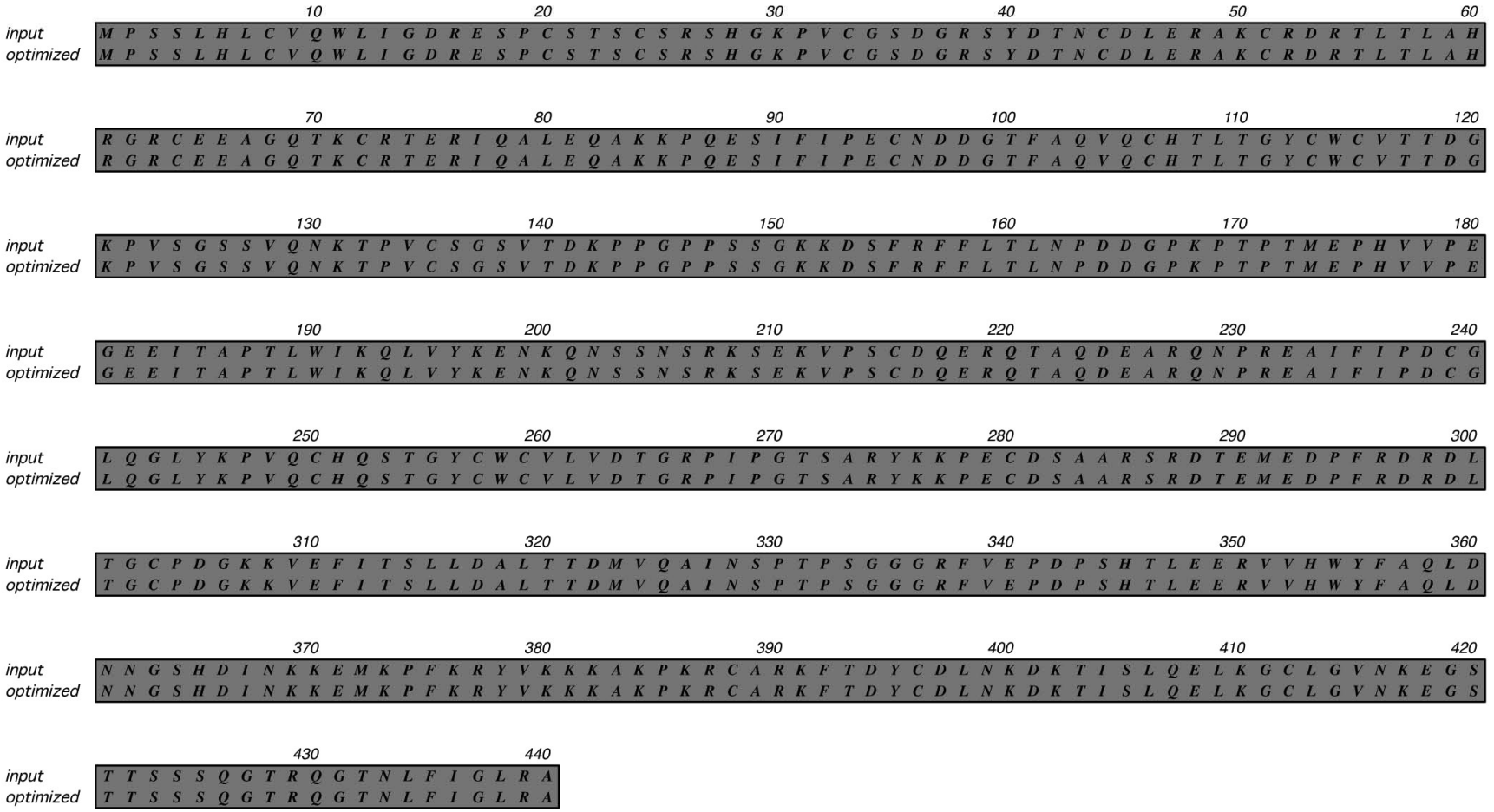

Figure 2.2: Amino acid alignment of the *smoc1* input sequence with the codon optimized output sequenced used to generate a *smoc1* overexpression construct.

Table 2.3: Primers used to generate templates for riboprobe synthesis.The T7 RNA polymerase binding site (italics) was added to the end of all primers. The melting temperature for each primer was determined without the T7 site. Asterisks indicate primers designed and probes synthesized by the author.

Gene	Name	Sequence (5'-3')	Tm (°C)	Size (bp)
eya2		ATGCGAGCTTACGGACAG		1000
		*TAATACGACTCACTATAGGG*GTTCTTGTATGTGTTGTAGATCTCTTTA		
grem2b*	pGREM2 F	TCCATGGGCTTCTTCATCATC	62.3	701
	pGREM2 R+T7	*TAATACGACTCACTATAGGG*GTGTTGTGGTAATCAGTCTTTGTG	58.6	
smoc1*	pSMOC1 F	TTCAGACGGACGCAGTTATG	59.9	846
	pSMOC1 R+T7	*TAATACGACTCACTATAGGG*CTTGCAGAGGTTCCAGGTATAG	58	
smoc2*	pSMOC2 F	CCATGCAGTAACTGACCCA	62	793
	pSMOC2 R+T7	*TAATACGACTCACTATAGGG*CCATGTGTGGTACAGGACTATAA	62	
tbx5a*	pTBX5A F	GTCACGTCTTACCAAAACCACA	60	899
	pTBX5A R+T7	*TAATACGACTCACTATAGGG*GACATGTGTGATGTGTCCAGTG	60	
vax2*	pVAX2 F	ACAGGAACGAACTTCGCTAGAC	60	1030
	pVAX2 R+T7	*TAATACGACTCACTATAGGG*GATTACAGGAGCGCTTTTAGGA	60	

Table 2.4: Information for plasmid-based riboprobes used in this study**.**

Gene	Vector	Linearize	RNA Polymerase
aldh1a2	pSPORT	EcoRI	Sp6
aldh1a3	pCR4-TOPO	NotI	T3
eGFP		NotI	T3

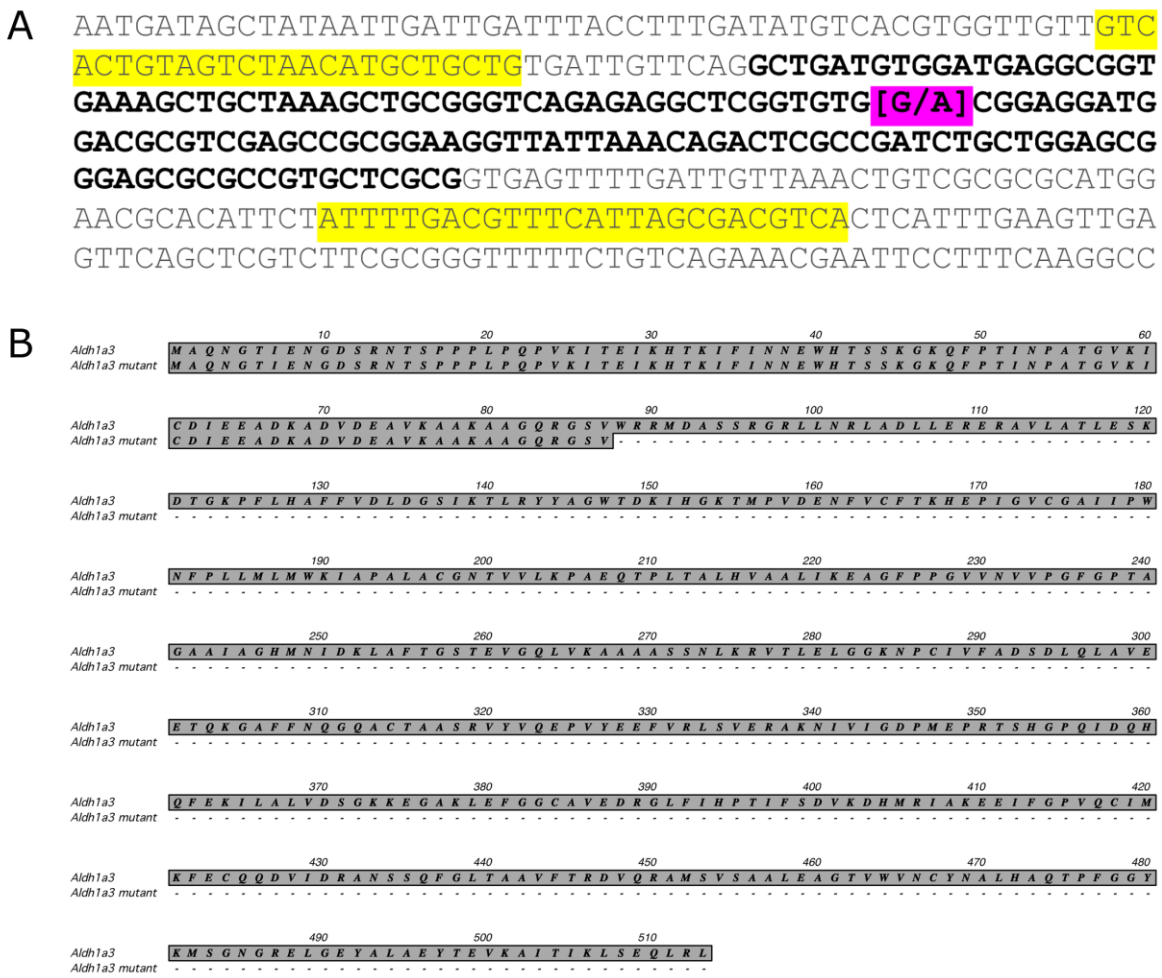

Figure 2.3: The *aldh1a3*^{sa118} mutant allele results in a severely truncated protein. (A) The G to A substitution (purple) that causes a premature stop codon is found within the third exon (bold). The primers, found in the surrounding introns, are highlighted yellow. (B) Amino acid alignment showing full length Aldh1a3 protein (top) and the truncated protein that results from the premature stop codon in the *aldh1a3*^{sa118} mutant allele (bottom).

Table 2.5: Primers used for *aldh1a3* genotyping.

Gene	Primer	Sequence (5'-3')	Tm(°C)	Size (bp)
aldh1a3	Forward	GTCACTGTAGTCTAACATGCTGCTG	60.4	253
	Reverse	TGAGCTCGCTAATGAAACGTCAAAAT	66	

Chapter 3

Investigating the role of Smoc1 and Smoc2 in vertebrate eye development

Introduction

During embryonic development, patterning typically occurs through morphogen gradients that can be modified by the opposing gradient of an antagonist. Patterning the eye axis is no different; the dorsoventral (DV) axis is patterned by a gradient of bone morphogenetic proteins (BMPs) originating from the extraocular ectoderm and later the dorsal retina (Kruse-Bend et al. 2012; French et al. 2009; Gosse & Baier 2009). Since BMPs form a gradient that is high in the dorsal and low in the ventral retina, it is expected that an opposing gradient of a BMP antagonist is needed to specify the ventral eye. One such inhibitor is Ventroptin, which in chicks is restricted to the ventral retina and is required for DV retinal patterning; however, in other vertebrates, Ventroptin is not expressed in the ventral retina (Sakuta et al. 2001). One BMP antagonist, SPARC related modular calcium binding 1 (Smoc1) has been reported to show restricted expression in the ventral eye in mice, zebrafish, and *Xenopus*, but the function of Smoc1 and its paralog, Smoc2, have yet to be characterized (Abouzeid et al. 2011; Okada et al. 2011).

Smoc1 was first identified in a cDNA library screen for its similarity to secreted protein acidic and rich in cysteine (SPARC) (Vannahme et al. 2002). Smoc2 was subsequently identified when screening for a potential Smoc1 paralog (Vannahme et al. 2003). Smoc1 and Smoc2 have four characteristic domains: a follistatin domain, two thyroglobulin domains, an EF-Hand calcium binding domain, and one domain unique to Smoc proteins (Figure 3.1 A, Figure 3.2 A) (Vannahme et al. 2002; Vannahme et al. 2003). The follistatin domain is thought to potentially confer TGF-β binding capabilities similar to follistatin while the thyroglobulin domains are likely necessary for interactions with extracellular matrix (ECM) proteins (Novinec et al. 2008). The EF-Hand calcium binding domain affects protein conformation and binding with ECM components in a calcium dependent manner (Vannahme et al. 2002; Vannahme et al. 2003; Novinec et al. 2008).

Little work has been done to determine if Smoc1 or Smoc2 binds TGF-β ligands and if these potential interactions have the ability to inhibit or facilitate

BMP signaling. The *Drosophila* ortholog of Smoc1, Pentagone, facilitates diffusion of Decapentaplegic (Dpp), the *Drosophila* BMP4 ortholog, across the wing disc and is essential for forming a Dpp gradient across the entire wing disc (Vuilleumier et al. 2010). Work in *Xenopus* has shown that overexpression of *Smoc1* dorsalizes the embryo, a phenotype that would be expected from the loss of BMPs or overexpression of an antagonist while a reduction in Smoc1 results in mild ventralization. Work in *Xenopus* has also shown that co-overexpression of *smoc1* with *bmp2* rescues the ventralized phenotypes caused by *bmp2* overexpression implying that there is a direct inhibitory interaction between Smoc1 and Bmp2. BMP antagonistic properties of Smoc1 were further tested in *Xenopus* animal cap explants by demonstrating that co-overexpression of *smoc1* and *bmp2* abrogates expression of the Bmp2 responsive gene *VENT homeobox 1 gene 2* (*Xvent-1*) when compared to overexpression of *bmp2* alone (Thomas et al. 2009). Smoc1 inhibitory activity appears to be restricted to BMP ligands as co-overexpression of *smoc1* with *activin* was not able to rescue Activin induced overexpression of *brachyury* (*bra*) in animal cap explants. Interestingly, a reduction in Smoc1 levels also resulted in anophthalmia, a phenotype that has been also observed in humans (Thomas et al. 2009).

Several studies have associated mutations in *SMOC1* with Waardenburg anophthalmia, a syndrome characterized by limb defects and eye defects that range from microphthalmia to true anophthalmia (Okada et al. 2011; Abouzeid et al. 2011; Gerth-Kahlert et al. 2013; Rainger et al. 2011). The associative mutations in *SMOC1* that have been identified are diverse and span the entire gene, with no apparent correlation between the location of the mutation and the phenotype (Slavotinek 2011; Rainger et al. 2011). In mice, *Smoc1* mutants do not have as severe of a phenotype as has been seen in humans but still includes microphthalmia in addition to coloboma and RPE defects (Okada et al. 2011; Rainger et al. 2011). Even less is known about Smoc2. One of the only studies on Smoc2 in development has linked Smoc2 to hematopoiesis in zebrafish (Mommaerts et al. 2014). Humans with mutations in *SMOC2* have dental malformations but no eye defects were observed (Bloch-Zupan et al. 2011).

Surprisingly, although there is a clear link between *Smoc1* and eye development, few functional studies have been done. The expression of *Smoc1/smoc1* in the ventral eye in mice and zebrafish and the eye abnormalities observed in *Smoc1* mutants suggests that *Smoc1* could function in DV retinal patterning by modulating BMP signaling. The ocular phenotypes observed in Waardenburg anophthalmia could at least partially be due to mispatterned eyes. This work utilized zebrafish to analyze the function of *smoc1* and *smoc2* during vertebrate eye development. It was found that Smoc1 and Smoc2 regulate ocular size through an unknown mechanism. Reduction in Smoc1 or Smoc2 protein levels and overexpression of *smoc1* and *smoc2* did not alter DV retinal patterning although the phenotypes observed and the use of a BMP reporter line indicates that both do function as BMP inhibitors during development. Interestingly, Smoc1 regulates BMP signaling throughout the eye and in a very defined region of the choroid fissure, a region of the eye where BMP signaling has not yet been studied.

Results & Discussion

Smoc1 sequence

Although Smoc1 is known to be extracellular, previous studies have reported that zebrafish Smoc1 lacks a signal peptide to target the protein for the secretory pathway (Abouzeid et al. 2011). Currently, the zebrafish *smoc1* sequences available on NCBI and Ensembl do not align well to other species when translated and appear to have multiple insertions and deletions or only fragments of the coding sequence are available with no information on the intervening sequences. As there are discrepancies in the *smoc1* sequence amongst online sources, primers were designed to amplify various regions of the *smoc1* coding sequence. Following PCR amplification, PCR products were sequenced and overlapping regions were aligned.

From this analysis, a full length *smoc1* coding sequence was generated, and unlike previous sequences, when translated the *smoc1* sequence aligned well with other species (Figure 3.1 A). Similar to other analyses, no evidence of a signal peptide was found. Only one Smoc1 isoform has been reported, but

sequencing revealed that there are two Smoc1 isoforms, with one missing the same 11 amino acids between the two thyroglobulin domains as one of the mouse isoforms (Figure 3.1). The intervening region between the thyroglobulin domains has been identified as a domain unique to Smoc proteins. The function of this domain has not been determined, but the similarity between the mouse and zebrafish isoform suggest that these amino acids serve an unknown function (Figure 3.1 B) (Vannahme et al. 2002).

Smoc2 sequence

The coding sequence of Smoc2 was also amplified and sequenced to verify that the *smoc2* morpholino oligonucleotide binding sites were within the gene and to confirm the nucleotide and amino acid sequence. From this analysis, a large deletion in the 3' region of the gene was found, corresponding to the loss of 8 amino acids C-terminal to the EF HAND domain when compared to the GenBank reference sequence (Figure 3.2 B). BLAST like alignment tool (BLAT) searches done on the Zv9 version of the zebrafish genome show that the start of the deletion does not map to an intron exon boundary while the end of the deletion does fall on an intron exon boundary, indicating potential problems with genome assembly and annotation. Furthermore, all Ensembl RNAseq datasets analyzed showed no evidence of the retained nucleotides in the GenBank reference sequence being present in *smoc2* transcripts. All plasmids sequenced contained the same deletion, indicating that this deletion is not due to Smoc2 having more than one isoform. As the deletion is in frame, the possibility that this deletion is a polymorphism present in the strain of zebrafish used cannot be ruled out without further sequencing of other strains.

***smoc1* & *smoc2* expression patterns**

To confirm *smoc1* and *smoc2* are expressed in the eye as has been reported previously and to determine where these genes are expressed at multiple developmental timepoints, *in situ* hybridization was done for *smoc1* and *smoc2* at various stages of eye development (Abouzeid et al. 2011; Mommaerts et al. 2014). Consistent with previous results, *smoc1* begins to be weakly expressed around 14 hpf next to the developing eye field (Figure 3.3 A). By 16 hpf, *smoc1* is expressed

adjacent to the presumptive ventral retina (Figure 3.3 B). As eye development progresses through lens formation and eye rotation, *smoc1* is expressed in the ventral portion of the retina next to the choroid fissure (Figure 3.3 C-E). By 48 hpf, *smoc1* expression is restricted to the ventral CMZ in the region directly adjacent to the choroid fissure (Figure 3.3 F).

Currently there is no evidence to suggest *smoc1* is expressed earlier than 14 hpf; however, *smoc2* is broadly expressed during gastrulation and becomes spatially restricted at 12 hpf when expression becomes localized to anterior somites (Mommaerts et al. 2014). *In situ* hybridization for *smoc2* shows it to be weakly expressed in the medial eye field at 14 hpf (Figure 3.3 G). By 16 hpf, *smoc2* expression becomes restricted to the most anterior region of the eye field in the presumptive ventral retina (Figure 3.3 H). After the eye rotates, *smoc2* is expressed in the ventral retina, but while *smoc1* is restricted to the most ventral portion of the retina, *smoc2* expression extends throughout the ventral retina (Figure 3.3 I-K). By 48 hpf, *smoc2* is expressed in the ventral CMZ, and similar to earlier stages, *smoc2* expression extends further dorsally than *smoc1* (Figure 3.3 L).

The overlapping but different expression patterns of *smoc1* and *smoc2* suggest that these two genes could be partially functionally redundant, particularly in the ventral portion of the retina surrounding the choroid fissure where both genes are expressed (Figure 3.3). It should be noted that the overlapping expression patterns, high conservation in amino acid sequence between Smoc1 and Smoc2, and the absence of phenotypes in many mutant lines with mutations in single genes suggest that further work will require the analysis of double mutants to resolve any issues of functional redundancy (Kettleborough et al. 2013; Kok et al. 2015). The localized expression of *smoc1* around the choroid fissure indicates that the primary role of Smoc1 could be to regulate choroid fissure closure whereas the expression of *smoc2* throughout the ventral retina suggests that Smoc2 might be involved in regulating BMP signaling throughout the eye and is likely a better candidate for restricting dorsal retinal identity.

The DV polarity of the CMZ has been described (French et al. 2013). The spatially restricted expression of *smoc1* and *smoc2* to the ventral CMZ along with the expression of *gdf6a* in the dorsal CMZ further supports that the dorsal and ventral progenitor pool in the CMZ is somehow different (French et al. 2013). Recent work has shown that inhibition of BMP signaling is required for epithelial streaming of cells to the presumptive ventral CMZ (Heermann et al. 2015). Based on the expression of *smoc1* and *smoc2* in the ventral eye and later in the ventral CMZ, Smoc1 and Smoc2 might be essential for this process to occur (Heermann et al. 2015). Why there appears to be BMP signaling through Gdf6a in the dorsal CMZ and the inhibition of BMP signaling by Smoc1 and Smoc2 in the ventral CMZ is unknown, but one possibility is that Smoc1 and Smoc2 antagonize Gdf6a to balance progenitor pool proliferation with cell cycle exit and differentiation.

If *smoc1* and *smoc2* are involved in the initiation of eye patterning, it would be expected that these genes would be expressed in the presumptive ventral retina by 12 hpf when dorsal retinal identity is being established by the diffusion extraocular BMPs to the lateral retina (Kruse-Bend et al. 2012; Veien et al. 2008). However, these results combined with the work of others show that *smoc1* and *smoc2* expression becomes restricted to the presumptive ventral retina at 14 hpf, 2 hours after dorsal eye identity has been established (Abouzeid et al. 2011; Mommaerts et al. 2014). The delayed expression of *smoc1* and *smoc2* suggest that if these genes are involved in DV retinal patterning, they are involved in the maintenance of DV retinal patterning rather than initiation. The timing of the onset of ocular *smoc1* and *smoc2* expression coincides with Wnt signaling from the dorsal RPE maintaining dorsal retinal identity, further strengthening the argument that instead of ventral retinal initiators, *smoc1* and *smoc2* are more likely involved in maintenance of ventral retinal identity (Veien et al. 2008; Holly et al. 2014). Congruent with the model of the BMP inhibitors smoc1 and smoc2 being involved in maintenance of ventral retinal identity, microarrays done on *Vax2*$^{-/-}$ mice show that *smoc1* is strongly downregulated when Vax2 is absent, suggesting that *smoc1* is downstream of *vax2* and that ventral retinal identity is already established from other factors that regulate *vax2* expression (Alfano et al. 2011).

Initially it was expected that *smoc1* and *smoc2* would be expressed during initiation of DV patterning as a way to balance dorsalizing BMP signals and to allow for the establishment of ventral retinal fate. Surprisingly, based on the expression pattern alone, the BMP inhibitors Smoc1 and Smoc2 are likely not involved in the initiation of ventral retinal identity. One possibility is that hedgehog signals originating from the midline are sufficient to initiate ventral retinal fate and the inhibition of BMP signaling only becomes necessary in the maintenance phase of DV retinal patterning. It is also possible that there are still other unidentified BMP inhibitors expressed near the presumptive ventral retina that are required for the inhibition of dorsal and initiation of ventral fate.

Expression of *smoc1* & *smoc2* is expanded in *gdf6a* mutants

The loss of Gdf6a results in a ventralized eye where genes normally restricted to the ventral half of the eye are expanded throughout the eye at the expense of dorsal retinal markers (French et al. 2009; Gosse & Baier 2009). The expression of *smoc1* and *smoc2* was examined using whole mount *in situ* hybridization on embryos from *gdf6a*$^{+/-}$ incrosses. While most 28 hpf embryos from these incrosses had *smoc1* expression surrounding the choroid fissure as has been seen in wild-type embryos, 36% of them had a slight expansion of *smoc1* expression to the midline of the eye (n = 28; Figure 3.4 A, B). At this same stage, 21% of embryos had *smoc2* expression expanded throughout the eye, as is seen with other ventral patterning genes (n = 28; Figure 3.4 C, D) (French et al. 2009). Although *gdf6a*$^{-/-}$ mutants do not have any discernable phenotype at 28 hpf, the embryos with expanded *smoc1* and *smoc2* expression are most likely homozygous mutants as the expanded expression was observed in close to 25% of embryos, corresponding to the Mendelian ratios expected from heterozygous mutant incrosses (Asai-Coakwell et al. 2013). By 48 hpf, when the *gdf6a*$^{-/-}$ microphthalmic phenotype is apparent, *smoc1* and *smoc2* expression was found to be expanded throughout the entire CMZ in *gdf6a*$^{-/-}$ mutants while the remaining embryos had *smoc1* and *smoc2* restricted to the ventral CMZ as is seen in wild-type embryos (Figure 3.4 E-H; n = 33 and 51, respectively).

The slight expansion of *smoc1* expression and the expansion of *smoc2* to encompass the entire retina in 28 hpf *gdf6a*$^{-/-}$ mutants argues that if *smoc1* and *smoc2* are involved in DV retinal patterning, Smoc2 likely plays a more important role than Smoc1 in maintaining ventral retinal fate by inhibiting BMP signals originating from the dorsal eye. The localized expression of *smoc1* to the ventralmost portion of the retina surrounding the choroid fissure and its incomplete expansion in *gdf6a*$^{-/-}$ mutants suggests that while Smoc1 could inhibit BMP signals from the dorsal retina, Smoc1 could also have a more specific role in regulating BMP signaling in the ventral retina and might be involved in choroid fissure closure.

Knockdown of *smoc1* and *smoc2* results in microphthalmia

Mutations in *SMOC1* have been associated with Waardenburg anophthalmia, a condition that when associated with mutations in *SMOC1* typically presents as bilateral true anophthalmia, syndactyly, metacarpal synostosis, and oligodactyly (Abouzeid et al. 2011; Rainger et al. 2011; Okada et al. 2011). In accordance with human studies, work done on two independently generated *Smoc1* mutant mouse lines has shown that the loss of Smoc1 results in similar limb abnormalities, but the eye defects observed in these mouse mutants are noticeably less severe and do not have true anophthalmia. Instead these mouse lines exhibit a suite of milder optic abnormalities including microphthalmia, coloboma, optic nerve aplasia and hypoplasia, RPE overgrowth to the optic nerve, and abnormalities in the retinal ganglion cell layer (Rainger et al. 2011; Okada et al. 2011). Because there are differences between the mouse and human phenotypes, Smoc1 and Smoc2 protein levels were reduced in zebrafish using translation blocking morpholino oligonucleotides to see if a reduction in Smoc1 and Smoc2 protein levels in zebrafish would more closely resemble the Waardenburg anophthalmia phenotype.

Injection of *smoc1* morpholino resulted in limited apoptosis throughout the embryo, but embryos otherwise appeared normal. Eye development was followed in *smoc1* morphants from 24-48 hpf. Eye morphology in morphants was largely normal when compared to uninjected embryos, with the only exception

being that morphants displayed mild microphthalmia (Figure 3.5 A-C). Because some mild apoptosis was observed in *smoc1* morphants, embryos were coinjected with *smoc1* and *p53* morpholinos to determine if the reduction in eye size could be due to apoptosis, which could be caused by non-specific morpholino effects. Eye area measurements show that *smoc1* morphants have a significantly smaller eye area when compared to uninjected embryos (n = >36 embryos each, $p < 0.01$), however this microphthalmic phenotype is partially rescued when *p53* morpholino is coinjected with *smoc1* morpholino with no statistically significant difference between *smoc1 p53* morphants and uninjected controls (Figure 3.5 D; n = 18-36 embryos each, $p > 0.05$).

Unlike the *smoc1* morpholino, the *smoc2* morpholino was highly toxic even at low doses and resulted in widespread severe apoptosis in most surviving embryos (not shown). Although there was widespread apoptosis, eye morphogenesis appeared normal in *smoc2* morphants, with surviving morphants exhibiting mild microphthalmia, with on average, a statistically significant 10% reduction in eye area when compared to uninjected embryos (Figure 3.6; n = 28 eyes, 14 embryos each, $p = 0.0016$).

Based on the statistically significant difference in eye size between *smoc1* morphants and uninjected embryos and the lack of a significant difference between *smoc1* morphants coinjected with *p53* morpholino and uninjected embryos indicates that *smoc1* morphants have microphthalmia due to increased apoptosis. It cannot be determined from this data whether the apoptotic effect is due to the reduction in Smoc1 protein levels or is from non-specific morpholino effects. The similarity in microphthalmic phenotype between *Smoc1* mutant mice and *smoc1* morphant zebrafish is promising and suggests that *smoc1* morphants can be used as a model to study Smoc1 function in eye development (Okada et al. 2011). The microphthalmic phenotype seen in *smoc2* morphants also suggests that Smoc2 regulates ocular size potentially through modulating BMP regulated apoptosis. Like the experiments using *smoc1* morpholino, it cannot be determined if the apoptotic effect observed is a result of a reduction in Smoc2 protein levels or from non-specific apoptosis caused by the morpholino.

Furthermore, the loss of BMP signaling caused by mutations in *gdf6a* results in increased apoptosis, which suggests two possibilities: 1) BMP signaling must be tightly balanced during eye development where either too little or too much signaling results in apoptosis or 2) Smoc1 or Smoc2, as has been seen with the Smoc1 *Drosophila* homolog Pentagone, can both inhibit and facilitate BMP signaling (French et al. 2013; Vuilleumier et al. 2010). If Smoc proteins inhibit BMP signaling and also allow for diffusion of BMP ligands, the dorsoventral BMP gradient in the eye would be narrowed, which would effectively reduce BMP signaling and cause increased apoptosis similar to what is seen in *gdf6a* mutants (Vuilleumier et al. 2010).

Smoc1 morphants have abnormal optic stalks

Following injection of *smoc1* morpholino oligonucleotides, *in situ* hybridization was done for retinal patterning markers including *vax2*, which also marks the optic stalk. Interestingly, although *vax2* expression in the retina of *smoc1* morphants appeared normal, expression in the optic stalk showed that in 68% of *smoc1* morphants the optic stalks of are abnormal. The optic stalks in *smoc1* morphants appeared more condensed and lacked constrictions near the retina when compared to uninjected embryos (n = 28). There also appeared to be a reduced distance between the optic stalk and the yolk when compared to the uninjected counterparts (Figure 3.7). These results appear to recapitulate the *Smoc1* mutant mouse phenotype where mice exhibit aplastic or hypoplastic optic nerves, but further work would be required with zebrafish *smoc1* mutants to determine if the abnormalities seen in the optic stalk during early eye development result in aplastic or hypoplastic optic nerves (Rainger et al. 2011; Okada et al. 2011).

***Smoc1* regulates BMP signaling in the choroid fissure**

Since Smoc1 has been implicated in regulating BMP signaling, the effects of Smoc1 knockdown on BMP signaling was examined in *Tg(BMPRE-AAV.Mlp:eGFP)* embryos using *in situ* hybridization for *GFP* (Collery & Link 2011). While BMP signaling is normally restricted to the dorsal portion of the retina at 28 hpf (Figure 3.8A), *smoc1* morphants exhibited a mild expansion of

BMP signaling to encompass more of the retina. Interestingly, closer examination of eyes from *smoc1* morphants showed the presence of BMP signaling in the proximal choroid fissure (36% of embryos, n = 33), which was not seen in any uninjected *Tg(BMPRE-AAV.Mlp:eGFP)* embryos (Figure 3.8 B).

These results show that although *smoc1* expression is restricted to the ventral portion of the eye surrounding the choroid fissure, Smoc1 protein is able to regulate BMP signaling throughout the eye and is able to diffuse throughout the eye. The finding that there is a defined region of BMP activity in the choroid fissure that is regulated by Smoc1 is surprising and further supports the hypothesis that in addition to DV retinal patterning, Smoc1 also has a ventral specific role. One potential source of BMP signaling in the proximal choroid fissure is Bmp7b, the human and mouse BMP7 ortholog, which in zebrafish is expressed in the eye adjacent to the choroid fissure and in mice is expressed in the proximal region of the ventral eye (Morcillo et al. 2006). BMP7 has been previously implicated in choroid fissure formation, which could mean that the balance between BMP7 signaling and the modulation of BMP7 signaling by Smoc1 is involved in coordinating choroid fissure formation and fissure closing (Morcillo et al. 2006).

Knockdown of *smoc1* alters dorsoventral retinal patterning

To determine if *smoc1* is involved in DV retinal patterning, translation blocking *smoc1* morpholino oligonucleotides were injected and eye patterning was assessed using *in situ* hybridization for the DV markers *vax2* and *tbx5a*. In uninjected embryos, *tbx5a* expression was confined to a narrow region in the dorsal retina (Figure 3.9 A) whereas in *smoc1* morphants, *tbx5a* expression is slightly downregulated (Figure 3.9 B). Conversely, *vax2* expression is restricted to the ventral retina in uninjected embryos (Figure 3.9 C) and in *smoc1* morphants *vax2* expression is slightly upregulated (Figure 3.9 D).

Together, these results suggest that Smoc1 is involved in patterning the DV retinal axis, but not in a manner that was initially expected. The differences in DV patterning between *smoc1* morphants and uninjected controls was only apparent at 48 hpf, suggesting that if Smoc1 does indeed pattern the DV axis, it does so

during a late maintenance stage. Furthermore, it would be expected that if Smoc1 is inhibiting BMP signaling during DV patterning, that loss of Smoc1 protein would result in a dorsalized eye, which is the opposite of what was observed. One possibility is that Smoc1, like the *Drosophila* ortholog Pentagone, is required for BMP diffusion and gradient formation; however this conflicts with the finding that a loss of Smoc1 results in expanded BMP signaling (Vuilleumier et al. 2010). It should also be noted that Pentagone inhibits Dpp, the *Drosophila* BMP4 ortholog, and in zebrafish Bmp4 does not appear to be essential for DV patterning (Vuilleumier et al. 2010; French et al. 2009). If the primary role of Smoc1 is to inhibit Bmp4 and it binds other BMPs including Bmp2b and Gdf6a with a lower affinity, it is possible that rather than regulating DV patterning, Smoc1 instead functions in another capacity within the ventral retina.

Knockdown of *smoc2* does not affect dorsoventral retinal patterning

Since *smoc2* is expressed in the ventral half of the eye while *smoc1* has a more restricted expression pattern, it was hypothesized that Smoc2 contributes more to DV retinal patterning than Smoc1 does. To test this hypothesis, translation blocking *smoc2* morpholino was injected into embryos and *in situ* hybridization was done for the DV patterning markers *tbx5a* and *vax2*. Surprisingly, there was no change in DV retinal patterning when Smoc2 protein levels were reduced (Figure 3.10).

Although this experiment suggests that *smoc2* is not involved in patterning the DV retina, one possibility is that *smoc2* does contribute to DV retinal patterning, but that these effects could not be observed in this experiment due to morpholino toxicity. Through previous experiments, it was observed that the *smoc2* translation blocking morpholino was highly toxic, resulting in few survivors and noticeable apoptosis throughout the embryo. Since the *smoc2* morpholino is highly toxic and a relatively low dose of morpholino was used, Smoc2 protein levels might not have been reduced enough to alter DV retinal patterning, but further knockdown cannot be achieved due to morpholino toxicity. One explanation for this high toxicity is that *smoc2* appears to be deposited maternally and is ubiquitously expressed during early development making the

use of a translation blocking morpholino to look at later onset phenotypes problematic (Mommaerts et al. 2014). Although a splice blocking morpholino can be used to avoid reducing protein produced from maternal transcripts and to potentially increase viability of *smoc2* morphants, there is still the possibility of non-specific morpholino effects which could confound this study (Kok et al. 2015). For future studies that attempt to elucidate the role of *smoc2* in later developmental events including the development and DV patterning of the eye, *smoc2* mutants will need to be generated.

smoc1 and *smoc2* do not act synergistically

Because *smoc1* and *smoc2* expression partially overlaps in the ventral retina and because of the high conservation of amino acid sequence between the two proteins, it was hypothesized that Smoc1 and Smoc2 act synergistically to pattern the DV axis of the eye and that knockdown of both proteins would be required to produce a completely dorsalized eye. Antisense translation blocking morpholinos for *smoc1* and *smoc2* were injected to the same total dose as was used for single injections of *smoc1* or *smoc2* morpholino. Following morpholino injection, *in situ* hybridization was done on 28 hpf embryos for the patterning markers *vax2* and *tbx5a*. In *smoc1 smoc2* double morphants, there were no changes to DV retinal patterning indicating that Smoc1 and Smoc2 do not act synergistically to pattern the dorsoventral axis of the eye (Figure 3.11). As previously mentioned, the efficacy of both of the morpholinos used is currently unknown. It is possible that the morpholinos used caused a sub-optimal reduction of Smoc1 and Smoc2 protein levels, which is why no synergistic effect was observed.

Overexpression of *smoc1* and *smoc2* does not alter dorsoventral retinal patterning

Next, to further determine the function of Smoc1 and Smoc2 during vertebrate eye development, *smoc1* and *smoc2* were overexpressed by injecting one-cell stage embryos with various doses of *smoc1* or *smoc2* mRNA. Multiple doses were used to test the possibility that Smoc1 or Smoc2 can facilitate ligand binding and BMP signaling at low concentrations and inhibit BMP signaling at

high concentrations similar to what has been observed with Sfrps during zebrafish eye development (Holly et al. 2014). Embryos were observed for axial patterning defects and classified into either dorsalized or ventralized categories based on the phenotypes described for the zebrafish *bmp2b* mutant (Kishimoto et al. 1997). Next, *in situ* hybridization for the DV retinal markers *tbx5a* and *vax2* was done to test if overexpression of Smoc1 or Smoc2 can alter DV retinal patterning.

Overexpressing *smoc1* at doses of 5 ng, 10 ng, 100 ng, 200 ng, and 300 ng did not cause many gross morphological defects. Surprisingly, no change in DV retinal patterning was observed for any of the doses used (Figure 3.12 A-L). Injection of *smoc1* mRNA at the higher doses (200 pg & 300 pg) did cause axial defects similar to that seen in *bmp2b* mutants where the loss of Bmp2b results in a dorsalized body axis (Figure 3.12 M-O; (Kishimoto et al. 1997)). The embryos with axial defects were classified as C3 and C4 dorsalized phenotypes (Figure 3.12 M-O). Since only dorsalized phenotypes were seen and only at the highest doses used, there is no evidence to suggest that Smoc1 can also facilitate BMP signaling during zebrafish development.

Similar to the experiments where *smoc1* was overexpressed, overexpression of *smoc2* did not cause any obvious changes in DV retinal patterning at any of the doses used (Figure 3.13 A-H). The axial phenotypes observed when *smoc2* was overexpressed were noticeably more severe when compared to the phenotypes seen when *smoc1* was overexpressed (Figure 3.13 I-L). A large proportion of embryos that were injected with 100 ng, 200 ng, and 300 ng had a dorsalized axis phenotype that ranged from mild dorsalization when 100 ng was injected (C3; Figure 3.13 I) to severe dorzalization when 200 and 300 ng of mRNA was injected (C4 & C5; Figure 3.13 J, K). The axial patterning defects observed further suggest that Smoc2 does act as a BMP inhibitor with no evidence to suggest that Smoc2 can also facilitate signaling.

Although no differences in DV retinal patterning were observed when *smoc1* and *smoc2* were overexpressed, it is still possible that Smoc1 and Smoc2 are involved in eye patterning. The morpholino experiments described suggest that Smoc1 likely has a late maintenance role in eye patterning. Since

maintenance of eye patterning starts at 14 hpf, it is possible that the mRNA injected at the one cell stage would not affect maintenance of DV patterning or that Smoc1 and Smoc2 proteins are relatively unstable with a short half life. These experiments have shown that overexpression of *smoc1* and *smoc2* results in axial defects similar to what is seen when BMPs are lost and the embryo becomes dorsalized (Kishimoto et al. 1997). These overexpression experiments further support the finding that in *Xenopus* Smoc1 does inhibit BMP signaling (Thomas et al. 2009). Interestingly, the lack of ventralized embryos at low mRNA doses suggests that Smoc1 and Smoc2, unlike the *Drosophila* ortholog Pentagone, do not also facilitate BMP signaling by aiding in diffusion of ligands (Vuilleumier et al. 2010).

Whether Smoc1 and Smoc2 are involved in DV retinal patterning also relies on the ligands that they can interact with. In zebrafish, Bmp2b and Gdf6a are the primary BMP ligands involved in DV retinal patterning and it has been shown that Bmp4 is not sufficient to pattern the DV axis (Kruse-Bend et al. 2012; French et al. 2009; Gosse & Baier 2009). If Smoc1 and Smoc2 have the highest affinity for Bmp4 and interact weakly with Bmp2b or Gdf6a, the contribution of Smoc1 and Smoc2 to DV retinal patterning would be relatively minor. In order to fully characterize the function of Smoc1 and Smoc2 in vertebrate eye development, protein interaction studies need to be done to identify binding partners of Smoc1. Ideally, tissue specific overexpression of *smoc1* and *smoc2* should be done to avoid axial defects seen with global overexpression and to determine at which stages Smoc1 and Smoc2 are involved in eye development.

Summary & Future directions

This work has found that the BMP inhibitors Smoc1 and Smoc2 are involved in multiple aspects of vertebrate ocular development. Expression of *smoc1* occurs in the ventral retina surrounding the choroid fissure while *smoc2* is expressed in the ventral half of the retina. The functions of Smoc1 and Smoc2 were tested primarily using a loss of function approach with translation blocking morpholino oligonucleotides. In both cases, *smoc1* and *smoc2* morphants exhibited microphthalmia likely due to increased apoptosis, a phenotype also

observed when BMP signaling is lost in *gdf6a* mutants (French et al. 2013). In addition, *smoc1* morphants had optic stalk defects, which could potentially lead to hypoplastic or aplastic optic nerves. The microphthalmic and optic stalk phenotypes observed in these morphants recapitulate the phenotype of *Smoc1* mutant mice (Okada et al. 2011; Rainger et al. 2011). In mice and zebrafish, a reduction in Smoc1 levels results in relatively mild ocular defects when compared to anophthalmia and severe microphthalmia seen in humans with mutations in *SMOC1* (Okada et al. 2011; Rainger et al. 2011; Abouzeid et al. 2014; Gerth-Kahlert et al. 2013; Williamson & Fitzpatrick 2014). Because it is thought that the mouse line analyzed may not be a true null and morpholinos cannot completely block translation, generation of a null *smoc1* zebrafish mutant is essential and will hopefully provide a more accurate model to study Waardenburg anophthalmia (Rainger et al. 2011).

Although it was initially hypothesized that Smoc1 and Smoc2 inhibit BMP signaling during DV retinal patterning and are involved in specifying ventral retinal fate, it could only be shown that Smoc1 is likely involved in maintenance rather than initiation of DV retinal patterning. Strikingly, *smoc1* morphants had what appeared to be a mildly ventralized eye, which could support studies in *Drosophila* that have shown that the Smoc1 ortholog, Pentagone, functions primarily as a facilitator of Dpp diffusion and signaling (Vuilleumier et al. 2010). Overexpression of *smoc1* and *smoc2* did not result in changes in DV retinal patterning despite the embryos having a ventralized body axis, which would be expected from a reduction in BMP signaling and is consistent with what has been seen in *Xenopus* when *smoc1* is overexpressed (Thomas et al. 2009). Together, these results show that Smoc1 and Smoc2 do inhibit BMP signaling, but if they are involved in DV patterning, they only have a maintenance role. To further determine the contribution of Smoc1 and Smoc2 to DV retinal patterning and to avoid potential problems with sub-optimal knockdown, single and double *smoc1* and *smoc2* mutants should be generated and evaluated for morphological eye defects and mispatterned eyes.

While it was expected that Smoc1 regulates BMP signaling from the dorsal eye during eye development and DV retinal patterning, it was not expected that

Smoc1 regulates BMP signaling in a clearly defined region in the proximal choroid fissure. The importance of inhibition of BMP signaling in the choroid fissure is unknown, but it is possible that Smoc1 mediated inhibition of BMP signaling is involved in choroid fissure closure or invasion of vasculature into the eye through the choroid fissure. The source of BMPs in the choroid fissure are unknown, but based on available expression patterns in mice and zebrafish, a strong candidate is Bmp7 in mice and Bmp7b in zebrafish (Morcillo et al. 2006; Shawi & Serluca 2008). In *Bmp7* mutant mice, the choroid fissure fails to form and there is reduced levels of apoptosis in the region where the fissure would form (Morcillo et al. 2006). If Smoc1 inhibits Bmp7b, it would block the apoptotic effect of Bmp7b, which could be important in allowing for choroid fissure closure. Inhibition of Bmp signaling in the choroid fissure could also be necessary to direct POM cells that will form the hyaloid vasculature to migrate to the choroid fissure. This argument is strengthened by the finding that another BMP inhibitor, *grem2b*, is expressed in a subpopulation of POM cells that migrates to the choroid fissure (Chapter 4). Future experiments should be done to determine potential sources of BMP signaling within the choroid fissure. In particular, experiments should be done to see if BMP signaling that occurs in the choroid fissure when Smoc1 levels are reduced is lost when Bmp7b levels are simultaneously reduced. If *smoc1* mutants are generated, there are a wide variety of transgenic vasculature lines that can also be used to further determine if Smoc1 is involved in formation of the hyaloid vasculature.

Lastly, the localization of *smoc1* and *smoc2* expression to the ventral CMZ later in development reveals that BMP inhibitors serve an unknown function in this cell population. Previous studies have shown that *gdf6a* expression marks a dorsal CMZ population and seems to regulate cell cycle progression in this cell population (French et al. 2013). It is currently not clear why there is regionalization of the CMZ, but recent work has implied that this regionalization of the CMZ is prepatterned early in eye morphogenesis as the optic cup is still forming and cells stream to the presumptive ventral CMZ in low BMP conditions (Heermann et al. 2015). As *smoc1* and *smoc2* are expressed early in eye development and later in the ventral CMZ, it is possible that inhibition of BMP

signaling by Smoc1 and Smoc2 early in eye morphogenesis contributes to the regionalization of the CMZ and epithelial streaming to the ventral region. Further investigating this possibility will be fairly complex and will require live imaging of zebrafish ocular morphogenesis using available transgenic lines that can be used to follow epithelial streaming as the optic cup is forming (Heermann et al. 2015).

A

Smoc1

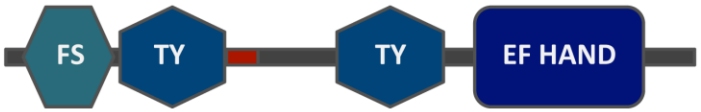
FS
TY
TY
EF HAND

B

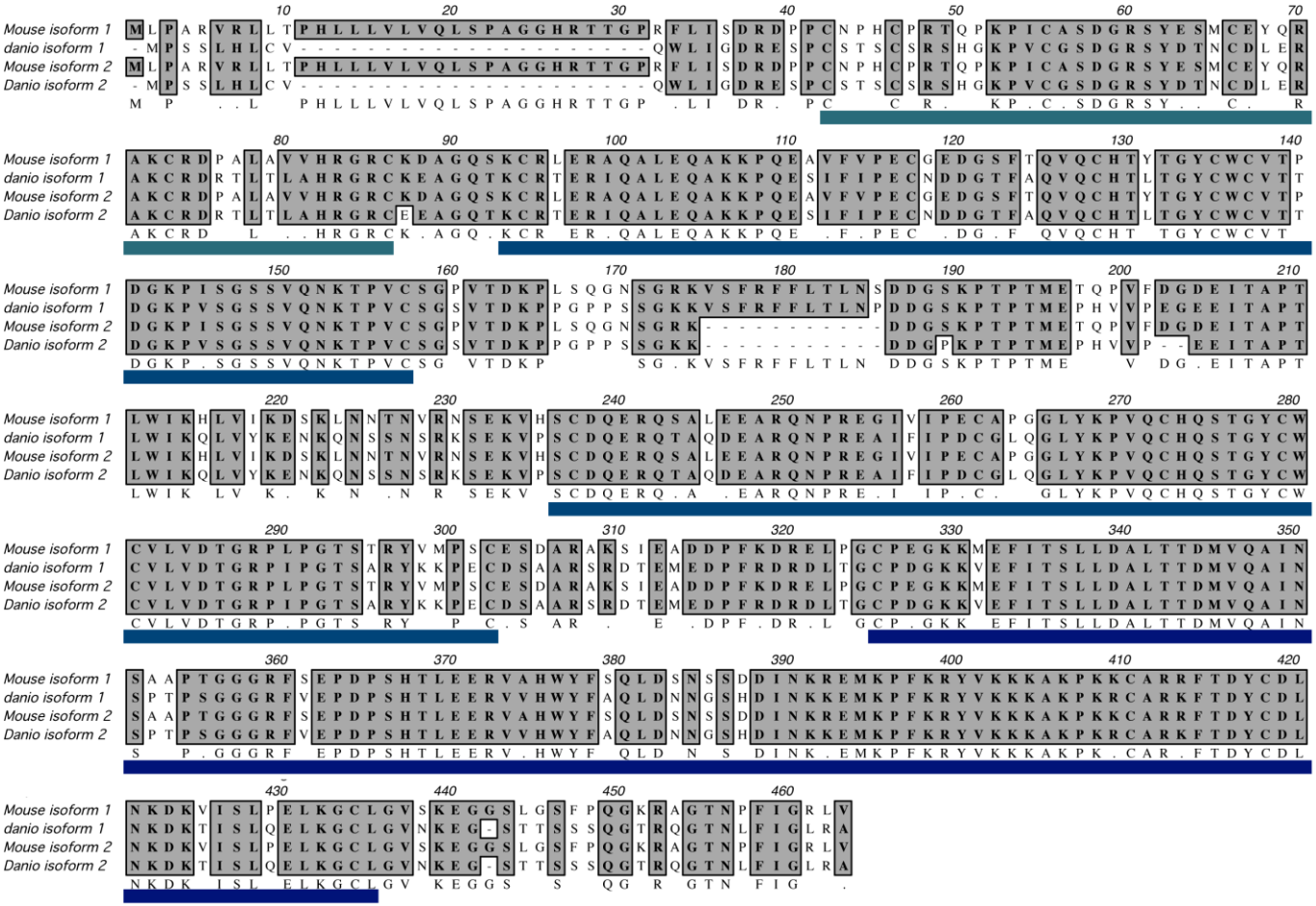
Mouse isoform 1
danio isoform 1
Mouse isoform 2
Danio isoform 2

Figure 3.1: Smoc1 is a highly conserved protein with two isoforms in zebrafish and mice. (A) Zebrafish Smoc1 has four conserved domains found in other classes of proteins: a follistatin (FS) domain (turquoise), two thyroglobulin (TY) domains (blue) and an EF HAND calcium binding domain (midnight). The region between the two thyroglobulin domains is a Smoc specific domain which contains an 11 amino acid deletion (red box) in one mouse and zebrafish isoform. (B) Alignment showing the isoforms and conservation of Smoc1. Conserved regions are shaded grey. The follistatin (turquoise), thyroglobulin (blue), and EF HAND (midnight) domains are highly conserved amongst mouse and zebrafish isoforms. Mouse Smoc1 isoform 2 lacks the same 11 amino acids within the Smoc specific domain as one of the zebrafish Smoc1 isoforms.

A

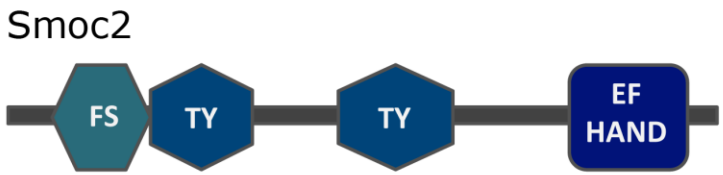
Smoc2
FS
TY
TY
EF
HAND

B

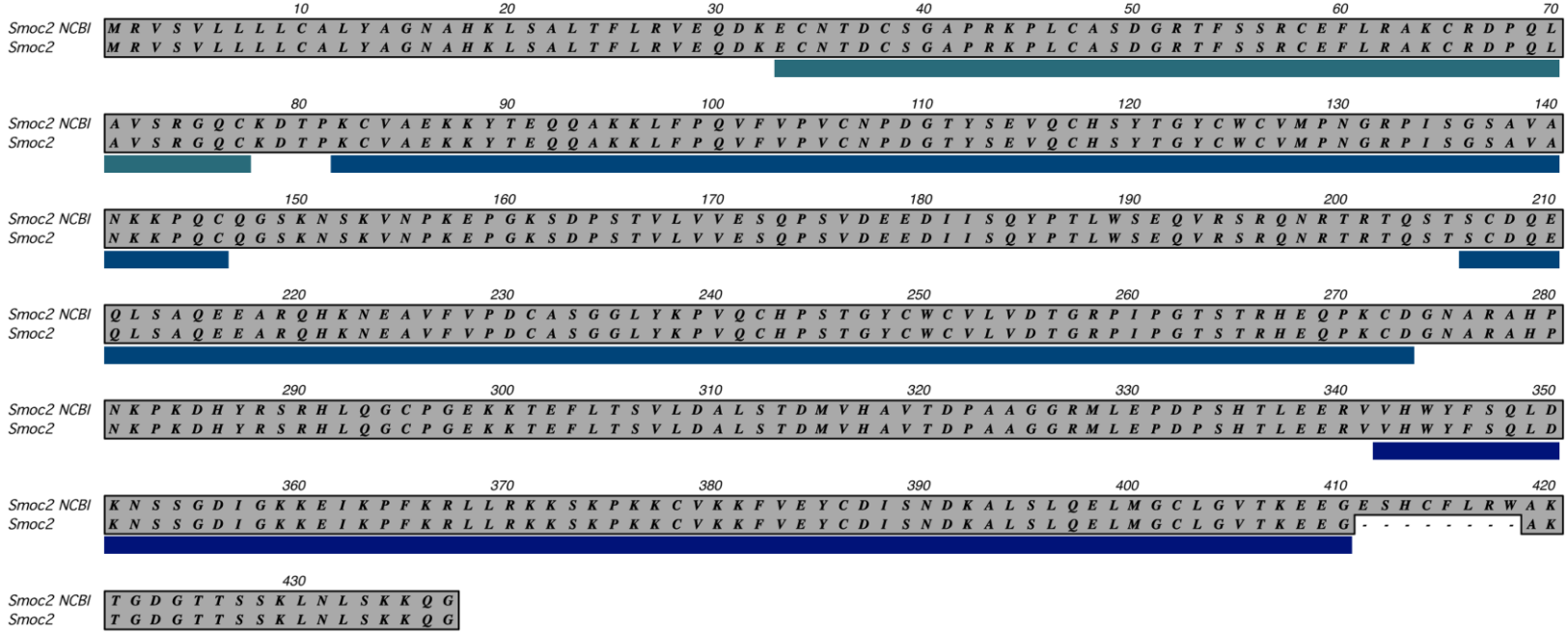
Smoc2 NCBI
Smoc2
MRVSVLLLLCALYAGNAHKLSALTFLRVEQDKECNTDCSGAPRKPLCASDGRTFSSRCEFLRAKCRDPQL
AVSRGQCKDTPKCVAEKKYTEQQAKKLFPQVFVPVCNPDGTYSEVQCHSYTGYCWCVMPNGRPISGSAVA
NKKPQCQGSKNSKVNPKEPGKSDPSTVLVVESQPSVDEEDIISQYPTLWSEQVRSRQNRTRTQSTSCDQE
QLSAQEEARQHKNEAVFVPDCASGGLYKPVQCHPSTGYCWCVLVDTGRPIPGTSTRHEQPKCDGNARAHP
NKPKDHYRSRHLQGCPGEKKTEFLTSVLDALSTDMVHAVTDPAAGGRMLEPDPSHTLEERVVHWYFSQLD
KNSSGDIGKKEIKPFKRLLRKKSKPKKCVKKFVEYCDISNDKALSLQELMGCLGVTKEEGE------AK
TGDGTTSSKLNLSKKQG
430

Figure 3.2: Conserved domains and alignment of zebrafish Smoc2. (A) Like Smoc1, Smoc2 has four conserved domains found in other protein families: a follistatin (FS) domain (turquoise), two thyroglobulin (TY) domains (blue), and an EF HAND calcium binding domain (midnight). (B) Amino acid alignment of the zebrafish Smoc2 reference sequence (GenBank: AEW31060.1) and the zebrafish Smoc2 amino acid sequence obtained by sequencing cDNA from 24 hpf zebrafish. The follistatin domain (turquoise), the two thyroglobulin domains (blue) and the EF HAND domain (midnight) are underlined. The smoc2 cDNA sequenced had a 24 bp deletion corresponding to a loss of 8 amino acids at the C-terminus of the EF HAND domain.

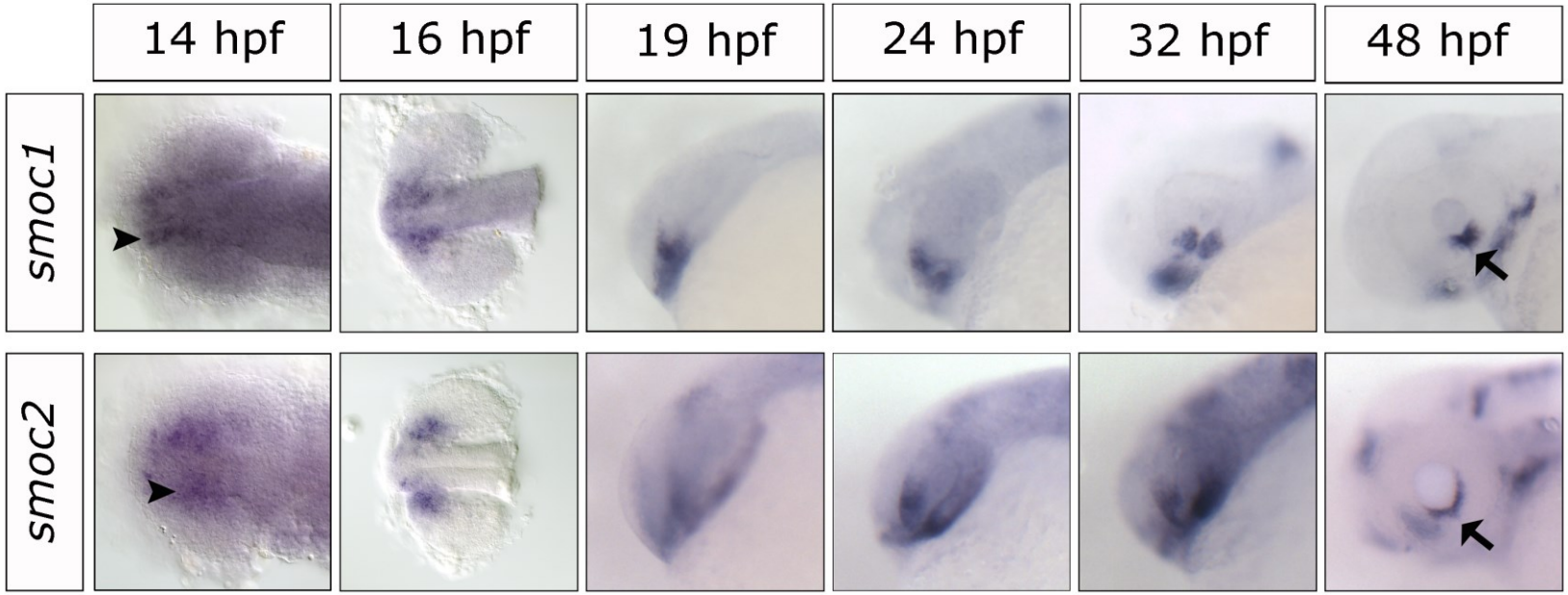

Figure 3.3: Expression of smoc1 and smoc2 in zebrafish from 14 hpf to 48 hpf. Both *smoc1* and *smoc2* are weakly expressed in the lateral forebrain adjacent to the eye at 14 hpf (A & G, arrowheads). By 16hpf, *smoc1* is expressed at the interface between the forebrain and anterior eye (B) and *smoc1* is expressed in the anteromedial eye (H). As the eye rotates, *smoc1* expression becomes restricted to the ventralmost portion of the eye surrounding the choroid fissure (C, D, E) while *smoc2* is expressed in the ventral half of the eye (I, J, K). At 48 hpf, *smoc1* and *smoc2* are expressed in the ventral CMZ (F, L, arrows).

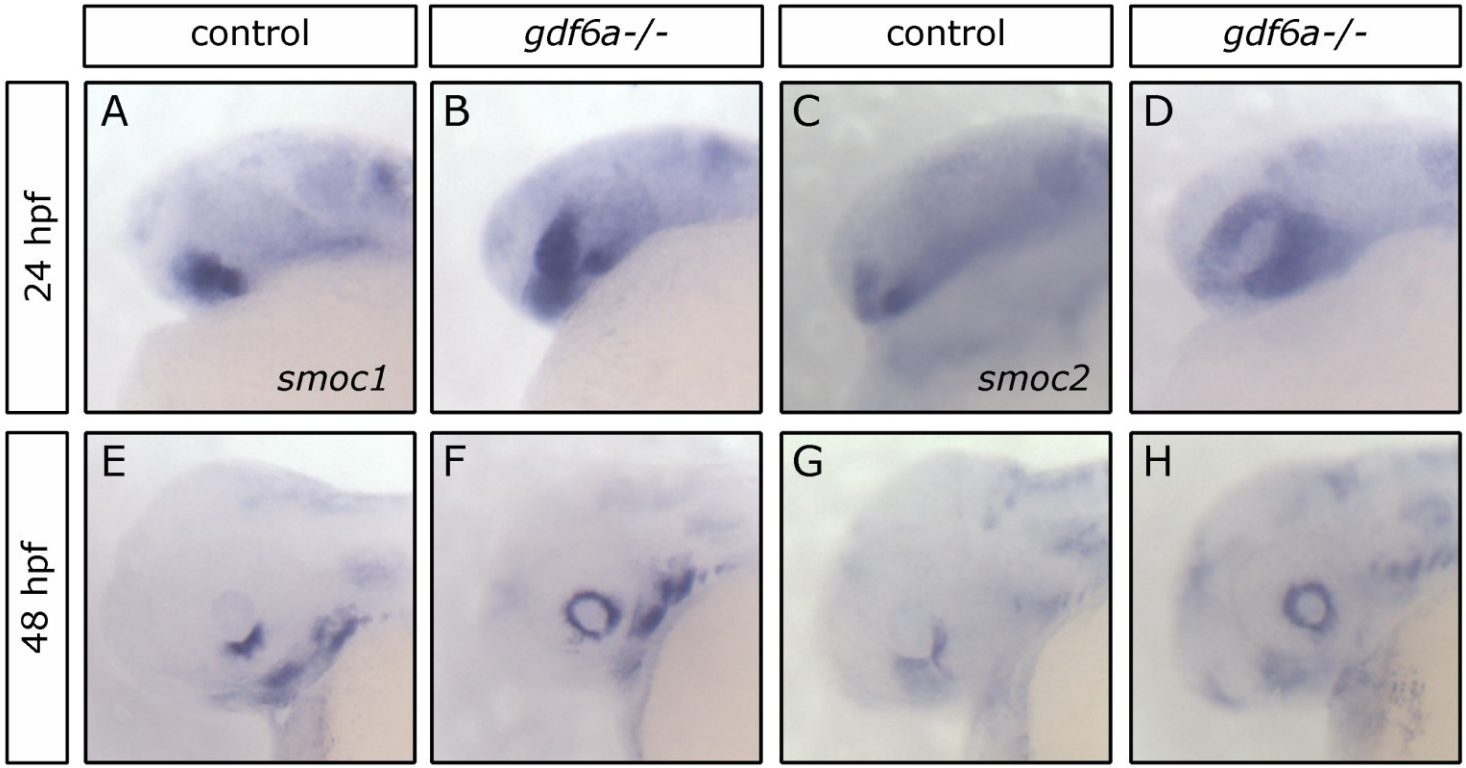

Figure 3.4: Expression of smoc1 and smoc2 is expanded in *gdf6a*$^{-/-}$ mutants. (A, B) Whole mount *in situ* hybridizations showing *smoc1* expression at 24 hpf in embryos from gdf6a$^{+/-}$ incrosses. Expression of *smoc1* is restricted to the ventral eye in 64% of the embryos (A) while the remaining 36% had a slight expansion of *smoc1* expression (B) (n = 28). (C, D) Whole mount *in situ* hybridization showing *smoc2* expression in embryos from the same incross as in (A). Expression of *smoc2* is normally restricted to the ventral half of the eye (C), but in 21% of the embryos, *smoc2* expression was expanded throughout the entire eye (D) (n = 28). (E-F) At 48 hpf, *smoc1* and *smoc2* is normally restricted to the ventral CMZ (E, G), but in *gdf6a*$^{-/-}$ mutants, expression of *smoc1* and *smoc2* is expanded throughout the entire CMZ (F, H).

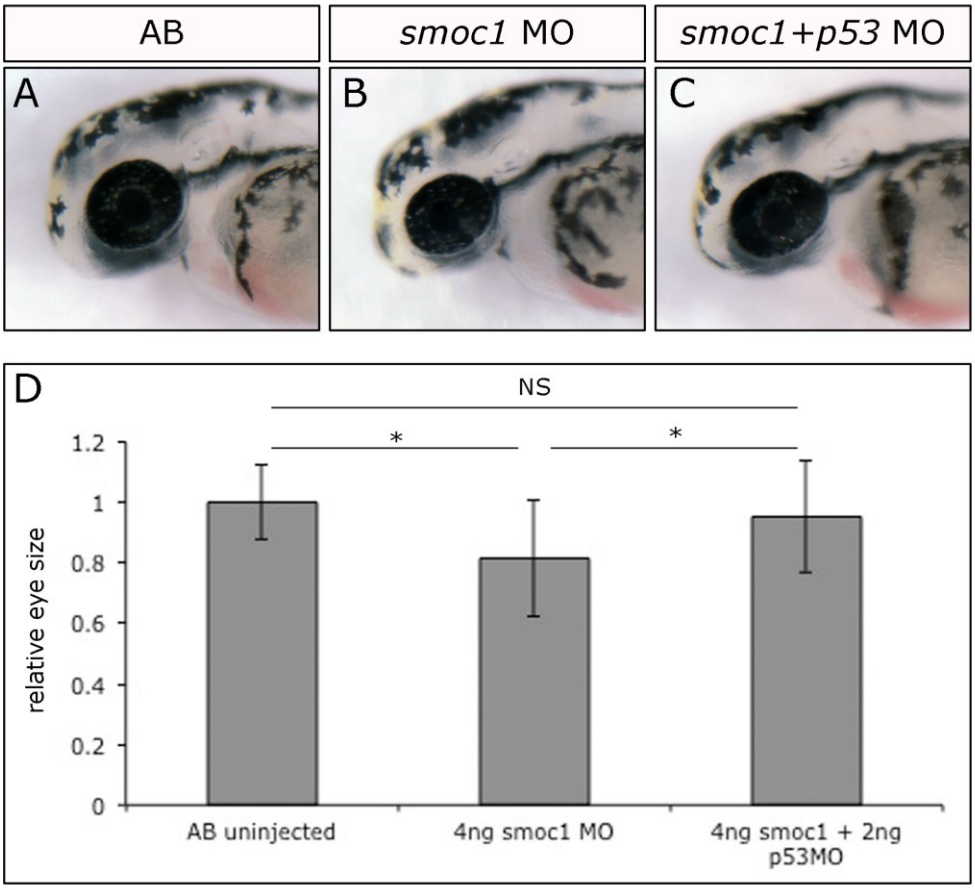

Figure 3.5: Reduction of Smoc1 protein levels results in microphthalmia in a p53 dependent manner.

(A-C) AB embryos injected with 4 ng of translation blocking smoc1 morpholino (B) had noticeably smaller eyes when compared to uninjected AB embryos (A). When smoc1 morpholino is coinjected with 2 ng p53 morpholino (C), the eye size appears similar to uninjected embryos (A). (D) Quantification of relative eye size obtained by measuring ocular area at 48 hpf. When compared to uninjected controls, smoc1 morphants have on average, a 20% reduction in eye area ($p < 0.01$, n = 35-36 embryos each). When smoc1 morpholino is coinjected with p53 morpholino, a statistically significant rescue in eye size is observed when compared to smoc1 morpholino alone ($p < 0.01$, n = 18, 35 embryos).

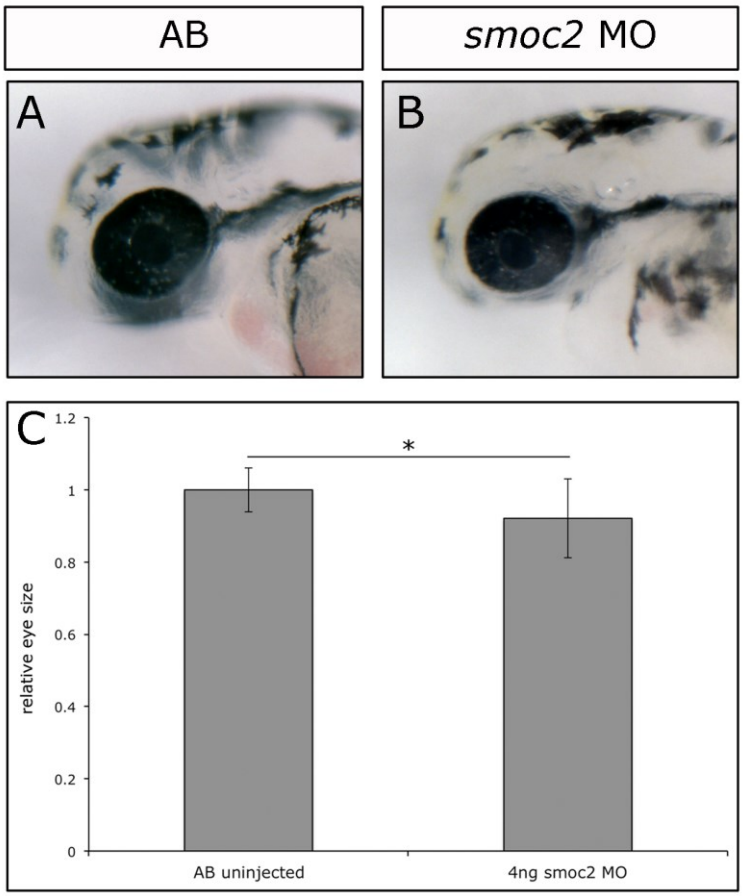

Figure 3.6: *smoc2* morphants have microphthalmia. (A, B) At 48 hpf, embryos injected with 4 ng of translation blocking *smoc2* morpholino (B) had a slight reduction in eye size when compared to uninjected AB controls (A). (C) Quantification of relative eye size obtained by measuring total ocular area at 48 hpf. On average, *smoc2* morphants have a 15% reduction in eye area when compared to AB uninjected controls (n = 14 embryos each, p = 0.0016).

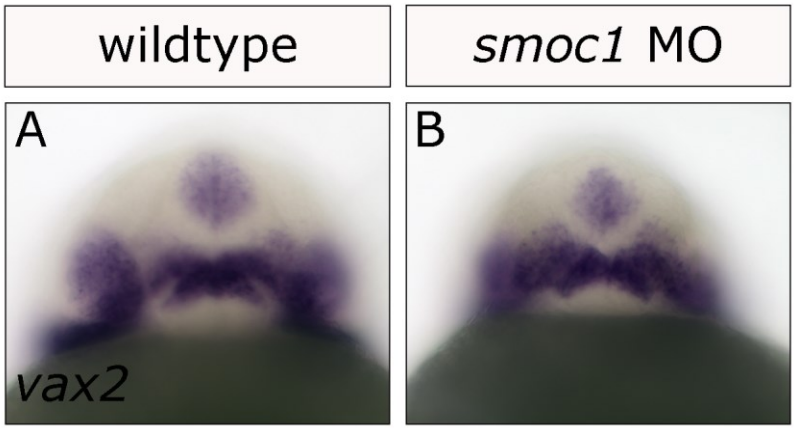

Figure 3.7: *smoc1* morphants have abnormal optic stalks. Frontal view of whole mount *in situ* hybridizations showing *vax2* expression in the optic stalks of uninjected AB embryos (A) and AB embryos injected with 4 ng of *smoc1* morpholino (B). The optic stalks in *smoc1* morphants (B) appear less constricted and are not as defined as the optic stalks seen in uninjected controls (A).

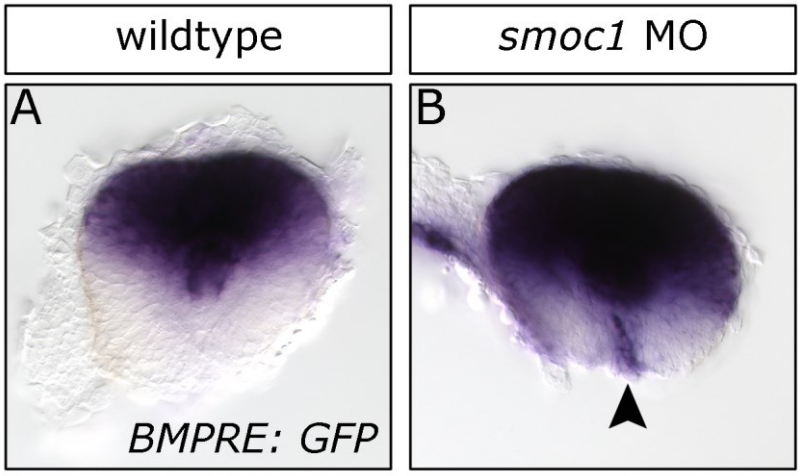

Figure 3.8: BMP signaling is expanded throughout the eye and into the choroid fissure when Smoc1 protein levels are reduced. *Tg(BMPRE-AAV.Mlp:eGFP)* embryos were injected with 4 ng *smoc1* morpholno and expression of *GFP* was used as a readout for BMP signaling. (A) In uninjected controls, GFP expression and BMP signaling are restricted to the dorsal quadrant of the retina. (B) In *smoc1* morphants, BMP signaling is expanded to encompass the entire dorsal half of the eye (100% of morphants) and in 36% of these morphants, BMP signaling was expanded into the proximal choroid fissure (arrowhead; n = 33).

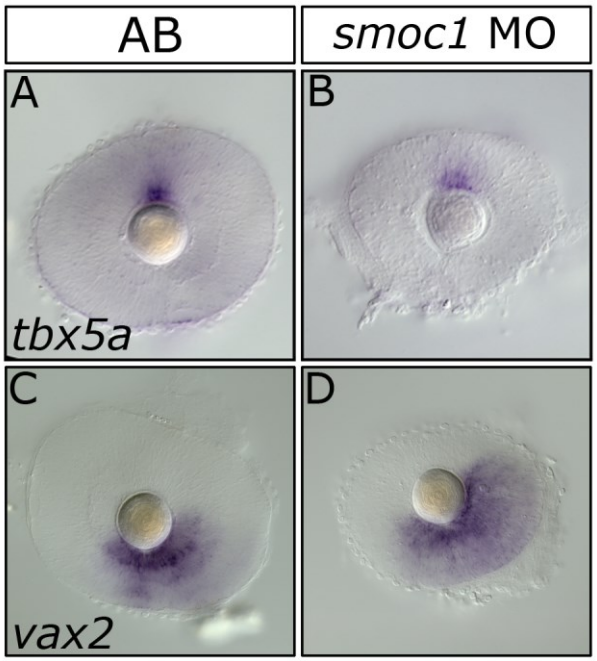

Figure 3.9: Smoc1 plays a minor role in patterning the DV retinal axis in zebrafish. Images show mounted eyes from 48 hpf embryos following *in situ* hybridization for the DV retinal markers *tbx5a* and *vax2*. (A, B) When compared to uninjected AB controls (A), *tbx5a* expression is slightly reduced in *smoc1* morphants (B). (C, D) Expression of the ventral marker *vax2* is slightly expanded in *smoc1* morphants (D) when compared to uninjected AB controls (C). Together, these results show that Smoc1 likely plays a minor role in the maintenance of DV retinal patterning.

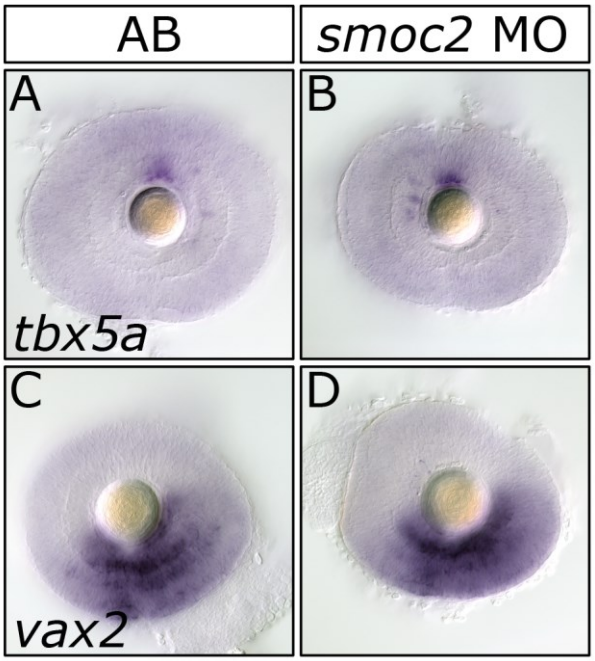

Figure 3.10: *smoc2* morphants have normal DV retinal patterning.Images are of eyes dissected from 48 hpf embryos following *in situ* hybridization for the DV retinal markers *tbx5a* and *vax2*. (A, B) There is no noticeable difference in *tbx5a* expression between uninjected AB controls (A) and embryos injected with 4 ng of translation blocking *smoc2* morpholino (B). (C, D) Similarly, no differences in *vax2* expression were observed between uninjected AB controls (C) and *smoc2* morphants (D).

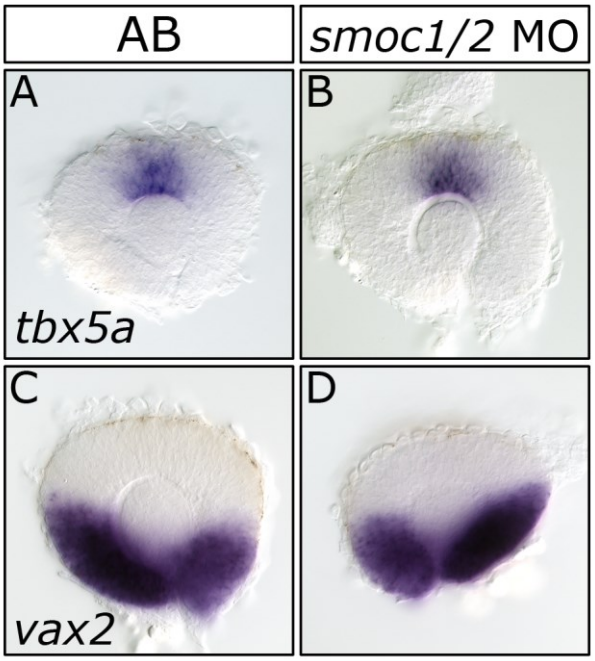

Figure 3.11: Smoc1 and Smoc2 do not act synergistically to pattern the DV retinal axis. Images are of eyes from 28 hpf embryos following *in situ* hybridization for the DV retinal patterning markers *tbx5a* and *vax2*. Embryos were injected with 2ng each of translation blocking *smoc1* and *smoc2* morpholino. (A, B) There is no noticeable difference in *tbx5a* expression between uninjected AB controls (A) and *smoc1/2* double morphants (B). (C, D) No differences were observed in *vax2* expression between uninjected AB controls (C) and *smoc1/2* morphants.

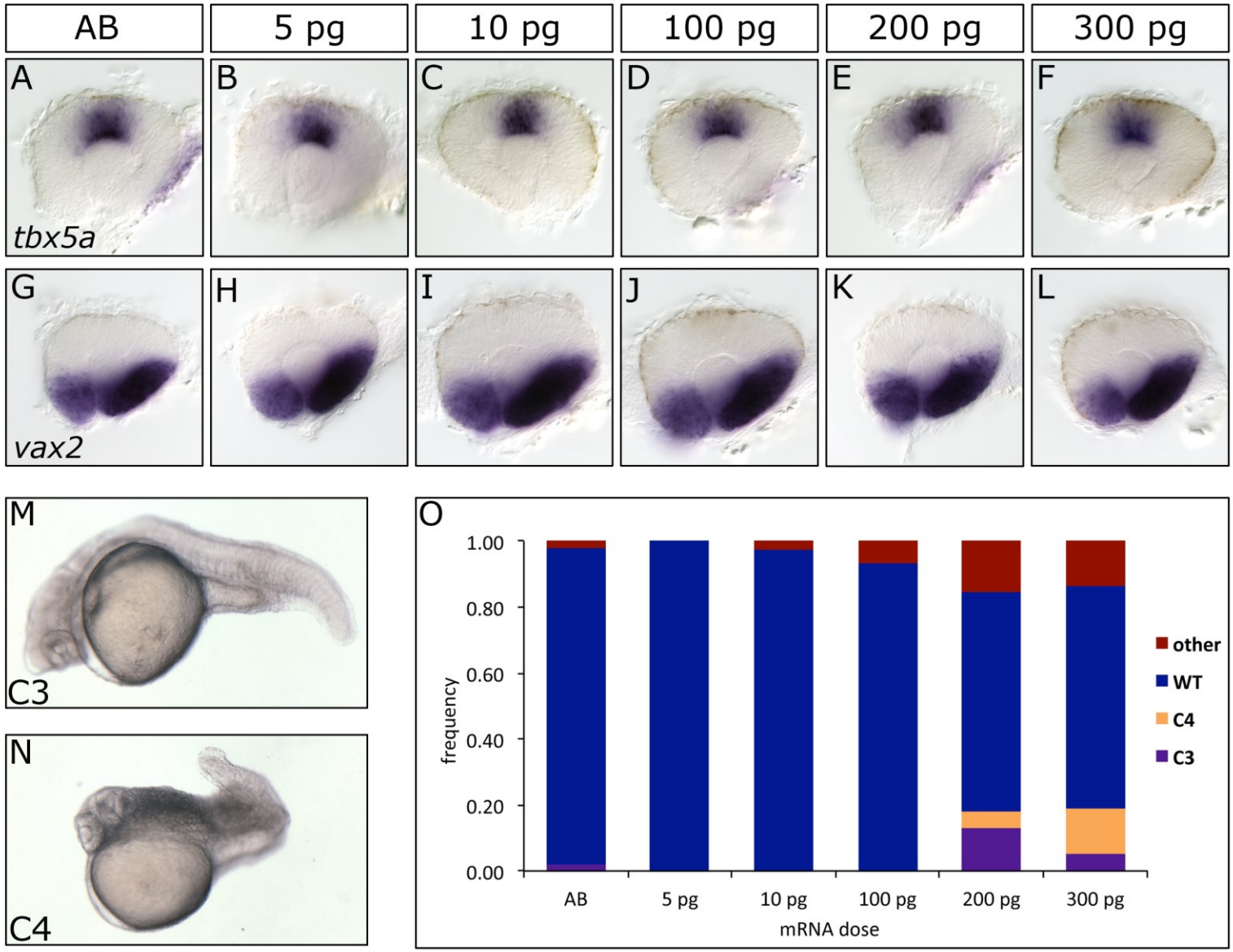
AB
5 pg
10 pg
100 pg
200 pg
300 pg
A
B
C
D
E
F
tbx5a
G
H
I
J
K
L
vax2
M
C3
N
C4
O
1.00
0.80
0.60
0.40
0.20
0.00
frequency
AB
5 pg
10 pg
100 pg
200 pg
300 pg
mRNA dose
other
WT
C4
C3

Figure 3.12: Overexpression of *smoc1* does not alter DV retinal patterning but does cause axis defects. (A-L) Dissected eyes from 28 hpf following injection with the indicated dose of *smoc1* mRNA and *in situ* hybridization for the DV patterning markers *tbx5a* and *vax2*. (A-F) When compared to uninjected AB controls (A), no change in *tbx5a* expression was seen at any of the *smoc1* mRNA doses used (B-F). (G-L) Similarly, no change was observed in *vax2* expression when comparing uninjected AB controls (A) to any of the *smoc1* mRNA doses used. (M, N) Overexpression of *smoc1* causes mild dorsalization phenotypes similar to loss of *bmp2*. Embryos were classified into the dorsalized classes C1-C5 based on descriptions from (Kishimoto et al. 1997). (O) Quantification of the proportion of embryos at each *smoc1* mRNA dose showing dorsalized phenotypes. The category other encompasses cyclopia and other gross morphological defects that do not resemble axis patterning defects.

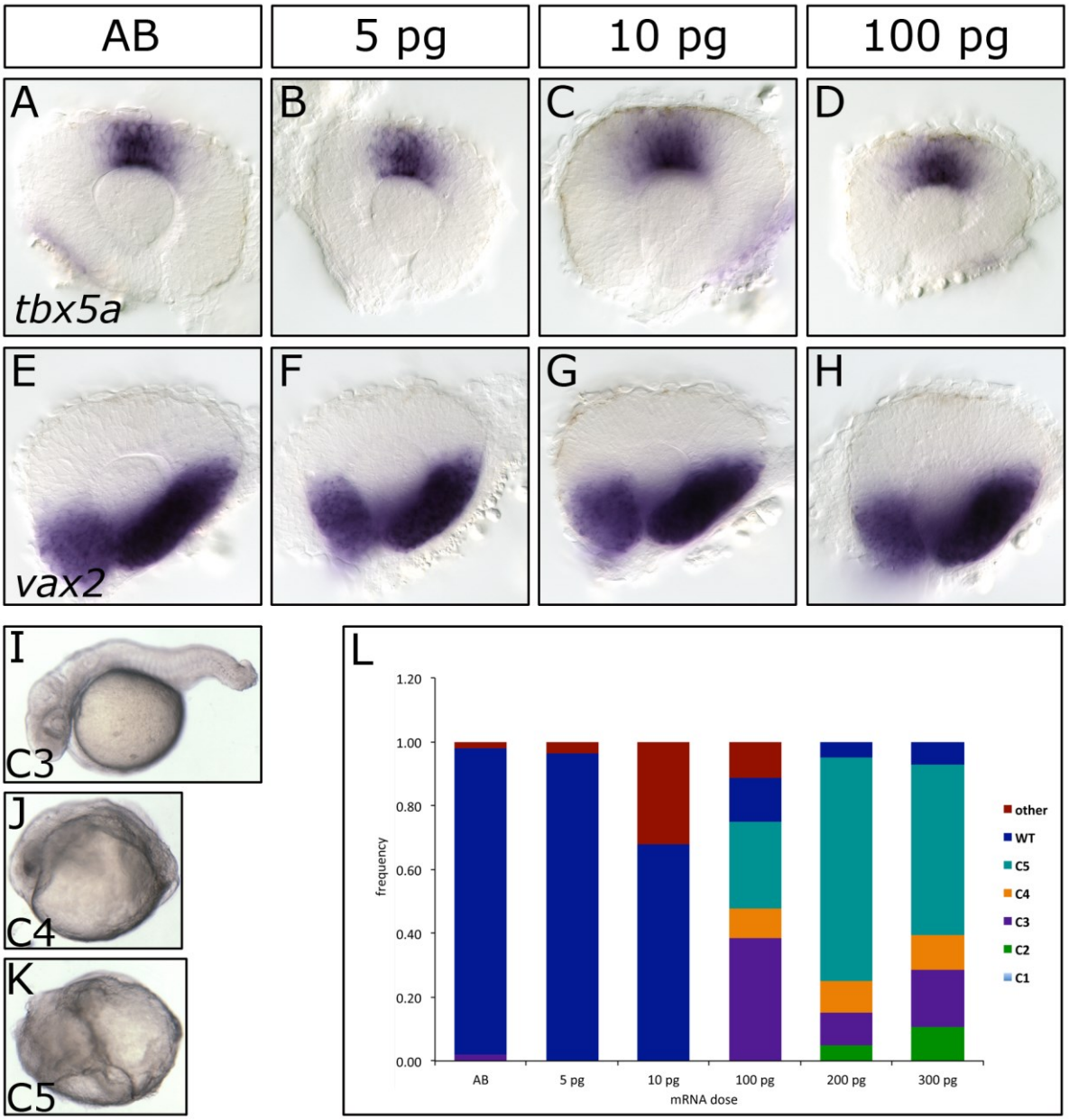

Figure 3.13: Overexpression of smoc2 does not alter DV retinal patterning, but it does cause axial defects similar to loss of a BMP. (A-H) Dissected eyes from 28 hpf embryos following injection of *smoc2* mRNA at the doses indicated and *in situ* hybridization for the DV retinal patterning markers *tbx5a* and *vax2*. (A-D) At all mRNA doses tested, no difference in *tbx5a* expression was observed between uninjected AB controls (A) and embryos injected with *smoc2* mRNA (B-D). (E-H) No change in *vax2* expression was observed when comparing uninjected AB controls (E) to embryos injected with the indicated dose of *smoc2* mRNA (F-H).

(I-K) Overexpression of *smoc2* dorsalizes embryos similar to what is seen in *bmp2b* mutants. (I) Embryo that is mildly dorsalized in the C3 phenotype category. (J, K) Embryos with severe dorsalization where only remnants of head structures can be observed were categorized as C4 (J) and C5 (K). (L) Quantification of the proportion of dorsalized embryos observed at each dose of *smoc2* mRNA. The other category encompasses holoprosencephaly, severe necrosis, tail and somite defects, and other gross morphological defects that do not fit in the categories outlined in (Kishimoto et al. 1997).

Chapter 4

Investigating the role of Grem2b in zebrafish eye development

Introduction

Gremlin, otherwise known as protein related to DAN and Cerberus (PRDC) or as down regulated by v-*mos* (DRM), proteins are members of the DAN family, which also includes the TGF-β inhibitors Cerberus, Coco, and Sclerostin (Avsian-Kretchmer & Hsueh 2004). The DAN family of TGF-β inhibitors is characterized by an eight-member cysteine knot domain, also known as the DAN domain. Within the DAN domain is a C-terminal cysteine knot (CTCK) domain, a cysteine knot domain structurally similar to the six-membered cysteine knot characteristic of TGF-β ligands (Avsian-Kretchmer & Hsueh 2004; Nolan et al. 2013). The additional two cysteines found in the DAN family of TGF-β inhibitors are thought to confer non-covalent dimerization and TGF-β inhibitory capabilities (Avsian-Kretchmer & Hsueh 2004; Kattamuri et al. 2012).

Gremlin is able to bind and inhibit, in decreasing order of affinity, BMP2, BMP4, and BMP7 (Hsu et al. 1998; Kriebitz et al. 2009; Church et al. 2015). Characterization of Gremlin has largely been done using biochemical approaches but little is known about the functions of Gremlin proteins in a developmental context. Studies on the role of Gremlin during development have used global or tissue specific overexpression of Gremlin which does not reveal much about the function of Gremlin, but rather provides information on how BMPs would normally function in the tissues being studied.

Gremlin2 (*Grem2*), initially named *PRDC*, was first described following a gene trap screen done to identify developmentally important genes in mice (Minabe-Saegusa et al. 1998). Concomitant with the initial description of *Grem2*, Gremlin was identified as a secreted TGF-β inhibitor in a screen for its ability to induce a secondary axis when overexpressed in *Xenopus* (Hsu et al. 1998). Further characterization of Gremlin has been done by studying avian limb development. During limb formation, Gremlin inhibits BMP regulated apoptosis thereby allowing the continuation of limb outgrowth and the persistence of interdigital tissue in species with webbed feet (Merino et al. 1999). *Gremlin*, and in zebrafish *grem2b*, are expressed in neural crest, but little is known about the

function of Gremlin proteins in this cell population (Kelly et al. 2004; Hsu et al. 1998; Tzahor et al. 2003; Müller et al. 2006).

In zebrafish, inhibition of BMP signaling is required for proper heart development, which is achieved by the close proximity of *grem2b* expressing cells in the ventral pharyngeal arches to the developing cardiac field. Inhibition of BMP signaling by Grem2b is required for the differentiation of atrial cardiomyocyte precursors as well as for cardiac looping and for normal atrial rhythms (Müller et al. 2013). During cranial neural crest cell (CNCC) migration, inhibition of BMP signaling by Grem2b is necessary to restrict BMP signaling to the ventral most portion of the CNCC population and allow for proper dorsoventral patterning of the craniofacial skeleton (Zuniga et al. 2011). Despite the characterization of Grem2b function in neural crest cells and previous work showing that *grem2b* is expressed in neural crest and in the eye, the function of Grem2b in eye development has yet to be studied.

In zebrafish, it has been reported that *grem2b* is expressed in the neural crest and periphery of the ventral retina (Müller et al. 2013). Since *grem2b* is expressed in the eye and Gremlin proteins are involved in regulating BMP signaling, it is hypothesized that Grem2b regulates ocular BMP signaling and other BMP mediated aspects of eye development. To test this hypothesis, loss of function studies in zebrafish using morpholino oligonucleotides were done to determine how a reduction in Grem2b levels affects eye development and ocular BMP signaling.

Results & Discussion

Gremlin proteins are highly conserved

Due to the teleost genome duplication, zebrafish have two *grem2* paralogs, *grem2a* on chromosome 17, and *grem2b* on chromosome 12, while higher vertebrates including humans and mice have a single *GREM2* ortholog. Protein alignments show that the amino acid sequence is highly conserved amongst Grem2a and Grem2b in zebrafish and human and mouse GREM2 (Figure 4.1). Grem2a has a stretch of 15 amino acids in the N-terminal region and 14 amino acids near the C-terminus that are not present in its paralog, Grem2b, or human

or mouse GREM2 (Figure 4.1). The high degree of conservation between zebrafish Grem2b and human and mouse GREM2 suggest that *grem2b* is the ortholog of *Grem2* in humans and mice.

Both Grem2a and Grem2b have a DAN domain characteristic of the DAN family of BMP inhibitors in addition to a CTCK domain within the DAN domain, which is characteristic of TGF-β ligands and is involved in dimerization (Figure 4.2) (Avsian-Kretchmer & Hsueh 2004; Nolan et al. 2013). The additional amino acids in Grem2a fall within the DAN domain and at the beginning of the CTCK domain, but the effect of these additional amino acids on protein function is unclear (Figure 4.2 A). Since the sequence of *grem2a* has only recently been made available, all of the following experiments only examined the role of *grem2b* in zebrafish eye development.

grem2b expression

Expression patterns for *grem2b* have already been published, but it was not entirely clear from the available images where exactly *grem2b* is expressed within the eye (Müller et al. 2006). In order to characterize *grem2b* expression, whole mount *in situ* hybridization was done at multiple developmental stages. Expression of *grem2b* was found to be restricted to neural crest from 16-19 hpf (Figure 4.3 A-B). At later stages, *grem2b* is expressed at the edges of the ventral eye in what appears to be a migratory neural crest population that migrates exclusively to the ventral eye (Figure 4.3 C-D). By 32 hpf, *grem2b* expressing cells appear to be migrating through the choroid fissure and over the ventral retina (Figure 4.3 D). Like other BMP inhibitors, *grem2b* expression at 48 hpf is restricted to the ventral CMZ (Figure 4.3 E).

This expression pattern of *grem2b* observed in this experiment is similar to published expression patterns at the developmental stages examined. In accordance with previously published expression patterns, *grem2b* expression was found to be in the neural crest. Although previous work has shown that *grem2b* is expressed in a subpopulation of cranial neural crest cells, no association was made between *grem2b* expressing cranial neural crest cells and the cells expressing *grem2b* at the periphery of the ventral eye (Müller et al.

2006). The finding that *grem2b* expression in the eye appears to be due to migratory cells suggests that *grem2b* marks a novel population of POM cells that has not previously been described. POM cells are essential for the formation of many anterior ocular components, and notably, the presence of POM cells in the choroid fissure is necessary for choroid fissure closure (Lupo et al. 2011; Gage et al. 2005; Creuzet et al. 2005). Since *grem2b* expressing cells appear to migrate exclusively to the ventral eye, it is possible that the cells that localize to the choroid fissure and regulate fissure closure are from the *grem2b* expressing population of POM cells. By further studying the dynamics and characteristics of this cell population, the mechanisms through which these extraocular cells direct choroid fissure closure can be further elucidated.

The observed expression pattern of *grem2b* is similar to the expression of *gremlin* in other species, indicating that Gremlin proteins have an evolutionarily conserved role during the development and migration of neural crest. *Gremlin* is expressed in the mandibular neural crest in mice, *Xenopus*, and chick (Kelly et al. 2004; Hsu et al. 1998; Tzahor et al. 2003). Unlike what has been observed in zebrafish, *gremlin* expressing mandibular neural crest cells in chick and *Xenopus* surround the entire eye. It is thought that these mandibular neural crest cells differentiate into extraocular muscles in low BMP conditions which occurs when the cells migrate away from the BMP secreting neural tube and secrete the BMP inhibitor Gremlin (Hsu et al. 1998; Tzahor et al. 2003; Sambasivan et al. 2011). It is possible that *grem2b* expressing cells in zebrafish serve a similar function, however lineage tracing experiments would be required to investigate this further.

grem2b expression is altered in *gdf6a* mutants

Since it was observed that *grem2b* expressing cells appear to migrate exclusively to the ventral eye, it was hypothesized that there is a chemoattractant signal originating from the ventral eye that directs this subpopulation of cells to the ventral eye. To test this hypothesis, *grem2b* expression was examined using whole mount *in situ* hybridization on embryos from *gdf6a*$^{+/-}$ incrosses since homozygous *gdf6a* mutants have ventralized eyes (French et al. 2009; Gosse & Baier 2009). Expression of *grem2b* at 28 hpf appeared to be normal in 77% of the

embryos from *gdf6a*$^{+/-}$ incrosses (Figure 4.4 A) while the remaining 23% of embryos (n = 26 embryos total) had a defined stripe of *grem2b* expression at the midline of the dorsal eye (Figure 4.4 B). As the ratio of the number of normal *grem2b* expressing embryos to abnormally expressing embryos is close to the expected Mendelian ratio from incrossing heterozygotes, it can be concluded that the embryos with the abnormal stripe of *grem2b* expression in the dorsal eye are *gdf6a*$^{-/-}$ mutants. At 48 hpf, when *gdf6a*$^{-/-}$ mutants exhibit a clear microphthalmic phenotype, *grem2b* expression was restricted to the ventral CMZ in wild-type embryos (Figure 4.4 C) and *gdf6a*$^{-/-}$ mutants had *grem2b* expression expanded throughout the CMZ (Figure 4.4 D).

While *grem2b* expression in the ventral eye of wild-type embryos is somewhat stochastic due to *grem2b*'s expression in what appears to be a migratory cell population, the expression of *grem2b* in the dorsal eye of *gdf6a* mutants did not vary and no stream of *grem2b* expressing cells migrating to the dorsal eye was observed (Figure 4.8 B), making it unclear if the aberrant *grem2b* expression is due to CNCC migrating to the dorsal eye or if the aberrant expression of *grem2b* occurs within the eye itself. If these *grem2b* expressing cells in the dorsal eye of *gdf6a*$^{-/-}$ mutants are indeed migratory, the migration of these cells to what appears to be the location of the posterior or dorsal groove in the ventralized eye of *gdf6a* mutants implies that the persistent dorsal groove observed in *gdf6a* morphants has a molecular signature reminiscent of the choroid fissure in the ventral eye rather than being a true persistent dorsal groove (Schmitt & Dowling 1994; Asai-Coakwell et al. 2007).

The migration of *grem2b* expressing cells exclusively to the ventral half of the eye in wild-type embryos and the presence of *grem2b* expressing cells in the ventralized dorsal eye of *gdf6a* mutants suggests that there are chemoattractants emanating from the ventral eye, and possibly from the choroid fissure that directs this subpopulation of cells to the ventral eye and through the choroid fissure. This hypothesis is further supported by a previous study that demonstrates that the eye must be present in embryos to direct the migration of POM cells to the eye (Langenberg et al. 2008). Further work is required to identify chemoattractants involved in this migratory process by examining the expression of candidate

chemoattractants in wild-type and *gdf6a*$^{-/-}$ mutants to see if the expression pattern of candidate genes is similar to the *grem2b* expression pattern in wild-type and mutant embryos. Candidate chemoattractants that appear to be expressed in the ventral eye and choroid fissure include: *eph receptor-b4a* (*ephb4a*), *ephrin-B2a* (*efnb2a*), *neuropilin 2b* (*nrp2b*), *semaphorin 3fa* (*sema3fa*), *semaphorin 3fb* (*sema3fb*), *slit homolog 2* (*slit2*) and *vasorin a* (*vasna*). Another possibility that has also been previously suggested in the literature is that RA could act to direct POM to the eye (Langenberg et al. 2008). Since the RA synthesis genes *aldh1a2* and *aldh1a3* are expressed in the dorsal and ventral regions of the eye respectively, this would imply that the subpopulation of *grem2b* expressing cranial neural crest cells could potentially respond to only high levels of RA in the ventral eye, or they migrate at an early enough timepoint where RA from the dorsal eye is at negligible levels. Further characterization of the expression of these genes in wild-type and *gdf6a* mutants could help to further elucidate the mechanisms through which POM cells migrate to the eye and could be used as a tool to determine why POM cells migrating to the choroid fissure are necessary for choroid fissure closure (Lupo et al. 2011).

grem2b morphants have microphthalmia

Previous studies have characterized the expression of *grem2b*, but little is known on its role in eye development. To further examine the function of *grem2b*, translation blocking antisense morpholinos were used to reduce Grem2b protein levels and eye development was observed throughout development. When Grem2b protein levels were reduced, groups of apoptotic cells were observed in the forebrain and what appeared to be neural crest cells. Although apoptosis from specific and off target morpholino effects cannot be differentiated in this experiment, the localized apoptosis of certain cell populations suggests that the apoptosis caused by *grem2b* morpholino is a result of a reduction in Grem2b protein levels and is not from non-specific morpholino effects. This finding is further supported by the previous characterization of Gremlin in limb and digit development where Gremlin was found to have an antiapoptotic role to prevent interdigital tissue regression in avian species (Merino et al. 1999).

In addition to the apoptotic phenotype observed when Grem2b protein levels are reduced, *grem2b* morphants also exhibited a range of ocular phenotypes including microphthalmia (53% of embryos, n = 51 embryos total; Figure 4.5 C-E) and of those microphthalmic embryos, some also had noticeable ventral eye defects with ventral eye thinning and coloboma (12% of embryos; Figure 4.5 D-E). To further characterize this microphthalmic phenotype, eye area was measured in *grem2b* morphants at 72 hpf. On average, *grem2b* morphants had a statistically significant 15% reduction in eye area ($p<0.0001$, n = 34 embryos) (Figure 4.6).

These results indicate that Grem2b regulates eye size, but the mechanisms through which it does this are still unknown. Since *grem2b* is expressed in an extraocular cell population that migrates to the eye early in eye development, it is possible that the secretion of Grem2b by this migratory cell population is required for cell survival within the eye or that *grem2b* expressing cells integrate into the eye and their contribution to the eye is necessary for normal eye size. The expression of *grem2b* in the CMZ at 48 hpf also suggests the possibility that Grem2b has an antiapoptotic function within the progenitor pool in the CMZ and the loss of cells in the progenitor pool could also contribute to the microphthalmic phenotype at later stages of eye development.

Understanding why *grem2b* morphants have microphthalmia can further our understanding on POM dynamics and how the interaction between POM and the developing eye regulates ocular morphogenesis. However, as mentioned above, the use of morpholinos to study Grem2b function is not ideal as one of the known off-target effects of morpholinos is apoptosis and Gremlin has been characterized as an antiapoptotic protein, making the generation and characterization of *grem2b* mutants necessary to further study the function of this gene.

The finding that *grem2b* morphants have ventral eye defects including coloboma is not entirely surprising because *grem2b* expressing cells migrate to the ventral eye and choroid fissure and previous studies demonstrate that POM migration to the choroid fissure is essential for proper ventral eye development and choroid fissure closure (Lupo et al. 2011). Although the ocular defects

observed in this experiment were expected, it is still not known how POM contributes to fissure closure, nor if the inhibition of BMP signaling by Grem2b is a necessary component of this process. It is known that POM cells contribute to multiple anterior structures within the eye including the cornea, sclera, trabecular meshwork, Schlemm's canal, extraocular and ciliary muscles, and vasculature (Gage et al. 2005). Further experiments are required to determine which, if any, structures in the eye the *grem2b* expressing subpopulation of cranial neural crest cells contributes to, which could further our understanding of the dynamics of POM cell migration.

grem2b morphants have expanded BMP signaling

Gremlin proteins have been characterized as BMP inhibitors that dimerize and inhibit BMP 2, 4, and 7 signaling (Hsu et al. 1998; Avsian-Kretchmer & Hsueh 2004) (Nolan et al. 2013; Church et al. 2015). The BMP inhibitory function of Gremlin proteins has largely been studied in cell culture or through overexpression experiments that result in dorsalized embryos, but nothing is known on whether the small population of *grem2b* expressing cells that localizes to the eye has the ability to regulate BMP signaling originating from the dorsal eye. To test if Grem2b can regulate BMP signaling in the eye, *grem2b* translation blocking antisense morpholino oligonucleotides were injected with translation blocking *p53* morpholino into the BMP reporter line *Tg(BMPRE-AAV.Mlp:eGFP)*. The *p53* morpholino was used to negate the apoptotic effects of the *grem2b* morpholino since the transgenic line used appears to be sensitized to changes in BMP signaling when compared to the wild-type AB line. Following injection of these morpholinos, *in situ* hybridization was done to examine GFP expression in the eye. Embryos injected with *grem2b* and *p53* morpholinos had mildly expanded GFP expression (53%) that expanded to the midline of the eye or GFP expression throughout the eye (48%) while uninjected embryos had GFP expression restricted to the dorsal quadrant of the eye (n= 54 embryos; Figure 4.7).

As the eyes are abnormal in *grem2b* morphants, it is not clear if BMP signaling is expanded throughout the eye or if there is a loss of ventral eye tissue

in these morphants. Since *grem2b* expressing cells are only found in the ventral eye, it is plausible that there is a loss of ventral eye tissue in *grem2b* morphants with the sensitized *Tg(BMPRE-AAV. Mlp:eGFP)* background. It is also surprising that a small population of cells has the capability to regulate ocular BMP signaling throughout the eye. In contrast with loss of another BMP inhibitor, Smoc1, *grem2b* morphants did not have any alterations in BMP signaling in the choroid fissure, which is surprising since *grem2b* expressing cells localize to this structure (Chapter 3, Figure 3.8). It is possible that alterations in BMP signaling at the choroid fissure occur, but the transgenic line is not sensitive enough to observe changes in BMP signaling. It is also possible that Smoc1 from the ventral eye alone is sufficient to inhibit BMP signaling in the choroid fissure.

Summary and Future directions

This work has provided an initial characterization of the BMP inhibitor Grem2b during zebrafish eye development. In agreement with previous studies, *grem2b* was found to be expressed in a subset of cranial neural crest cells and at the periphery of the eye, but this is the first work that has associated *grem2b* expression with POM cells, a subset of neural crest cells that migrates to the eye and contributes to many anterior ocular structures (Müller et al. 2006). Strikingly, *grem2b* expressing cells appear to migrate only to the ventral eye indicating that expression of *grem2b* marks a subset of POM cells that could have a specialized function in ventral eye development. To date, no other POM marker has been described as marking a specific subset of POM cells that migrate to a precise location in the eye (Lupo et al. 2011). The migration of *grem2b* expressing cells to the choroid fissure could mean that inhibition of BMP signaling is required for choroid fissure closure, vascularization of the eye, or for POM cell differentiation.

Reducing Grem2b protein levels using translation blocking morpholinos resulted in microphthalmia and coloboma, further strengthening the hypothesis that Grem2b is involved in choroid fissure closure and that cells that express *grem2b* somehow regulate ocular development. During avian limb development, Gremlin acts as an anti-apoptotic factor, so it is not entirely surprising that

grem2b morphants had localized apoptosis in addition to microphthalmia (Merino et al. 1999). In order to further characterize the potential anti-apoptotic function of Grem2b in eye development and regulation of ocular size, *grem2b* mutants will need to be generated so that the non-specific apoptotic effects of morpholinos can be avoided.

It is not clear from this work if Grem2b directs eye development extraocularly or if these cells integrate into the eye and contribute to eye size and anterior structures including the hyaloid vasculature. One possibility is that Grem2b in the choroid fissure neutralizes the apoptotic effects of Bmp7b thereby allowing for choroid fissure closure and vascularization of the eye (Morcillo et al. 2006). In addition to regulating ocular size, Grem2b could also be necessary for extraocular muscle differentiation since in other species, Gremlin is secreted by mandibular neural crest cells and it is thought the low BMP conditions in the mandibular neural crest allows these cells to differentiate into extraocular muscles (Kelly et al. 2004; Hsu et al. 1998; Tzahor et al. 2003). In addition to generating *grem2b* mutants, *grem2b* transgenic lines should also be generated to follow the migration of *grem2b* expressing cells and if possible, lines should be generated that would allow for lineage tracing of *grem2b* expressing cells to determine which ocular and extraocular structures *grem2b* expressing cells contribute to.

The migration of *grem2b* expressing cells to the choroid fissure implies that migratory cues are being secreted by the ventral eye. One possibility is that the *grem2b* subpopulation of POM cells that migrate to the ventral eye respond to high RA levels established by the RA synthesis enzyme Aldh1a3. As RA has been shown to be necessary to direct POM cells to the choroid fissure and to direct fissure closure, it would be expected that there would be a reduction of *grem2b* cells in the ventral eye and choroid fissure when RA signaling is ablated (Lupo et al. 2011). Other candidate chemoattractants restricted to the ventral eye should be further investigated for their ability to direct *grem2b* expressing cells to the ventral eye and choroid fissure. Understanding how the subpopulation of *grem2b* cells differs from other POM cells could provide further clues on how *grem2b* cells migrate to the ventral eye. Generation of transgenic lines would be

greatly beneficial in understanding what exactly makes this subpopulation different from other neural crest populations by generating a molecular profile using fluorescence activated cell sorting (FACs) to isolate *grem2b* expressing cells followed by RNA-seq to examine expression levels of key transcription factors and cell migration factors. FACs analysis also opens up the possibility of transplanting *grem2b* cells to the dorsal eye to observe their behavior or to the ventral eye to see how excess *grem2b* expressing cells affects ventral eye development.

Surprisingly, it was shown that Grem2b can regulate BMP signaling in the dorsal retina. Reducing Grem2b protein levels resulted in expanded BMP signaling throughout the eye, an unexpected finding based on the small population of cells that *grem2b* expression is restricted to. BMP sources from the dorsal retina include Bmp2b, Gdf6a, and Bmp4 (Kruse-Bend et al. 2012; Gosse & Baier 2009; French et al. 2009). Since Grem1 has been described as having the highest affinity for Bmp2 followed by Bmp4, these two Bmp ligands are strong candidates for being inhibited by Grem2b during zebrafish ocular development (Church et al. 2015). Further work could investigate the possible interactions between Grem2b, Bmp2b, and Bmp4. Ideally, interactions could be tested using tissue specific overexpression of *bmp2b*, *bmp4*, and *grem2b* to see if *grem2b* can rescue *bmp2b* or *bmp4* overexpression and by examining how BMP signaling and expression of BMP target genes is altered in *grem2b* mutants.

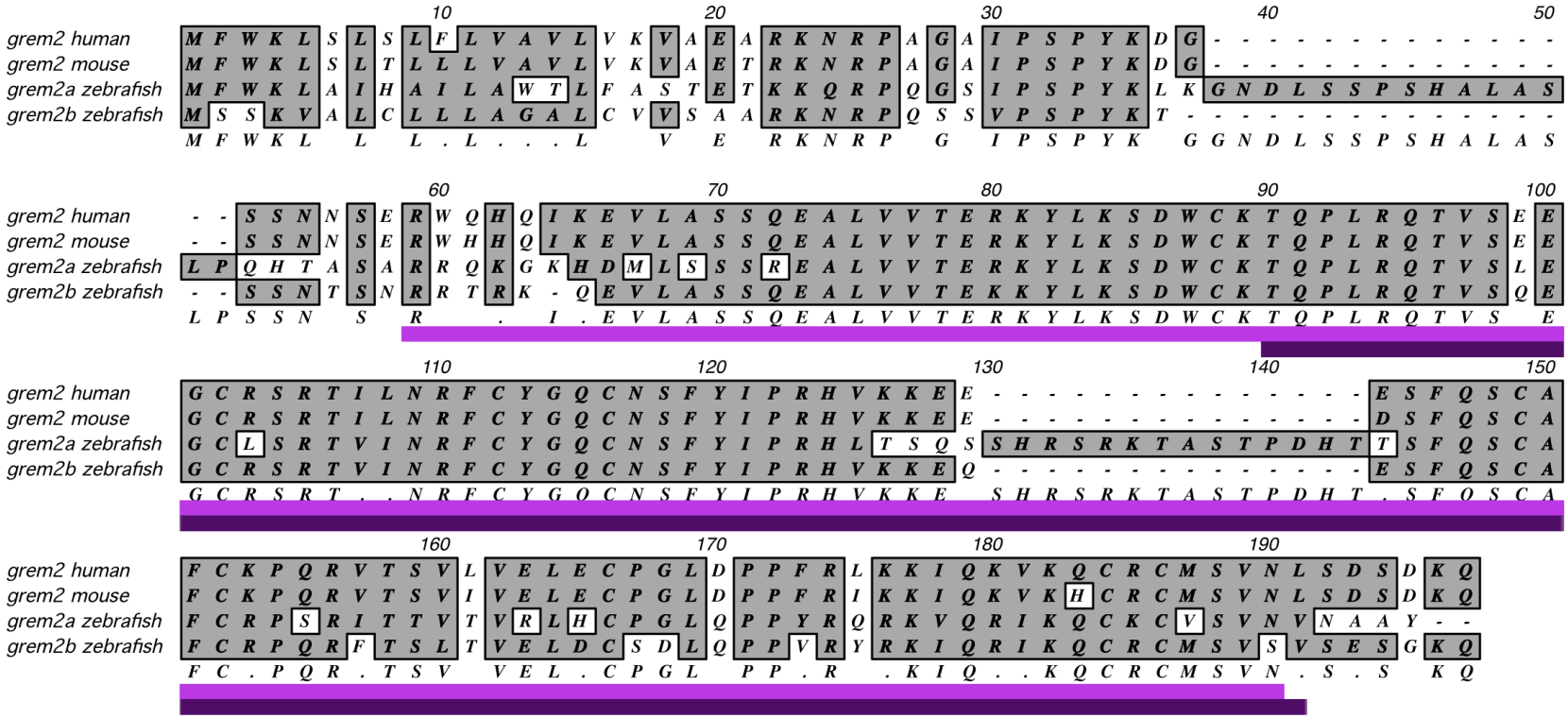

Figure 4.1: Grem2 proteins are highly conserved. Amino acid alignment showing the high degree of conservation between Grem2 in humans and mice and Grem2a and Grem2b in zebrafish. Zebrafish Grem2a has two regions of amino acids not present in the other grem2 proteins suggesting that Grem2b is the Grem2 homolog in zebrafish. The conserved functional domains are underlined in magenta (DAN domain) and eggplant (C-terminal cysteine knot domain).

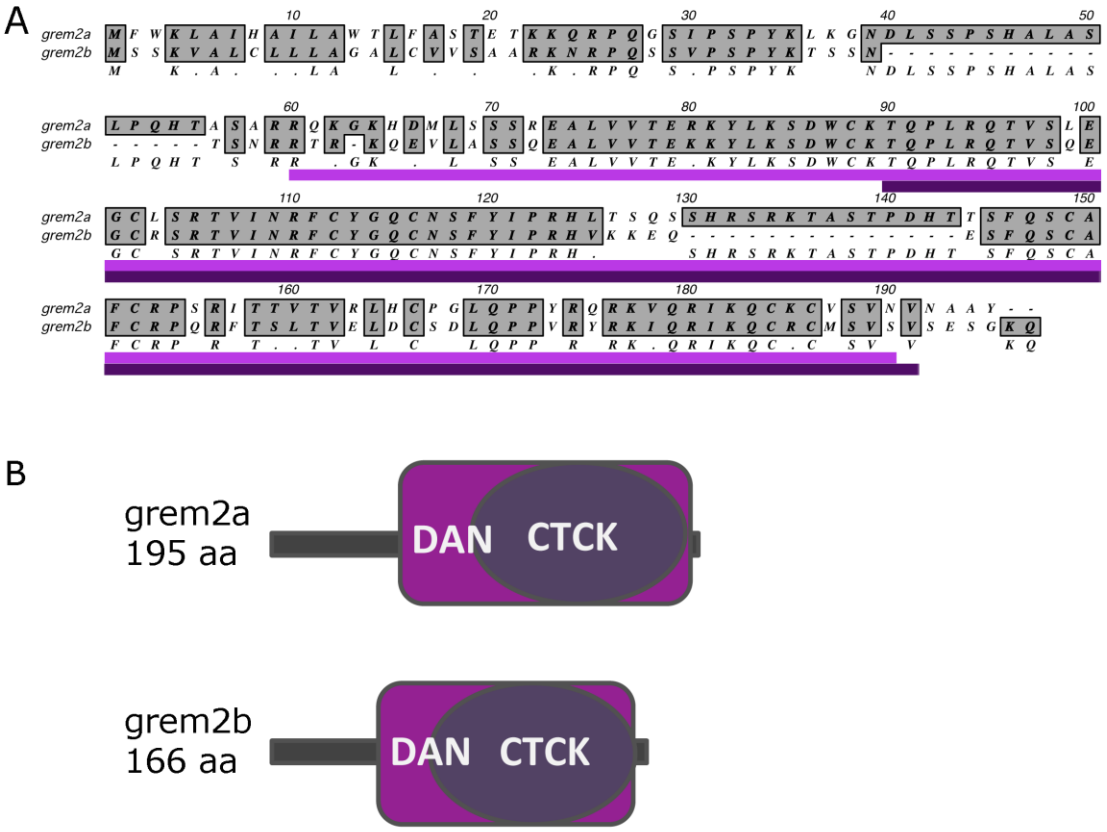

Figure 4.2: The zebrafish Grem2 paralogs, Grem2a and Grem2b, are highly conserved. (A) Alignment of zebrafish Grem2a and Grem2b proteins with the functional domains underlined in magenta (DAN domain) and eggplant (C-terminal cysteine knot domain; CTCK). There are an extra 14 amino acids within the CTCK domain of Grem2a. (B) Diagrams showing the functional domains in Grem2a and Grem2b. The C-terminal cysteine knot domain is found within the DAN domain.

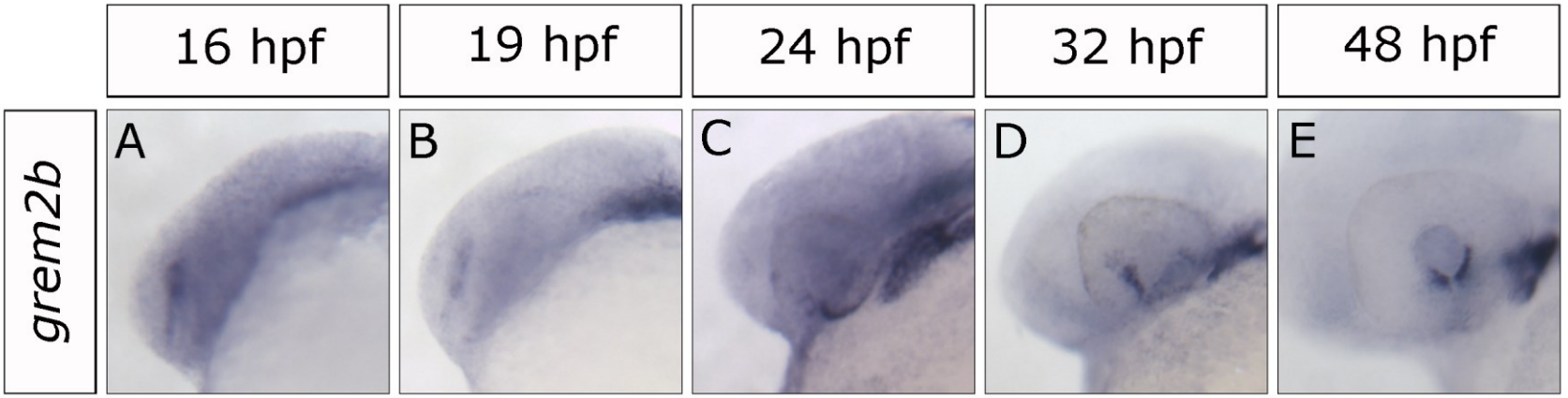

Figure 4.3: Expression of *grem2b* between 16 and 48 hpf of zebrafish development. *grem2b* is expressed within the neural crest at 16 hpf (A) and 19 hpf (B). By 24 hpf, *grem2b* appears to be expressed in neural crest cells that are beginning to reach the ventral eye (C). At 32 hpf, *grem2b* expression encompasses neural crest and cells found within the ventral eye (D). *grem2b* expression becomes restricted within the eye to the ventral CMZ by 48 hpf (E).

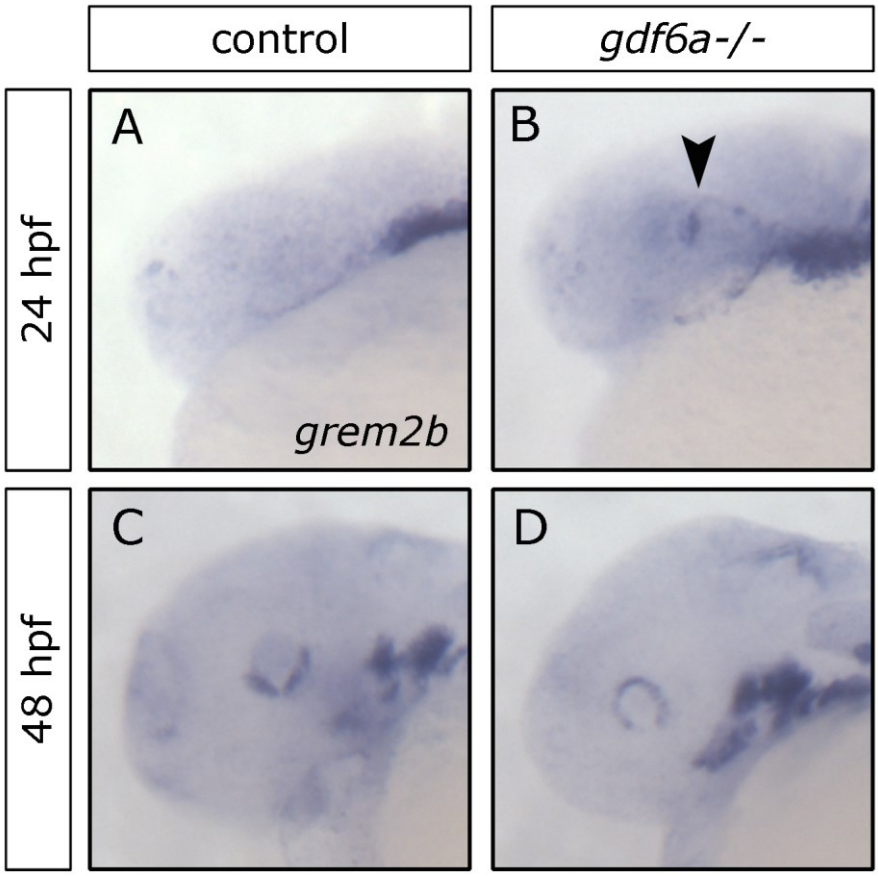

Figure 4.4: Expression of *grem2b* is altered in *gdf6a*$^{-/-}$ mutants. In 24 hpf wild-type embryos, *grem2b* expressing cells are beginning to reach the ventral eye (A), whereas in *gdf6a*$^{-/-}$ mutants, there is a stripe of *grem2b* expression at the midline of the dorsal eye (B; arrowhead). At 48 hpf, *grem2b* is expressed in the ventral CMZ (C) in wild-type embryos while in *gdf6a*$^{-/-}$ mutants, *grem2b* expression is expanded throughout the entire CMZ (D).

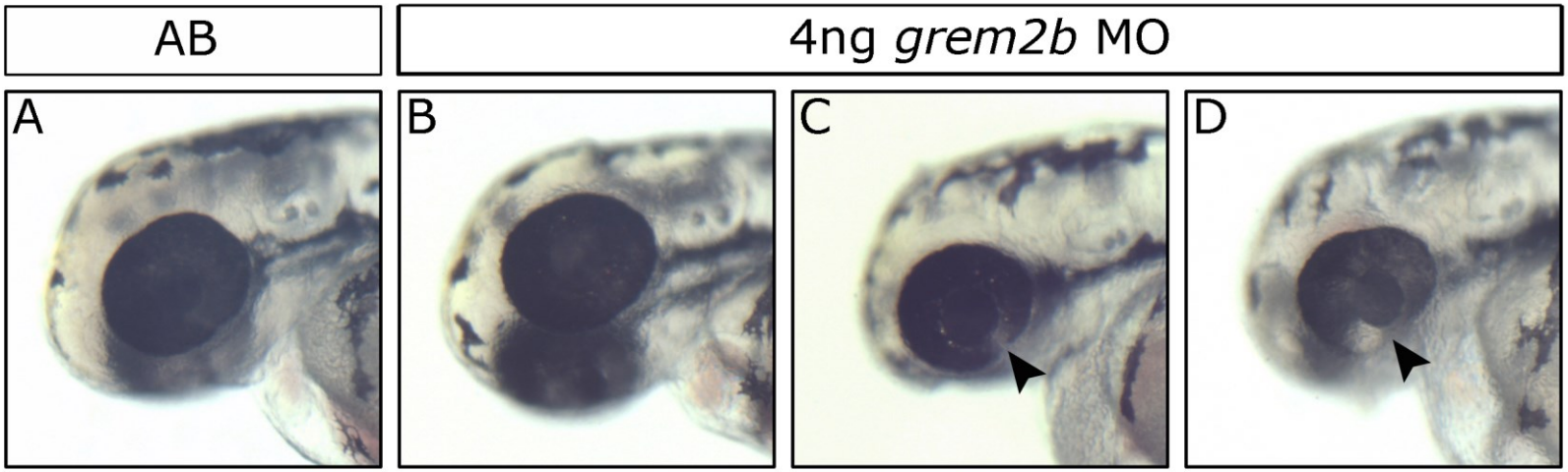

Figure 4.5: Reduction of Grem2b protein levels results in microphthalmia and ventral eye defects. At 48 hpf, comparable eye morphology was observed between wild-type AB uninjected embryos (A) and 47% of the *grem2b* morphants (B). The remaining 53% of embryos exhibited microphthalmia with 12% having obvious ventral eye defects (C-D, arrowheads) that ranged from ventral eye thinning (C) to incomplete choroid fissure closure (D).

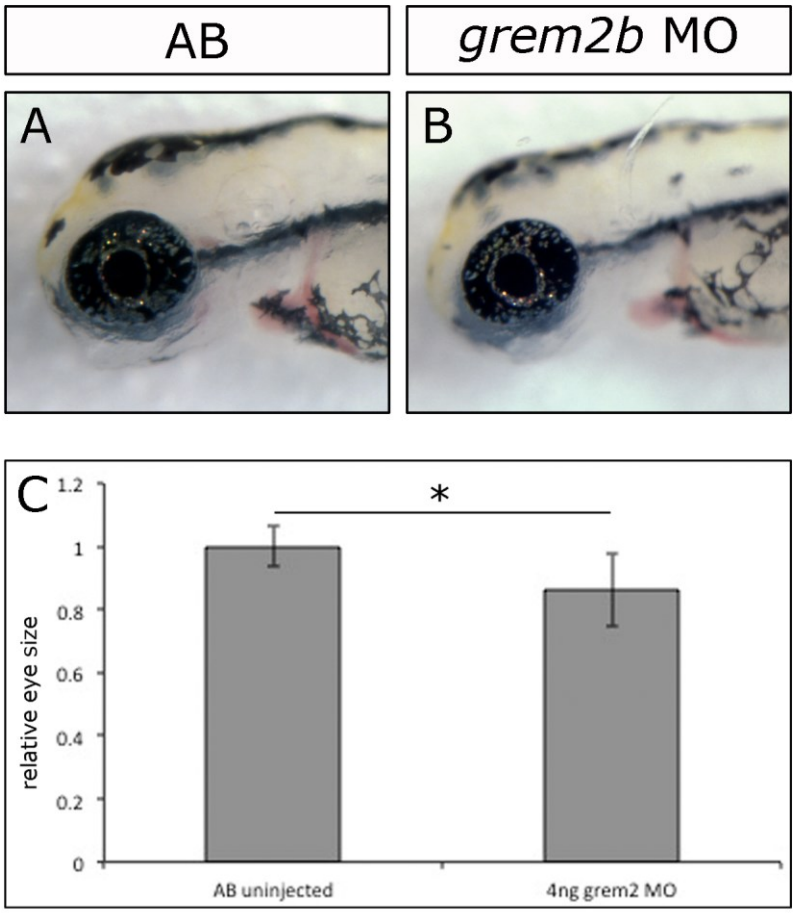

Figure 4.6: *grem2b* morphants exhibit microphthalmia. At 3 dpf, wild-type uninjected AB embryos (A) have noticeably larger eyes than *grem2b* morphants (B). (C) Relative average eye area was significantly reduced by approximately 15% in *grem2b* morphants ($p < 0.0001$, $n = 34$ embryos each).

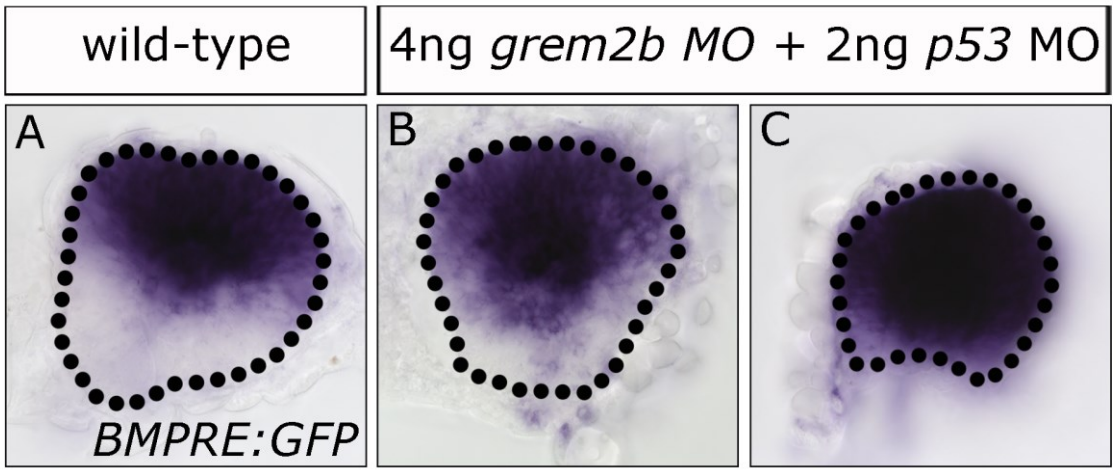

Figure 4.7: BMP signaling is expanded in *grem2b* morphants. *Tg(BMPRE-AAV.Mlp:eGFP)* embryos were injected with 4 ng of *grem2b* morpholino and 2ng of *p53* morpholino to prevent morpholino toxicity. (A) Dissected eye of an uninjected embryo showing BMP signaling is restricted to the dorsal quadrant of the eye. (B) In 53% of the *grem2b* morphants, BMP signaling was expanded, but did not encompass the entire eye. (C) 47% of *grem2b* morphants had BMP signaling expanded throughout the eye in addition to severe microphthalmia (n = 54 embryos). Eye tissue is outlined in black.

Chapter 5

Examining the function of the retinoic acid synthesis enzyme Aldh1a3 in vertebrate eye development

Some of the experiments (Figures 5.2-5.6) done in this chapter were done as part of a Biology 499 undergraduate research project.

Introduction

Retinoic acid (RA) is a diffusible vitamin A metabolite that acts as a morphogen during embryonic development. Retinol, one form of vitamin A, is imported into the cell by STRA6 (Figure 5.1). Once in the cell, retinol is oxidized to retinal by retinol dehydrogenase (RDH) enzymes. Retinal is then oxidized to RA by aldehyde dehydrogenases (ALDH) otherwise known as retinaldehyde dehydrogenases (RALDH) (Rhinn & Dollé 2012). There is also evidence suggesting that the cytochrome p450 enzyme CYP1B1 can catalyze both oxidation steps (Chambers et al. 2007). Further oxidation of RA by the cytochrome p450 26 (CYP26) enzymes to polar metabolites abolishes the biological activity of RA and promotes RA degradation (Duester 2008). RA can signal in an autocrine fashion or diffuse to nearby cells in a paracrine fashion by binding to nuclear RA receptors (RAR) heterodimerized to retinoid X receptors (RXR) which are bound to retinoic acid response elements (RAREs). Binding of RA to receptors displaces corepressors and recruits coactivators thereby activating of downstream gene expression (Figure 5.1).

In humans, maternal Vitamin A deficiency and mutations in multiple genes involved in RA synthesis and signaling have been associated with MAC (Gregory-Evans, Williams, et al. 2004b; Williamson & Fitzpatrick 2014). Mutations in *STRA6* and *RARB* manifest as microphthalmia and anophthalmia with extraocular developmental anomalies (Williamson & Fitzpatrick 2014). Mutations in *STRA6* and *RARB* are rare, likely due to the syndromic phenotypes observed and the resulting reduced viability (Williamson & Fitzpatrick 2014). Lesions in *ALDH1A3* have been identified as an autosomal recessive cause of MAC with phenotypes that range from mild microphthalmia to microphthalmia with coloboma and anophthalmia (Williamson & Fitzpatrick 2014; Yahyavi et al. 2013; Fares-Taie et al. 2013; Mory et al. 2013; Aldahmesh et al. 2013; Abouzeid et al. 2014; Semerci et al. 2014). Mutations in *ALDH1A3* have been estimated to account for up to 10% of MAC cases, making mutations in this gene one of the most common causes of inherited MAC (Abouzeid et al. 2014; Gerth-Kahlert et al. 2013; Williamson & Fitzpatrick 2014). Although human studies have clearly

demonstrated a strong correlation between MAC and mutations in genes involved in RA synthesis and signaling, studies in vertebrate model systems that have attempted to elucidate the role of RA in eye development has produced conflicting results.

Within the developing embryo, RA morphogen gradients are established through spatially restricted expression of RA synthesis and degradation enzymes. During eye development, the RA synthesis genes *retinol dehydrogenase 10a* (*rdh10a*) and *aldehyde dehydrogenase 1a3* (*aldh1a3*) are expressed within the ventral retina while *aldh1a3* is expressed in the dorsal retina and *cyp1b1* is expressed in the dorsal and ventral eye (French et al. 2009). The spatial restriction of RA synthesis genes within the developing vertebrate eye indicates that high levels of RA are required in the ventral and dorsal regions of the eye, but how RA functions during eye development is still not fully understood. One possibility is that high levels of RA in the dorsal and ventral regions of the eye are required for dorsoventral retinal patterning. In *Xenopus* and zebrafish, exogenous RA results a ventralized eye and the expansion of the ventral patterning marker, *vax2*, suggesting that RA can regulate ventral retinal patterning by regulating *vax2* expression; however studies in mice and zebrafish have produced conflicting results (Gregory-Evans, Williams, et al. 2004b; Hyatt, Schmitt, Marsh-Armstrong, McCaffery, Dräger & Dowling 1996a; Lupo et al. 2005). Analysis of mouse *Raldh* mutants has found that RA is not necessary for dorsoventral retinal patterning but instead signals to POM cells to regulate apoptosis and coordinate eye development (Matt et al. 2005; Molotkov et al. 2006).

In mice, mutations in the ventrally expressed RA synthesis gene, *Raldh3,* have been reported to be non-viable with mild ventral eye defects or viable with the fully penetrant loss of anterior eye structures (Dupé et al. 2003; Matt et al. 2005; Molotkov et al. 2006). Although *Raldh1*, expressed in the dorsal retina in mice, is not necessary for eye morphogenesis, RA synthesized by this enzyme is sufficient to direct POM migration to the eye (Molotkov et al. 2006). *Raldh1 Raldh3* double mutants exhibit POM overgrowth from reduced POM apoptosis, resulting in thickened eyelids and more severe ventral eye defects when

compared to *Raldh3* mutants (Matt et al. 2005; Molotkov et al. 2006). In zebrafish, RA appears to be necessary for normal POM dynamics and for the regulation of the POM marker *eya2*; however, in contrast to mice, pharmacological inhibition of RA signaling in zebrafish results in increased apoptosis of POM cells and fewer POM cells migrating to the choroid fissure (Matt et al. 2008; Molotkov et al. 2006; Lupo et al. 2011).

Previous studies on how RA affects zebrafish eye development have relied mainly on pharmacological inhibition of RA signaling or exogenous RA treatment. While this approach has shown that POM migration is likely affected by RA and that RA is involved mainly in ventral eye development, pan-inhibition of RA signaling or exogenous RA treatment is insufficient to fully determine what role RA has in eye development, and the exact spatial requirements for RA cannot be determined based on this approach alone. To better understand how RA synthesized in the ventral eye affects vertebrate eye development, eye development, POM migration, and DV retinal patterning in zebrafish *aldh1a3* mutants were characterized. This work demonstrates that *aldh1a3* regulates RA levels within the entire eye; however, loss of *aldh1a3* alone does not result in any eye phenotypes suggesting that there are likely multiple sources of RA within the eye that are involved in eye development.

Results and Discussion

aldh1a3 mutants are strong hypomorphs

The *aldh1a3* mutant allele contains a premature stop codon early in the gene, leading to the hypothesis that if the mutant allele is not functional, there should be a reduction in *aldh1a3* expression. A strong reduction in *aldh1a3* expression was observed in the ventral eye of *aldh1a3*$^{-/-}$ mutants with a weaker reduction in *aldh1a3* expression seen in heterozygous mutants (Figure 5.2). The reduced expression in heterozygous and homozygous *aldh1a3* mutants indicate that nonsense mediated decay could be occurring to reduce mutant *aldh1a3* transcript levels. Although from this analysis, it cannot be concluded that *aldh1a3* mutants are null mutants, it can be inferred that these mutants are at least strong hypomorphs based on the noticeable reduction in *aldh1a3* expression.

aldh1a3 mutant phenotype

Eye development was followed in embryos from *aldh1a3*$^{+/-}$ crosses from 24 hpf to 5 dpf. Since mouse *Raldh3* mutants have completely penetrant eye defects and humans with mutations in *ALDH1a3* have eye defects on the MAC spectrum, it was expected that zebrafish *aldh1a3* mutants would also have completely penetrant eye defects (Matt et al. 2005; Molotkov et al. 2006). Surprisingly, eye development progressed normally and mild ventral eye defects were observed in only a small proportion of embryos. At 28 hpf, 8.8% (n = 330 embryos) of embryos had a slightly larger choroid fissure, which could be indicative of coloboma; however, this phenotype disappeared by 48 hpf where only 2% of embryos (n = 150 embryos) still had a visibly open choroid fissure (Figure 5.3 A, B). Although *aldh1a3* mutants do not appear to have coloboma, it is possible that in these mutants, the two lobes of the eye are tightly opposed but do not fuse. Laminin staining should be done on *aldh1a3* mutants to more definitively determine if these mutants have coloboma.

Embryos were grown to 5 dpf to see if the eyes continue to develop normally. At 5 dpf, 16% (n = 150) of embryos had a variety of ventral eye defects that ranged from mild ventral eye flattening to microphthalmia and coloboma (Figure 5.3 C-G). Genotyping of these embryos showed that eye defects are associated with heterozygous or homozygous *aldh1a3* mutants. At all stages in development examined, eye defects were seen in less than 25% of the embryos examined, which could indicate that mutations in zebrafish *aldh1a3* result in an incompletely penetrant phenotype. Because the *aldh1a3* mutants were generated by ENU mutagenesis where the F1 generation had on average 7 nonsense, 3 splice site, and 90 non-synonymous induced mutations, it is more likely that the eye defects seen in *aldh1a3* mutants is from a background mutation (Kettleborough et al. 2013). The possibility of background mutations causing eye defects is further reinforced by the lack of eye defects and wild-type eye size seen in later generations of *aldh1a3* mutants produced through outcrosses (not shown; Caroline Cheng, personal communication).

Retinal patterning is normal in *aldh1a3* mutants

The spatially restricted expression of RA synthesis genes to the dorsal and ventral regions of the developing eye suggests that RA might be involved in dorsoventral retinal patterning. Based on previous studies in zebrafish where treatment with exogenous RA produces a ventralized eye, it was hypothesized that *aldh1a3* mutants would have a dorsalized eye with reduced ventral eye identity (Hyatt, Schmitt, Marsh-Armstrong, McCaffery, Dräger & Dowling 1996a). *In situ* hybridization was done on embryos from *aldh1a3*$^{+/-}$ heterozygous incrosses using probes for the dorsal and ventral markers *tbx5a* and *vax2*, respectively. There was no correlation between expression of *tbx5a* or *vax2* and *aldh1a3* genotype (Figure 5.4). While these results conflict with previous studies that have used exogenous RA treatment in zebrafish, the absence of patterning defects in *aldh1a3* mutants coincides with analysis of mouse *Raldh1 Raldh3* double mutants as well as experiments done in zebrafish using an RA receptor inhibitor where no dorsoventral patterning defects were found (Matt et al. 2008; Matt et al. 2005; Molotkov et al. 2006; Lupo et al. 2005).

POM migration is normal in *aldh1a3* mutants

Previous studies in zebrafish using pharmacological inhibition of RA signaling has shown a reduction in POM migration to the choroid fissure and increased POM apoptosis, whereas in mice, *Rald1 Raldh3* double mutants have POM overgrowth and reduced apoptosis (Molotkov et al. 2006). Because many studies have linked RA signaling from the eye to POM migration and POM gene expression, *eya2* expression was examined as a marker for POM in *aldh1a3* mutants. Although *eya2* expression was variable from *aldh1a3*$^{+/-}$ incrosses, there was no correlation between POM migration or POM gene expression and *aldh1a3* genotype (Figure 5.5). The lack of a POM phenotype in *aldh1a3* mutants is suprising since this has been observed in multiple model systems. One likely possibility is that there is still enough RA synthesized by other RA synthesis enzymes (Aldh1a2 and Cyp1b1) to direct POM migration to the eye. In order to determine if RA regulates POM migration or survival in zebrafish, analysis on double or triple *aldh1a3; aldh1a2; cyp1b1* mutants is necessary. Expression of

POM markers in these mutants can be examined in addition to using already available neural crest and POM transgenic lines to follow POM migration during development.

Retinoic acid signaling in *aldh1a3* mutants

Aldh1a3 mutants do not have any obvious phenotype during early eye development and there are no changes in expression of genes involved in the RA synthesis pathway other than *aldh1a3*. To test if there are any alterations in RA signaling in *aldh1a3* mutants, *aldh1a3* mutants were crossed to a transgenic RA reporter line, *Tg(12xRARE-ef1a:GFP)* and *in situ* hybridization for GFP was done as a readout for RA signaling. At 32 hpf, GFP is expressed in the ventral eye, which corresponds to the region of *aldh1a3* expression. A noticeable reduction in GFP expression in the ventral eye was observed in *aldh1a3* heterozygous mutants and *aldh1a3* homozygous mutants had no noticeable GFP expression within the ventral eye (Figure 5.6 A-C). At 48 hpf, GFP is expressed in the dorsal and ventral regions of the eye in wild type *Tg(12xRARE-ef1a:GFP)* embryos (Figure 5.6 D). Interestingly, although *aldh1a3* is expressed only in the ventral eye, *aldh1a3*$^{+/-}$ mutants exhibited a range of GFP expression, with some having a mild reduction in GFP expression in the dorsal and ventral eye, or a reduction in the ventral eye with complete absence of GFP expression in the dorsal eye (Figure 5.6 E-G). *aldh1a3*$^{-/-}$ mutants exhibited a similar range of GFP expression, but with more noticeable reductions in GFP expression in the dorsal and ventral regions of the eye in addition to embryos that had little to no GFP expression in the eye (Figure 5.6 H-J).

Aldh1a3 mutants have a noticeable reduction in RA signaling in the ventral eye during early eye development and surprisingly show that *aldh1a3* is involved in regulating dorsal and ventral RA levels, although the mechanism through which this happens is still unknown. These results could explain why mouse *Raldh1* mutants have no discernable eye defects, since it appears *Raldh3* contributes to RA signaling in the dorsal eye (Matt et al. 2005; Molotkov et al. 2006). The strong reduction of RA signaling in *aldh1a3* mutants at 32 hpf indicates that Aldh1a3 is the main RA synthesis gene involved in early eye

development. If this is indeed the case, high levels of RA might be needed only for ventral eye development which could explain why pharmacological treatments altering RA signaling results in ventral and not dorsal eye defects (Hyatt, Schmitt, Marsh-Armstrong, McCaffery, Dräger & Dowling 1996b; Lupo et al. 2011). It should be noted that although these results show an absence of GFP expression in *aldh1a3* mutants which could be interpreted as the absence of RA signaling in the eye, there is probably still residual RA signaling occurring from other RA synthesis enzymes that are not detected by the transgenic method used. To further quantify RA levels in the eye and to determine exactly how Aldh1a3 contributes to RA signaling within the eye, a more sensitive assay is required, such as using Gepra B transgenics that have been developed to measure RA concentrations in the developing embryo using a FRET based assay (Shimozono et al. 2013).

Development of photoreceptors in *aldh1a3* mutants

In mice and medaka, the ventral retinal patterning marker *vax2* has been shown to regulate the distribution of RA in the eye, which in turn results in aberrant opsin distribution in the retina. In *Vax2* mutant mice, *Raldh3* expression is lost in the developing ventral retina accompanied with a loss of RA signaling in the ventral half of the eye (Alfano et al. 2011). Since zebrafish *aldh1a3* mutants also have a reduction of RA signaling in the eye, it was hypothesized that zebrafish *aldh1a3* mutants could phenocopy mouse *Vax2* mutants and have altered opsin distribution. To test this hypothesis, *in situ* hybridization for *opsin 1, short-wave sensitive 2* (*opn1sw2)* was done on 4 dpf zebrafish larvae from *aldh1a3*$^{+/-}$ incrosses. Almost all larvae (n = 38/40) showed an even distribution of *opn1sw2* indicating that *opn1sw2* expression and photoreceptor distribution is unchanged in *aldh1a3*$^{-/-}$ mutants (Figure 5.7).

Unlike mice and medaka, where short-wave cones are found mainly in the ventral retina and medium-wave cones are found predominantly in the dorsal retina, zebrafish have a uniform distribution of cones throughout the retina (Alfano et al. 2011; Stenkamp 2007). Since mice, medaka, and zebrafish have RA synthesis restricted to the dorsal and ventralmost regions of the retina, it is

possible that zebrafish have lost the requirement of RA for cone distribution. Although *aldh1a3* mutants do not have altered cone distribution, it is not clear if photoreceptors in these mutants have further morphology. In order to further determine if RA, and in particular *aldh1a3*, is involved in photoreceptor development, photoreceptor morphology and rod distribution should be examined, since unlike cones, rods are unevenly distributed and are found in the dorsal and ventral regions of the zebrafish retina (Fadool 2003).

Discussion and conclusions

Human studies that have clearly demonstrated that ALDH1A3 is essential for eye development. Suprisingly, the MAC phenotypes observed in humans with mutations in *ALDH1A3* was not recapitulated in zebrafish *aldh1a3* mutants although these mutants were found to be, at the very least, strong hypomorphs. The absence of any discernable ocular phenotype in these mutants is not entirely surprising as only 6% of nonsense and essential splice mutations generated via the same ENU screen as the *aldh1a3* mutants caused an observable phenotype (Kettleborough et al. 2013). Unexpectedly, the loss of *aldh1a3* reduces RA signaling in the dorsal and ventral retina, suggesting the intriguing possibility that somehow RA synthesized in the ventral eye contributes to RA in the dorsal eye. These findings suggest that either RA synthesized by Aldh1a3 can diffuse throughout the eye, which contributes to RA signaling in the dorsal retina, or that RA produced by Aldh1a3 could be involved in the regulation of RA synthesis genes or enzymes in the dorsal eye. Although RA signaling was markedly reduced or appeared to be completely absent in *aldh1a3*$^{-/-}$ mutants, it is possible that residual RA produced by other synthesis enzymes including Aldh1a2 and Cyp1b1 are sufficient to direct eye development, but at levels too low to be detected by the transgenic line used.

Further investigation into the role of RA in vertebrate eye will have to take the potential functional redundancy of RA synthesis genes into account. In particular, early eye phenotypes including MAC, POM migration, RA signaling levels, and potential loss of photoreceptors should be investigated in double and triple *aldh1a3*, *aldh1a2*, and *cyp1b1* mutants. The use of double and triple

mutants should fully ablate RA synthesis within the eye, but advanced imaging techniques and the use of more sensitive transgenic lines, such as the GepraB FRET based transgenic reporter, will have to be used in conjunction with mutant analysis to determine if RA synthesis in the eye is truly ablated (Shimozono et al. 2013). Fully understanding the function of RA in the eye, and in particular in ventral eye development, has the potential to provide further mechanistic insight on choroid fissure closure and eye morphogenesis which could further our understanding of congenital eye malformations.

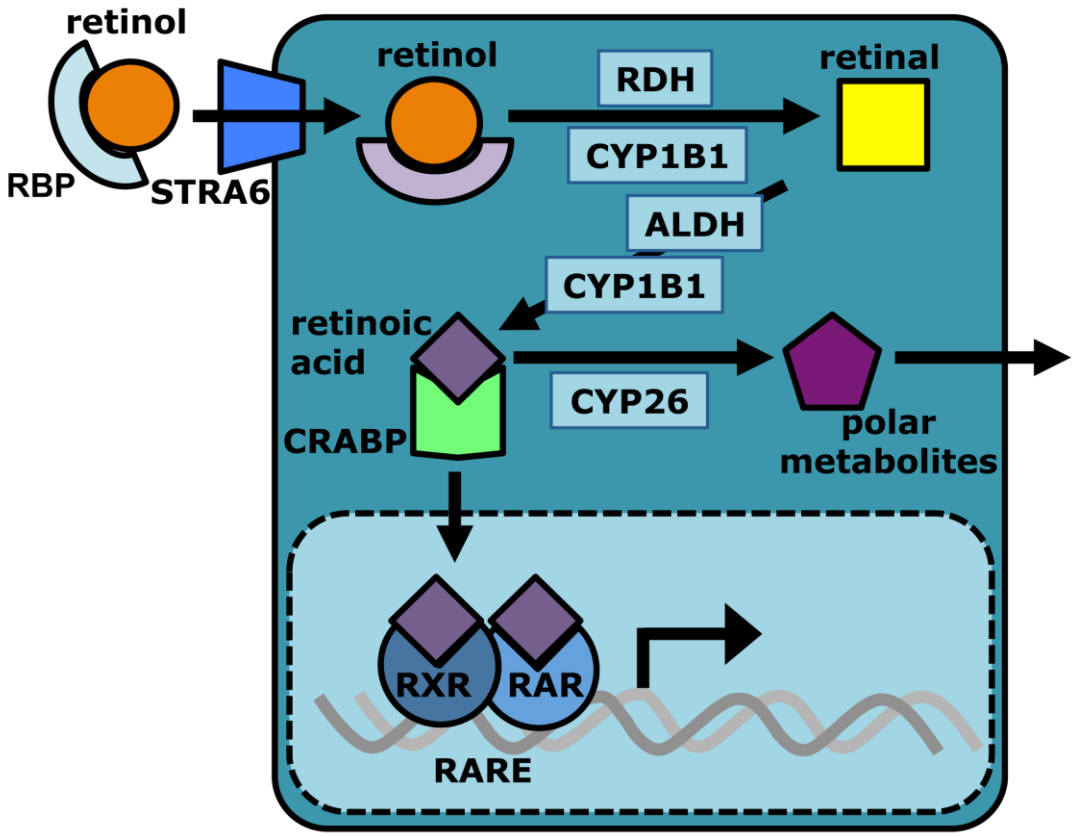

Figure 5.1: Retinoic acid (RA) synthesis and signaling pathway. Extracellular retinol, or vitamin A, is bound to retinol binding protein (RBP). Retinol is imported into the cell by the transporter Stimulated by retinoic acid 6 (STRA6) and is then converted into retinal by retinol dehydrogenase (RDH) and cytochrome p450 Cyp1b1 enzymes. Retinal is then converted into RA by aldehyde dehydrogenase (ALDH) and Cyp1b1 enzymes. Intracellular RA is bound by cellular retinoic acid binding protein (CRABP) and is imported into the nucleus where it interacts with nuclear retinoic acid receptors (RAR) and retinoid X receptors (RXR) that are bound to retinoic acid response elements (RAREs). RA can be targeted for degradation through oxidation by CYP26 enzymes resulting in polar metabolites being exported from the cell.

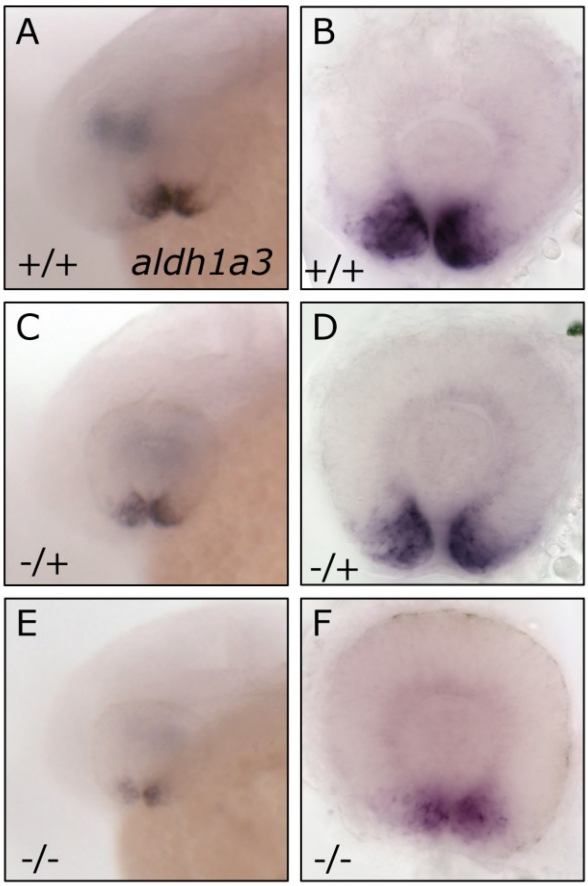

Figure 5.2: Expression of *aldh1a3* is reduced in *aldh1a3* mutants. (A, C, E) Lateral views of 28 hpf whole zebrafish embryos with the indicated genotype. (B, D, F) Dissected and mounted eyes from 28 hpf zebrafish embryos. (A, B) In 28 hpf embryos, *aldh1a3* is restricted to the ventral eye. In *aldh1a3*$^{+/-}$ mutants, *aldh1a3* expression is slightly reduced (C, D) whereas in *aldh1a3*$^{-/-}$ mutants, *aldh1a3* expression is almost completely lost (E, F).

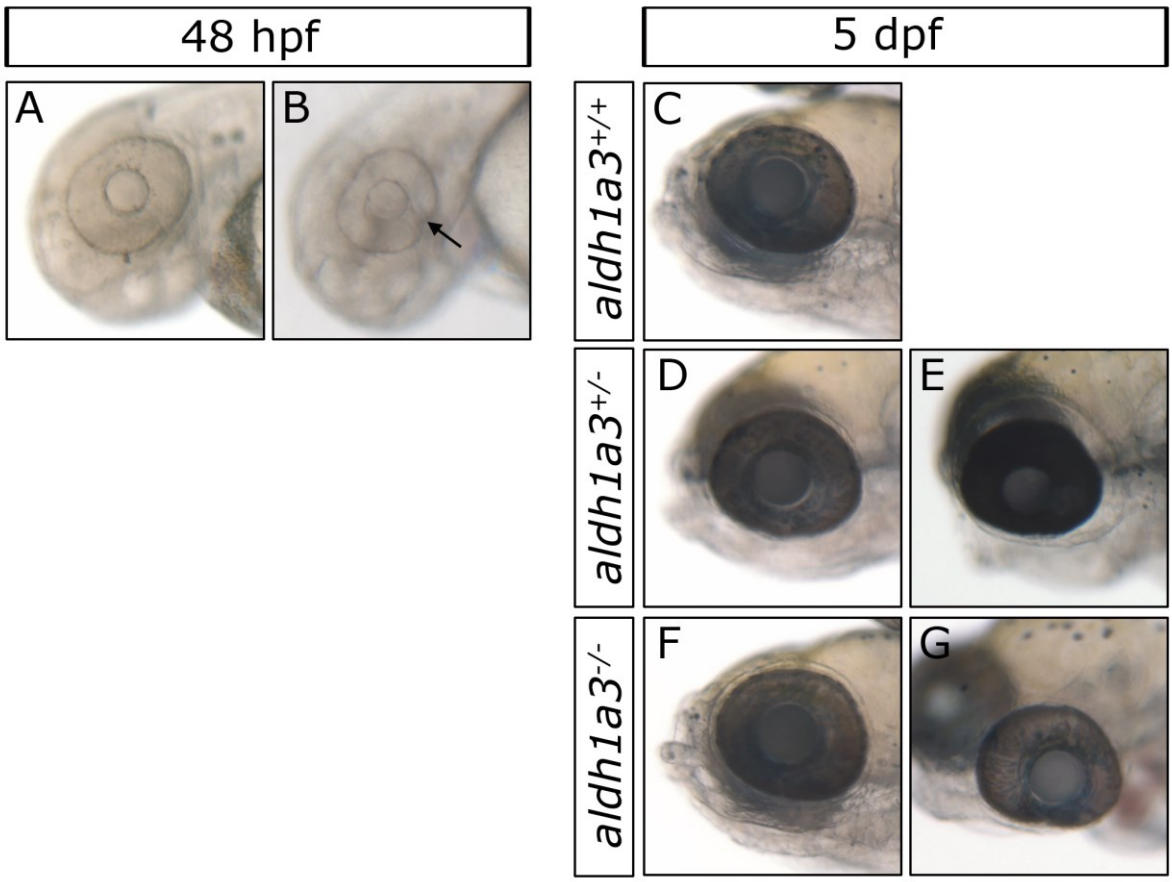

Figure 5.3: Eye defects observed in embryos from *aldh1a3*$^{+/-}$ incrosses. (A, B) At 48 hpf, 2% of embryos had noticeably open choroid fissures (n = 150; B, arrow). (C-G) Eye phenotypes observed in 5 dpf larvae with the associated genotype indicated. Phenotypes ranged from wild-type eyes in *aldh1a3*$^{+/-}$ and *aldh1a3*$^{-/-}$ mutants (D, F) to mild microphthalmia in *aldh1a3*$^{+/-}$ mutants (E) and microphthalmia with coloboma in *aldh1a3*$^{-/-}$ mutants (E, G).

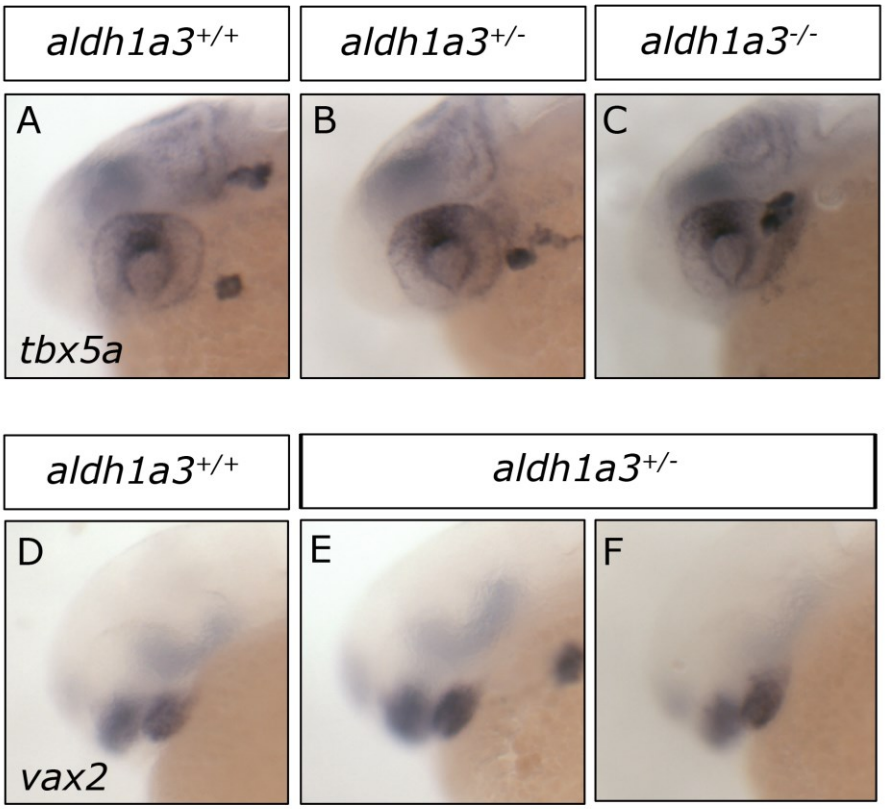

Figure 5.4: *aldh1a3* mutants have normal dorsoventral retinal patterning. Wholemount *in situ* hybridization showing expression of the dorsal retinal marker *tbx5a* (A-C) or the ventral retinal marker *vax2* (D-F) in 28 hpf embryos from *aldh1a3*$^{+/-}$ incrosses. No correlation was found between expression of *tbx5a* and *aldh1a3* mutant genotype (B, C) or between *vax2* expression and *aldh1a3* genotype (E, F).

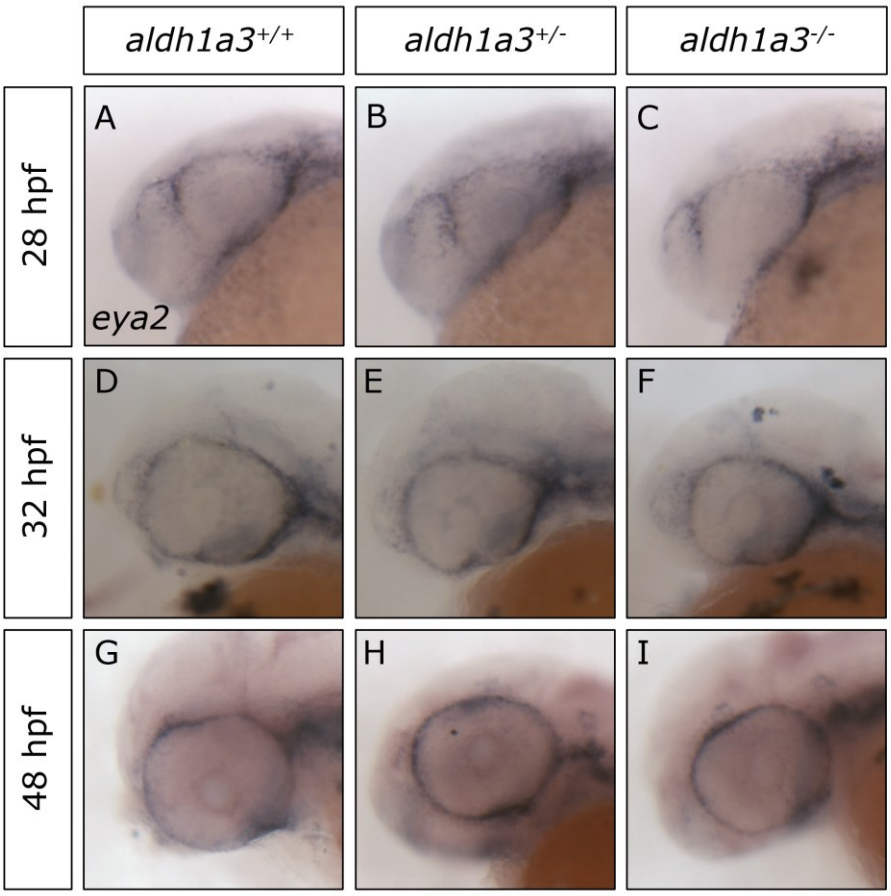

Figure 5.5: POM migration is unaffected in *aldh1a3* mutants. Whole mount *in situ* hybridization showing expression of the POM marker *eya2* in at 28 hpf (A-C), 32 hpf (D-F), and at 48 hpf (G-I). At all time points, *eya2* expression in wild-type siblings (A, D, G) was comparable to expression in *aldh1a3*$^{+/-}$ mutants (B, E, H) and *aldh1a3*$^{-/-}$ mutants (C, F, I).

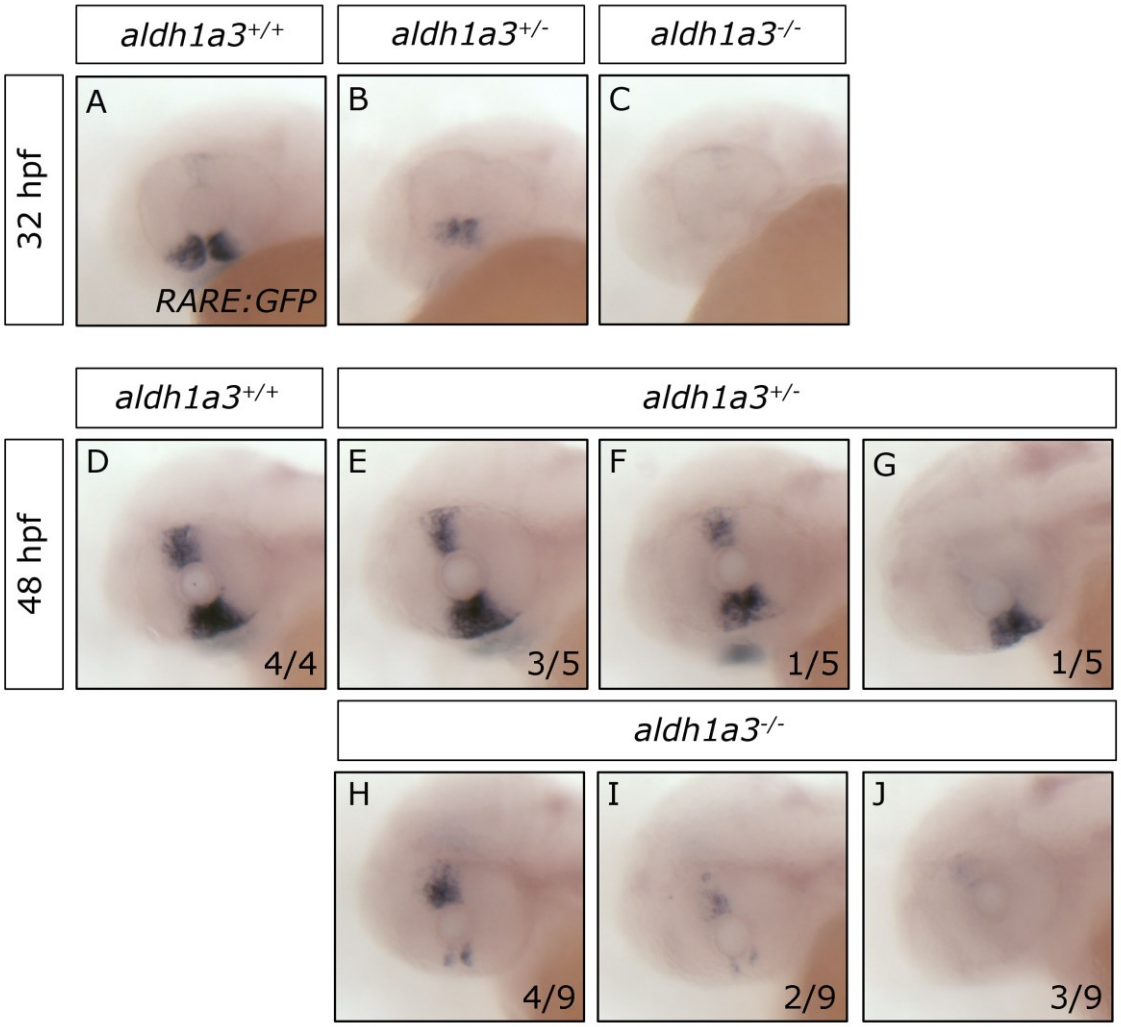

Figure 5.6: RA signaling is attenuated in *aldh1a3* mutants. Whole-mount *in situ* hybridization showing the expression of GFP at 32 hpf (A-C) and 48 hpf (D-J) in embryos from *aldh1a3*$^{+/-}$ *; Tg(12xRARE-ef1μ:eGFP)* incrosses. When compared to wild-type (A), *aldh1a3*$^{+/-}$ mutants have reduced RA signaling (B) and *aldh1a3*$^{-/-}$ mutants have no detectable RA signaling in the ventral eye at 32 hpf (C). (D) At 48 hpf, RA signaling occurs in the dorsal and ventral regions of the eye (n = 4 *aldh1a3*$^{+/+}$ embryos). (E-G) RA signaling is slightly reduced in the dorsal retina (E; n = 3 *aldh1a3*$^{+/-}$ embryos), in the dorsal and ventral retina (F; n = 1 *aldh1a3*$^{+/-}$ embryo) or absent in the dorsal retina and strongly reduced in the ventral retina (G; n = 1 *aldh1a3*$^{+/-}$ embryo) in *aldh1a3*$^{+/-}$ mutants. (H-J) In *aldh1a3*$^{-/-}$ mutants, RA signaling is slightly reduced (H; n = 4 *aldh1a3*$^{-/-}$ embryos), strongly reduced

(I; n = 2 *aldh1a3*$^{-/-}$ embryos) or undetectable in the dorsal and ventral regions of the eye at 48 hpf (J; n = 3 *aldh1a3*$^{-/-}$ embryos). Numbers in figure indicate the proportion of each genotype with the displayed RA signaling phenotype.

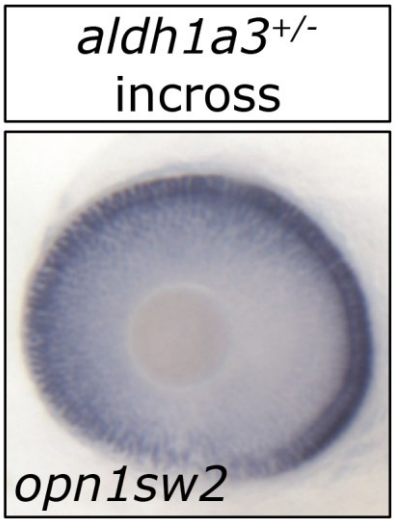

Figure 5.7: *aldh1a3* mutants have normal *opn1sw2* expression and cone distribution. *In situ* hybridization was done on 4 dpf larvae from heterozygous incrosses. From these incrosses, 95% (n = 40) of larvae had evenly distributed *opn1sw2* expression indicating that there is no difference in *opsin* gene expression or cone distribution amongst wild-type siblings and *aldh1a3* mutants.

Chapter 6

Conclusions and Future Directions

BMP signaling is essential for many aspects of eye development. BMP ligands are involved in establishing dorsal eye identity, regulating apoptosis and proliferation to control eye size, and directing eye morphogenesis. While the function of BMP ligands during early eye development have been thoroughly studied, much less is known about how BMP signaling is regulated and the potential role that BMP inhibitors have in vertebrate eye development. This work aimed to further understand the role of the putative BMP inhibitors, Sparc related modular calcium binding 1 (Smoc1), Smoc2, and Gremlin2b (Grem2b) in zebrafish eye morphogenesis and dorsoventral retinal patterning. As BMP ligands play an essential role in establishing the dorsal eye and regulating eye morphogenesis and size, it was hypothesized that Smoc1, Smoc2, and Grem2b regulate BMP signaling originating from the dorsal eye to establish ventral eye identity and to modulate eye morphogenesis and control eye size.

Expression of *smoc1* and *smoc2* is restricted to the ventral retina shortly after the DV retinal axis is established with *smoc1* expression restricted to the ventralmost portion of the retina. The later onset of expression suggests that rather than establishing ventral eye identity, the inhibition of BMP signaling by these molecules maintains ventral eye identity. Unlike *smoc1* and *smoc2*, which are both expressed within the ventral eye, *grem2b* is expressed in what appears to be a migratory POM cell population that migrates exclusively to the ventral eye and choroid fissure.

Loss of function experiments done using morpholino oligonucleotides resulted in a reduction in eye area when levels of Smoc1, Smoc2, or Grem2b levels were reduced. Eye area was rescued in *smoc1* morphants with the addition of *p53* morpholino, indicating that the reduction in eye area was due to increased apoptosis. Previous work has found that a loss of the BMP ligand *Gdf6a* also results in microphthalmia with increased apoptosis, suggesting that the balance between BMP signaling and BMP inhibition is essential in regulating ocular apoptosis and ocular size (French et al. 2013). Future work to determine how the inhibition of BMP signaling by Smoc1, Smoc2, and Grem2b regulates ocular size will require mutants to be generated in order to rule out the possibility that non-specific apoptosis was induced by the morpholinos used in this study.

In addition to the reduction in eye area observed in *smoc1* loss of function experiments, *smoc1* morphants had abnormal optic stalks, a phenotype similar to the hypoplastic optic nerves in *Smoc1* mutant mice (Okada et al. 2011). The microphthalmic phenotype along with abnormal optic stalks seen in zebrafish *smoc1* morphants appears to recapitulate the phenotypes seen in *Smoc1* mutant mice, however, *smoc1* mutants will need to be generated to see if the early optic stalk phenotype later results in hypoplastic optic nerves.

Further loss of function experiments done examined DV retinal patterning and BMP signaling. The mild alterations in DV retinal patterning observed in *smoc1* morphants suggests that reducing Smoc1 levels perturbs ocular BMP signaling. This was further explored using *smoc1* morpholino in a transgenic BMP reporter line. From this experiment, Smoc1 was shown to regulate BMP signaling in the dorsal eye and surprisingly, in the proximal choroid fissure. While the source of BMP ligands that Smoc1 inhibits in the choroid fissure has not yet been identified, a strong candidate is Bmp7, which is involved in choroid fissure formation, apoptosis, and vascularization (Morcillo 2006). Although *grem2b* is expressed in a small cell population outside of the eye, like Smoc1, Grem2b was found to regulate BMP signaling in the dorsal eye (Figure 6.1). Together, these results show how different BMP inhibitors within and adjacent to the ventral eye work together to regulate ocular BMP signaling in the dorsal and proximal choroid fissure.

The finding that Grem2b from POM cells that migrate to the ventral eye can regulate BMP signaling within the dorsal eye further illustrates how POM cells are essential for normal eye development (Figure 6.1). POM cells migrate to the eye and choroid fissure where these cells direct fissure closure through an unknown mechanism. To date no other ventral specific POM marker other than *grem2b* has been described. Loss of function experiments done using *grem2b* morpholino oligonucleotides demonstrate how *grem2b* is essential for ventral eye development and choroid fissure closure, and by extension, also shows the necessity of *grem2b* expressing POM cells in these processes.

Using *grem2b* as a ventral specific POM marker will be advantageous and allow for the further study of POM migration to the choroid fissure which can

further our understanding of how POM cells direct fissure closure. POM cells are likely directed to the choroid fissure and ventral eye by cell migratory cues emanating from this region since the migration of *grem2b* expressing cells is altered when the entire eye is ventralized. Identification of candidate chemoattractants can be done using a similar system where the aberrant expression of chemoattractants normally restricted to the ventral eye and choroid fissure is screened for in a ventralized eye model. Understanding the dynamics of the *grem2b* expressing population of cells can also be done using live imaging following the generation of *grem2b* transgenic lines. Further work to generate transgenic lines that will allow for fate mapping this cell population will further elucidate how exactly this cell population contributes to the developing eye.

POM migration and eye morphogenesis was also studied through the characterization of eye development in *aldh1a3* mutants. Retinoic acid (RA) has been implicated in POM migration to the choroid fissure and in directing fissure closure, but the exact spatial requirements for RA in the eye is not known (Lupo et al. 2011). This work used *aldh1a3* mutants, which lack an RA synthesis enzyme restricted to the ventral eye, to study if RA from the ventral eye is involved in eye development and POM migration. From this analysis, *aldh1a3* mutants were found to have only mild ventral eye defects and no change in POM migration to the eye or in DV retinal patterning. Interestingly, although these mutants appear largely normal, homozygous and heterozygous mutants had a strong reduction in RA signaling in the ventral eye at early stages and at later stages had a strong reduction in dorsal and ventral RA signaling within the eye. These experiments show that through an unknown mechanism, RA produced in the ventral eye by Aldh1a3 is involved in RA signaling in the dorsal eye. Further work using a FRET based assay will need to be done to quantify RA gradients and contributions of each RA synthesis enzyme in the eye and to examine if RA can diffuse from the ventral to the dorsal eye (Shimozono et al. 2013).

This thesis has examined the function of four genes that have spatially-restricted expression in either the ventral eye or surrounding tissues during zebrafish eye development. The complexity of vertebrate eye development is illustrated by the multifaceted roles of the BMP inhibitors Smoc1, Smoc2, and

Grem2b along with the RA synthesis enzyme Aldh1a3 during zebrafish eye morphogenesis. BMP ligands initiate and maintain dorsal retinal identity which is refined by the BMP inhibitor Smoc1. Smoc1 from the ventral eye, along with Grem2b secreted by migratory ventral specific POM cells, inhibits BMP signaling in the dorsal eye while Smoc1 also inhibits BMP signaling in the choroid fissure. During this time, *grem2b* expressing cells continue to migrate to the ventral eye where Grem2b is involved in ventral eye development, choroid fissure closure, and regulation of eye size (Figure 6.1). Smoc1 and Smoc2, like Grem2b, are also involved in regulating eye size during eye morphogenesis. Concomitantly RA synthesized in the ventral eye by Aldh1a3 appears to be involved in regulating RA levels and RA signaling throughout the eye; however RA signaling within the eye serves an as of yet unknown function.

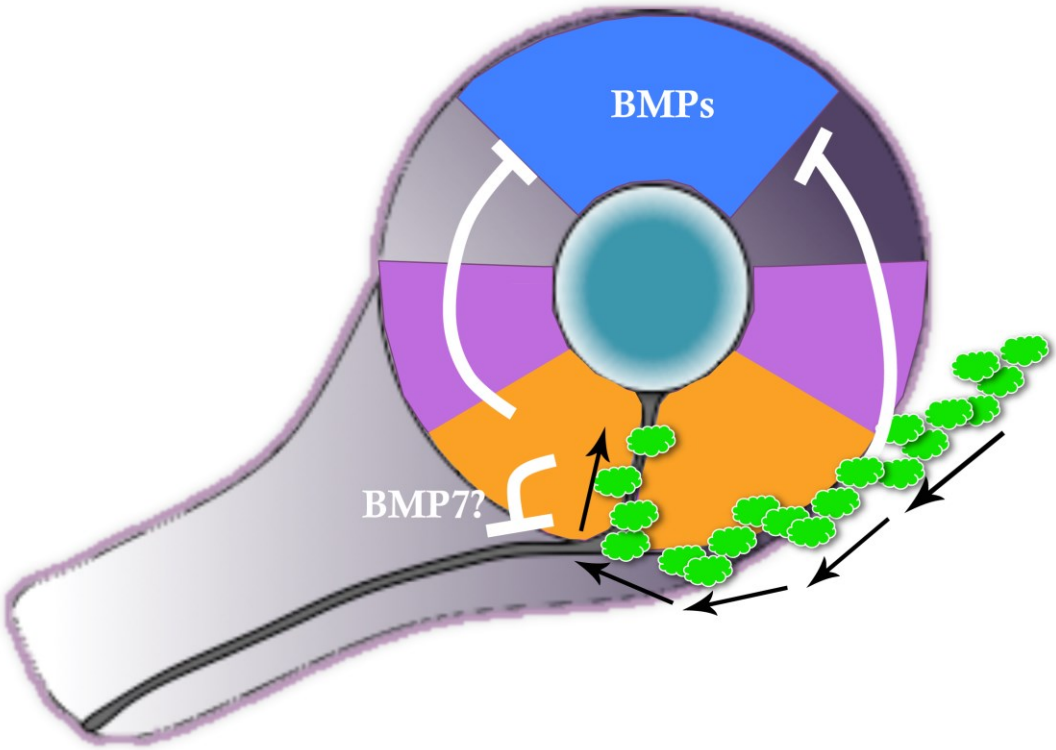

Figure 6.1: The BMP inhibitors Smoc1, Smoc2, and Grem2b are involved in early zebrafish eye morphogenesis.
Bmp ligands (blue) are restricted to the dorsal retina during vertebrate eye development. *Smoc1* (orange) expression is restricted to the ventralmost portion of the eye while expression of *smoc2* is restricted to the ventral half of the eye. Smoc1 regulates BMP signaling in the dorsal eye and in the proximal choroid fissure. One possible source of BMP ligands in the proximal choroid fissure is Bmp7. POM cells expressing *grem2b* (green) migrate to the ventral eye and choroid fissure where Grem2b regulates BMP signaling in the dorsal eye and is also involved in ventral eye development and choroid fissure closure.

Literature Cited

Ablain, J. & Zon, L.I., 2013. Of fish and men: using zebrafish to fight human diseases. *Trends in cell biology*, 23(12), pp.584–586.

Abouzeid, H. et al., 2014. Mutations in ALDH1A3 represent a frequent cause of microphthalmia/anophthalmia in consanguineous families. *Human mutation*, 35(8), pp.949–953.

Abouzeid, H. et al., 2011. Mutations in the SPARC-related modular calcium-binding protein 1 gene, SMOC1, cause waardenburg anophthalmia syndrome. *American journal of human genetics*, 88(1), pp.92–98.

Adler, R. & Canto-Soler, M.V., 2007. Molecular mechanisms of optic vesicle development: complexities, ambiguities and controversies. *Developmental Biology*, 305(1), pp.1–13.

Aldahmesh, M.A. et al., 2013. Mutations in ALDH1A3 cause microphthalmia. *Clinical genetics*, 84(2), pp.128–131.

Alfano, G. et al., 2011. Vax2 regulates retinoic acid distribution and cone opsin expression in the vertebrate eye. *Development (Cambridge, England)*, 138(2), pp.261–271.

Asai-Coakwell, M. et al., 2013. Contribution of growth differentiation factor 6-dependent cell survival to early-onset retinal dystrophies. *Human molecular genetics*, 22(7), pp.1432–1442.

Asai-Coakwell, M. et al., 2007. GDF6, a novel locus for a spectrum of ocular developmental anomalies. *American journal of human genetics*, 80(2), pp.306–315.

Avsian-Kretchmer, O. & Hsueh, A.J.W., 2004. Comparative genomic analysis of the eight-membered ring cystine knot-containing bone morphogenetic protein antagonists. *Molecular endocrinology (Baltimore, Md.)*, 18(1), pp.1–12.

Balemans, W. & Van Hul, W., 2002. Extracellular regulation of BMP signaling in vertebrates: a cocktail of modulators. *Developmental Biology*, 250(2), pp.231–250.

Barbieri, A.M. et al., 2002. Vax2 inactivation in mouse determines alteration of the eye dorsal-ventral axis, misrouting of the optic fibres and eye coloboma.

Beby, F. & Lamonerie, T., 2013. The homeobox gene Otx2 in development and disease. *Experimental eye research*, 111, pp.9–16.

Beccari, L. et al., 2012. Sox2-mediated differential activation of Six3.2 contributes to forebrain patterning. *Development (Cambridge, England)*, 139(1), pp.151–164.

Behesti, H., Holt, J.K.L. & Sowden, J.C., 2006. The level of BMP4 signaling is critical for the regulation of distinct T-box gene expression domains and growth along the dorso-ventral axis of the optic cup. *BMC developmental biology*, 6, p.62.

Bloch-Zupan, A. et al., 2011. Homozygosity mapping and candidate prioritization identify mutations, missed by whole-exome sequencing, in SMOC2, causing major dental developmental defects. *American journal of human genetics*, 89(6), pp.773–781.

Bragdon, B. et al., 2011. Bone morphogenetic proteins: a critical review. *Cellular signalling*, 23(4), pp.609–620.

Carl, M., Loosli, F. & Wittbrodt, J., 2002. Six3 inactivation reveals its essential role for the formation and patterning of the vertebrate eye. *Development (Cambridge, England)*, 129(17), pp.4057–4063.

Cavodeassi, F., Ivanovitch, K. & Wilson, S.W., 2013. Eph/Ephrin signalling maintains eye field segregation from adjacent neural plate territories during forebrain morphogenesis. *Development (Cambridge, England)*, 140(20), pp.4193–4202.

Centanin, L. & Wittbrodt, J., 2014. Retinal neurogenesis. *Development (Cambridge, England)*, 141(2), pp.241–244.

Chambers, D. et al., 2007. RALDH-independent generation of retinoic acid during vertebrate embryogenesis by CYP1B1. *Development (Cambridge, England)*, 134(7), pp.1369–1383.

Chuang, J.C. & Raymond, P.A., 2001. Zebrafish genes rx1 and rx2 help define the region of forebrain that gives rise to retina. *Developmental Biology*, 231(1), pp.13–30.

Church, R.H. et al., 2015. Gremlin1 preferentially binds to bone morphogenetic protein-2 (BMP-2) and BMP-4 over BMP-7. *The Biochemical journal*, 466(1), pp.55–68.

Collery, R.F. & Link, B.A., 2011. Dynamic smad-mediated BMP signaling revealed through transgenic zebrafish. *Developmental Dynamics*, 240(3), pp.712–722.

Creuzet, S., Vincent, C. & Couly, G., 2005. Neural crest derivatives in ocular and periocular structures. *The International journal of developmental biology*, 49(2-3), pp.161–171.

De Robertis, E.M., 2006. Spemann's organizer and self-regulation in amphibian embryos. *Nature Reviews Molecular Cell Biology*, 7(4), pp.296–302.

Duester, G., 2009. Keeping an eye on retinoic acid signaling during eye development. *Chemico-biological interactions*, 178(1-3), pp.178–181.

Duester, G., 2008. Retinoic acid synthesis and signaling during early organogenesis. *Cell*, 134(6), pp.921–931.

Dupé, V. et al., 2003. A newborn lethal defect due to inactivation of retinaldehyde dehydrogenase type 3 is prevented by maternal retinoic acid treatment. *Proceedings of the National Academy of Sciences of the United States of America*, 100(24), pp.14036–14041.

Duval, M.G., Oel, A.P. & Allison, W.T., 2014. gdf6a is required for cone photoreceptor subtype differentiation and for the actions of tbx2b in determining rod versus cone photoreceptor fate. *PLoS ONE*, 9(3), p.e92991.

Ekker, S.C. et al., 1995. Patterning activities of vertebrate hedgehog proteins in the developing eye and brain. *Current biology : CB*, 5(8), pp.944–955.

Esteve, P. et al., 2011. Secreted frizzled-related proteins are required for Wnt/β-catenin signalling activation in the vertebrate optic cup. *Development (Cambridge, England)*, 138(19), pp.4179–4184.

Fadool, J.M., 2003. Development of a rod photoreceptor mosaic revealed in transgenic zebrafish. *Developmental Biology*, 258(2), pp.277–290.

Fares-Taie, L. et al., 2013. ALDH1A3 Mutations Cause Recessive Anophthalmia and Microphthalmia. *American journal of human genetics*.

French, C.R. et al., 2013. Apoptotic and proliferative defects characterize ocular development in a microphthalmic BMP model. *Investigative ophthalmology & visual science*, 54(7), pp.4636–4647.

French, C.R. et al., 2009. Gdf6a is required for the initiation of dorsal-ventral retinal patterning and lens development. *Developmental Biology*, 333(1), pp.37–47.

Gage, P.J. et al., 2005. Fate maps of neural crest and mesoderm in the mammalian eye. *Investigative ophthalmology & visual science*, 46(11), pp.4200–4208.

Gerth-Kahlert, C. et al., 2013. Clinical and mutation analysis of 51 probands with anophthalmia and/or severe microphthalmia from a single center. *Molecular genetics & genomic medicine*, 1(1), pp.15–31.

Gosse, N.J. & Baier, H., 2009. An essential role for Radar (Gdf6a) in inducing dorsal fate in the zebrafish retina. *Proceedings of the National Academy of Sciences*, 106(7), pp.2236–2241.

Gregory-Evans, C.Y., Vieira, H., et al., 2004a. Ocular coloboma and high myopia with Hirschsprung disease associated with a novel ZFHX1B missense mutation and trisomy 21. *American journal of medical genetics. Part A*, 131(1), pp.86–90.

Gregory-Evans, C.Y., Williams, M.J., et al., 2004b. Ocular coloboma: a reassessment in the age of molecular neuroscience. *Journal of medical genetics*, 41(12), pp.881–891.

Hammerschmidt, M., Serbedzija, G.N. & McMahon, A.P., 1996. Genetic analysis of dorsoventral pattern formation in the zebrafish: requirement of a BMP-like ventralizing activity and its dorsal repressor. *Genes & development*, 10(19), pp.2452–2461.

Heermann, S. et al., 2015. Eye morphogenesis driven by epithelial flow into the optic cup facilitated by modulation of bone morphogenetic protein. *eLife*, 4.

Hemmati-Brivanlou, A., Kelly, O.G. & Melton, D.A., 1994. Follistatin, an antagonist of activin, is expressed in the Spemann organizer and displays direct neuralizing activity. *Cell*, 77(2), pp.283–295.

Holly, V.L. et al., 2014. Sfrp1a and Sfrp5 function as positive regulators of Wnt and BMP signaling during early retinal development. *Developmental Biology*.

Hoon, M. et al., 2014. Functional architecture of the retina: development and disease. *Progress in retinal and eye research*, 42, pp.44–84.

Houart, C. et al., 2002. Establishment of the telencephalon during gastrulation by local antagonism of Wnt signaling. *Neuron*, 35(2), pp.255–265.

Hsu, D.R. et al., 1998. The Xenopus dorsalizing factor Gremlin identifies a novel family of secreted proteins that antagonize BMP activities. *Molecular cell*, 1(5), pp.673–683.

Hyatt, G.A., Schmitt, E.A., Marsh-Armstrong, N., McCaffery, P., Dräger, U.C. & Dowling, J.E., 1996a. Retinoic acid establishes ventral retinal characteristics. *Development (Cambridge, England)*, 122(1), pp.195–204.

Hyatt, G.A., Schmitt, E.A., Marsh-Armstrong, N., McCaffery, P., Dräger, U.C. & Dowling, J.E., 1996b. Retinoic acid establishes ventral retinal characteristics.

Hyer, J., Mima, T. & Mikawa, T., 1998. FGF1 patterns the optic vesicle by directing the placement of the neural retina domain. *Development (Cambridge, England)*, 125(5), pp.869–877.

Iemura, S. et al., 1998. Direct binding of follistatin to a complex of bone-morphogenetic protein and its receptor inhibits ventral and epidermal cell fates in early Xenopus embryo. *Proceedings of the National Academy of Sciences of the United States of America*, 95(16), pp.9337–9342.

Kattamuri, C. et al., 2012. Members of the DAN family are BMP antagonists that form highly stable noncovalent dimers. *Journal of molecular biology*, 424(5), pp.313–

327.

Kelly, R.G., Jerome-Majewska, L.A. & Papaioannou, V.E., 2004. The del22q11.2 candidate gene Tbx1 regulates branchiomeric myogenesis. *Human molecular genetics*, 13(22), pp.2829–2840.

Kettleborough, R.N.W. et al., 2013. A systematic genome-wide analysis of zebrafish protein-coding gene function. *Nature*, 496(7446), pp.494–497.

Khokha, M.K. et al., 2005. Depletion of three BMP antagonists from Spemann's organizer leads to a catastrophic loss of dorsal structures. *Developmental cell*, 8(3), pp.401–411.

Kimmel, C.B. et al., 1995. Stages of embryonic development of the zebrafish. *Developmental Dynamics*, 203(3), pp.253–310.

Kishimoto, Y. et al., 1997. The molecular nature of zebrafish swirl: BMP2 function is essential during early dorsoventral patterning. *Development (Cambridge, England)*, 124(22), pp.4457–4466.

Kita, E.M., Scott, E.K. & Goodhill, G.J., 2014. Topographic wiring of the retinotectal connection in zebrafish. *Developmental neurobiology*.

Kobayashi, M. et al., 2001. The homeobox protein Six3 interacts with the Groucho corepressor and acts as a transcriptional repressor in eye and forebrain formation. *Developmental Biology*, 232(2), pp.315–326.

Kok, F.O. et al., 2015. Reverse Genetic Screening Reveals Poor Correlation between Morpholino-Induced and Mutant Phenotypes in Zebrafish. *Developmental cell*, 32(1), pp.97–108.

Koshiba-Takeuchi, K. et al., 2000. Tbx5 and the retinotectum projection. *Science (New York, N.Y.)*, 287(5450), pp.134–137.

Kriebitz, N.N. et al., 2009. PRDC regulates placode neurogenesis in chick by modulating BMP signalling. *Developmental Biology*, 336(2), pp.280–292.

Kruse-Bend, R. et al., 2012. Extraocular ectoderm triggers dorsal retinal fate during optic vesicle evagination in zebrafish. *Developmental Biology*.

Langenberg, T. et al., 2008. The eye organizes neural crest cell migration. *Developmental Dynamics*, 237(6), pp.1645–1652.

Lee, J. et al., 2008. Zebrafish blowout provides genetic evidence for Patched1-mediated negative regulation of Hedgehog signaling within the proximal optic vesicle of the vertebrate eye. *Developmental Biology*, 319(1), pp.10–22.

Lemke, G. & Reber, M., 2005. Retinotectal mapping: new insights from molecular

genetics. *Annual review of cell and developmental biology*, 21, pp.551–580.

Loosli, F. et al., 2003. Loss of eyes in zebrafish caused by mutation of chokh/rx3. *EMBO reports*, 4(9), pp.894–899.

Loosli, F. et al., 2001. Medaka eyeless is the key factor linking retinal determination and eye growth. *Development (Cambridge, England)*, 128(20), pp.4035–4044.

Loosli, F., Winkler, S. & Wittbrodt, J., 1999. Six3 overexpression initiates the formation of ectopic retina. *Genes & development*, 13(6), pp.649–654.

Lupo, G. et al., 2005. Dorsoventral patterning of the Xenopus eye: a collaboration of Retinoid, Hedgehog and FGF receptor signaling. *Development (Cambridge, England)*, 132(7), pp.1737–1748.

Lupo, G. et al., 2011. Retinoic acid receptor signaling regulates choroid fissure closure through independent mechanisms in the ventral optic cup and periocular mesenchyme. *Proceedings of the National Academy of Sciences of the United States of America*, 108(21), pp.8698–8703.

Martínez-Morales, J.R. & Wittbrodt, J., 2009. Shaping the vertebrate eye. *Current opinion in genetics & development*, 19(5), pp.511–517.

Matt, N. et al., 2008. Impairing retinoic acid signalling in the neural crest cells is sufficient to alter entire eye morphogenesis. *Developmental Biology*, 320(1), pp.140–148.

Matt, N. et al., 2005. Retinoic acid-dependent eye morphogenesis is orchestrated by neural crest cells. *Development (Cambridge, England)*, 132(21), pp.4789–4800.

Meeker, N.D. et al., 2007. Method for isolation of PCR-ready genomic DNA from zebrafish tissues. *BioTechniques*, 43(5), pp.610–612– 614.

Merino, R. et al., 1999. The BMP antagonist Gremlin regulates outgrowth, chondrogenesis and programmed cell death in the developing limb. *Development (Cambridge, England)*, 126(23), pp.5515–5522.

Minabe-Saegusa, C. et al., 1998. Sequence and expression of a novel mouse gene PRDC (protein related to DAN and cerberus) identified by a gene trap approach. *Development, growth & differentiation*, 40(3), pp.343–353.

Molotkov, A., Molotkova, N. & Duester, G., 2006. Retinoic acid guides eye morphogenetic movements via paracrine signaling but is unnecessary for retinal dorsoventral patterning. *Development (Cambridge, England)*, 133(10), pp.1901–1910.

Mommaerts, H. et al., 2014. Smoc2 modulates embryonic myelopoiesis during

zebrafish development. *Developmental Dynamics*, 243(11), pp.1375–1390.

Morcillo, J., 2006. Proper patterning of the optic fissure requires the sequential activity of BMP7 and SHH. *Development (Cambridge, England)*, 133(16), pp.3179–3190.

Morcillo, J. et al., 2006. Proper patterning of the optic fissure requires the sequential activity of BMP7 and SHH. *Development (Cambridge, England)*, 133(16), pp.3179–3190.

Morrison, D. et al., 2002. National study of microphthalmia, anophthalmia, and coloboma (MAC) in Scotland: investigation of genetic aetiology. *Journal of medical genetics*, 39(1), pp.16–22.

Mory, A. et al., 2013. A missense mutation in ALDH1A3 causes isolated microphthalmia/anophthalmia in nine individuals from an inbred Muslim kindred. *European journal of human genetics : EJHG*.

Mui, S.H. et al., 2002. The homeodomain protein Vax2 patterns the dorsoventral and nasotemporal axes of the eye. *Development (Cambridge, England)*, 129(3), pp.797–804.

Müller, I.I. et al., 2013. Functional modeling in zebrafish demonstrates that the atrial-fibrillation-associated gene GREM2 regulates cardiac laterality, cardiomyocyte differentiation and atrial rhythm. *Disease models & mechanisms*, 6(2), pp.332–341.

Müller, I.I., Knapik, E.W. & Hatzopoulos, A.K., 2006. Expression of the protein related to Dan and Cerberus gene--prdc--During eye, pharyngeal arch, somite, and swim bladder development in zebrafish. *Developmental Dynamics*, 235(10), pp.2881–2888.

Neff, M.M., Turk, E. & Kalishman, M., 2002. Web-based primer design for single nucleotide polymorphism analysis. *Trends in genetics : TIG*, 18(12), pp.613–615.

Nohe, A. et al., 2004. Signal transduction of bone morphogenetic protein receptors. *Cellular signalling*, 16(3), pp.291–299.

Nolan, K. et al., 2013. Structure of protein related to Dan and Cerberus: insights into the mechanism of bone morphogenetic protein antagonism. *Structure (London, England : 1993)*, 21(8), pp.1417–1429.

Novinec, M. et al., 2008. Recombinant human SMOCs produced by in vitro refolding: calcium-binding properties and interactions with serum proteins. *Protein expression and purification*, 62(1), pp.75–82.

Okada, I. et al., 2011. SMOC1 is essential for ocular and limb development in humans

and mice. *American journal of human genetics*, 88(1), pp.30–41.

Onwochei, B.C., Simon, J.W. & Bateman, J.B., 2000. Ocular Colobomata. *Survey of ….*

Ozeki, H. et al., 2000. Apoptosis is associated with formation and persistence of the embryonic fissure. *Current eye research*, 20(5), pp.367–372.

Picker, A. & Brand, M., Fgf signals from a novel signaling center determine axial patterning of the prospective neural retina.

Picker, A. et al., 2009. Dynamic coupling of pattern formation and morphogenesis in the developing vertebrate retina. *PLoS biology*, 7(10), p.e1000214.

Rainger, J. et al., 2011. Loss of the BMP antagonist, SMOC-1, causes Ophthalmo-acromelic (Waardenburg Anophthalmia) syndrome in humans and mice. *PLoS genetics*, 7(7), p.e1002114.

Rembold, M. et al., 2006. Individual cell migration serves as the driving force for optic vesicle evagination. *Science (New York, N.Y.)*, 313(5790), pp.1130–1134.

Rhinn, M. & Dollé, P., 2012. Retinoic acid signalling during development. *Development (Cambridge, England)*, 139(5), pp.843–858.

Rider, C.C. & Mulloy, B., 2010. Bone morphogenetic protein and growth differentiation factor cytokine families and their protein antagonists. *The Biochemical journal*, 429(1), pp.1–12.

Sakuta, H. et al., 2001. Ventroptin: a BMP-4 antagonist expressed in a double-gradient pattern in the retina. *Science (New York, N.Y.)*, 293(5527), pp.111–115.

Sambasivan, R., Kuratani, S. & Tajbakhsh, S., 2011. An eye on the head: the development and evolution of craniofacial muscles. *Development (Cambridge, England)*, 138(12), pp.2401–2415.

Sasagawa, S. et al., 2002. Axes establishment during eye morphogenesis in Xenopus by coordinate and antagonistic actions of BMP4, Shh, and RA. *Genesis (New York, N.Y. : 2000)*, 33(2), pp.86–96.

Sasai, Y. et al., 1994. Xenopus chordin: a novel dorsalizing factor activated by organizer-specific homeobox genes. *Cell*, 79(5), pp.779–790.

Schmidt, J.E. et al., 1995. Localized BMP-4 mediates dorsal/ventral patterning in the early Xenopus embryo. *Developmental Biology*, 169(1), pp.37–50.

Schmitt, E.A. & Dowling, J.E., 1994. Early eye morphogenesis in the zebrafish, Brachydanio rerio. *The Journal of comparative neurology*, 344(4), pp.532–542.

See, A.W.-M. & Clagett-Dame, M., 2009. The temporal requirement for vitamin A in

the developing eye: mechanism of action in optic fissure closure and new roles for the vitamin in regulating cell proliferation and adhesion in the embryonic retina. *Developmental Biology*, 325(1), pp.94–105.

Semerci, C.N. et al., 2014. Novel splice-site and missense mutations in the ALDH1A3 gene underlying autosomal recessive anophthalmia/microphthalmia. *The British journal of ophthalmology*, 98(6), pp.832–840.

Shawi, M. & Serluca, F.C., 2008. Identification of a BMP7 homolog in zebrafish expressed in developing organ systems. *Gene expression patterns : GEP*, 8(6), pp.369–375.

Shimozono, S. et al., 2013. Visualization of an endogenous retinoic acid gradient across embryonic development. *Nature*.

Sieber, C. et al., 2009. Recent advances in BMP receptor signaling. *Cytokine & growth factor reviews*, 20(5-6), pp.343–355.

Sinn, R. & Wittbrodt, J., 2013. An eye on eye development. *Mechanisms of development*, 130(6-8), pp.347–358.

Slavotinek, A.M., 2011. Eye development genes and known syndromes. *Molecular Genetics and Metabolism*, 104(4), pp.448–456.

Smith, J.C. & Slack, J.M., 1983. Dorsalization and neural induction: properties of the organizer in Xenopus laevis. *Journal of embryology and experimental morphology*, 78, pp.299–317.

Smith, W.C. & Harland, R.M., 1992. Expression cloning of noggin, a new dorsalizing factor localized to the Spemann organizer in Xenopus embryos. *Cell*, 70(5), pp.829–840.

Stenkamp, D.L., 2007. Neurogenesis in the Fish Retina. In *International review of cytology*. International Review of Cytology. Elsevier, pp. 173–224.

Stigloher, C. et al., 2006. Segregation of telencephalic and eye-field identities inside the zebrafish forebrain territory is controlled by Rx3. *Development (Cambridge, England)*, 133(15), pp.2925–2935.

Stuermer, C.A., 1988. Retinotopic organization of the developing retinotectal projection in the zebrafish embryo. *The Journal of neuroscience : the official journal of the Society for Neuroscience*, 8(12), pp.4513–4530.

Takahashi, H. et al., 2009. Functional mode of FoxD1/CBF2 for the establishment of temporal retinal specificity in the developing chick retina. *Developmental Biology*.

Take-uchi, M., Clarke, J.D.W. & Wilson, S.W., 2003. Hedgehog signalling maintains the optic stalk-retinal interface through the regulation of Vax gene activity. *Development (Cambridge, England)*, 130(5), pp.955–968.

Thisse, C. & Thisse, B., 2008. High-resolution in situ hybridization to whole-mount zebrafish embryos. *nature protocols*, 3(1), pp.59–69.

Thomas, J.T. et al., 2009. Xenopus SMOC-1 Inhibits bone morphogenetic protein signaling downstream of receptor binding and is essential for postgastrulation development in Xenopus. *The Journal of biological chemistry*, 284(28), pp.18994–19005.

Tzahor, E. et al., 2003. Antagonists of Wnt and BMP signaling promote the formation of vertebrate head muscle. *Genes & development*, 17(24), pp.3087–3099.

Umulis, D., O'Connor, M.B. & Blair, S.S., 2009. The extracellular regulation of bone morphogenetic protein signaling. *Development (Cambridge, England)*, 136(22), pp.3715–3728.

Vannahme, C. et al., 2002. Characterization of SMOC-1, a novel modular calcium-binding protein in basement membranes. *The Journal of biological chemistry*, 277(41), pp.37977–37986.

Vannahme, C. et al., 2003. Characterization of SMOC-2, a modular extracellular calcium-binding protein. *The Biochemical journal*, 373(Pt 3), pp.805–814.

Varga, Z.M., Wegner, J. & Westerfield, M., 1999. Anterior movement of ventral diencephalic precursors separates the primordial eye field in the neural plate and requires cyclops. *Development (Cambridge, England)*, 126(24), pp.5533–5546.

Veien, E.S. et al., 2008. Canonical Wnt signaling is required for the maintenance of dorsal retinal identity. *Development (Cambridge, England)*, 135(24), pp.4101–4111.

Verma, A.S. & FitzPatrick, D.R., 2007. University of Alberta Libraries. *Orphanet J Rare Dis*.

Vuilleumier, R. et al., 2010. Control of Dpp morphogen signalling by a secreted feedback regulator. *Nature cell biology*, 12(6), pp.611–617.

Waxman, J.S. & Yelon, D., 2011. Zebrafish retinoic acid receptors function as context-dependent transcriptional activators. *Developmental Biology*, 352(1), pp.128–140.

Westerfield, M., 2007. *The zebrafish book. A guide for the laboratory use of zebrafish (Danio rerio).* 5 ed., Eugene, OR: University of Oregon Press.

Williamson, K.A. & Fitzpatrick, D.R., 2014. The genetic architecture of microphthalmia, anophthalmia and coloboma. *European journal of medical genetics*, 57(8), pp.369–380.

Wilson, S.W. & Houart, C., 2004. Early steps in the development of the forebrain. *Developmental cell*, 6(2), pp.167–181.

Yahyavi, M. et al., 2013. ALDH1A3 loss of function causes bilateral anophthalmia/microphthalmia and hypoplasia of the optic nerve and optic chiasm. *Human molecular genetics*.

Zhang, X.M. & Yang, X.J., 2001. Temporal and spatial effects of Sonic hedgehog signaling in chick eye morphogenesis. *Developmental Biology*, 233(2), pp.271–290.

Zhao, L. et al., 2010. Sonic hedgehog is involved in formation of the ventral optic cup by limiting Bmp4 expression to the dorsal domain. *Mechanisms of development*, 127(1-2), pp.62–72.

Zuniga, E. et al., 2011. Gremlin 2 regulates distinct roles of BMP and Endothelin 1 signaling in dorsoventral patterning of the facial skeleton. *Development (Cambridge, England)*, 138(23), pp.5147–5156.